

---

# DROP JET IN CROSSFLOW: ALE/FINITE ELEMENT SIMULATIONS AND INTERFACIAL EFFECTS

D.Sc. thesis final exam of  
Gustavo Charles Peixoto de Oliveira  
at PPG-EM/UERJ  
Rio de Janeiro, February 20th 2015

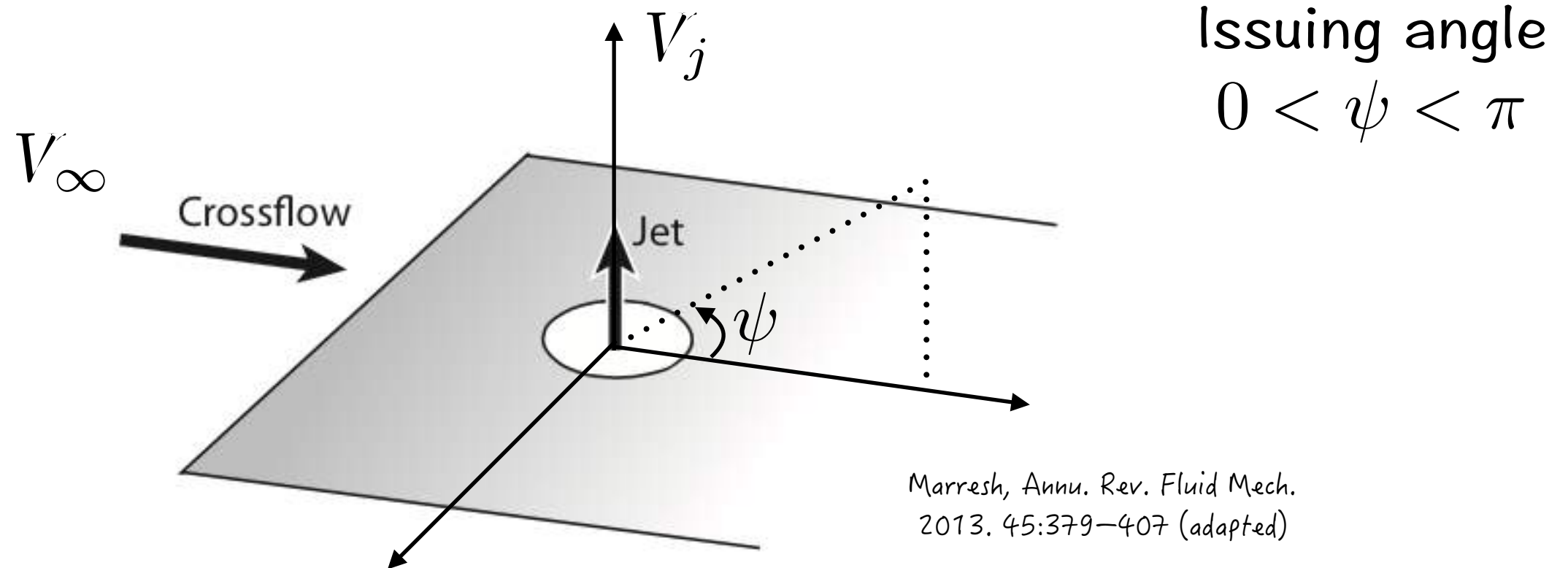
# Outline

1. Motivations & purposes of this thesis
2. Technicalities & tools
3. ALE/FEM modelling
4. PBC implementation
5. Validation of the methodology
6. The DJICF problem and results

---

# 1. Motivations & purposes of this thesis

- The canonical flow of a Jet in Crossflow (JICF): the inspiration

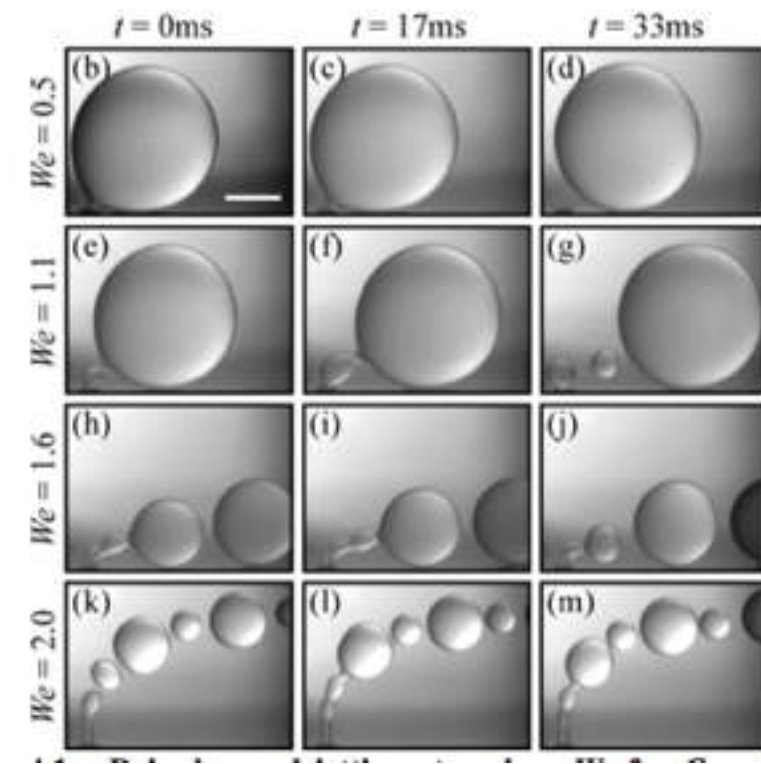
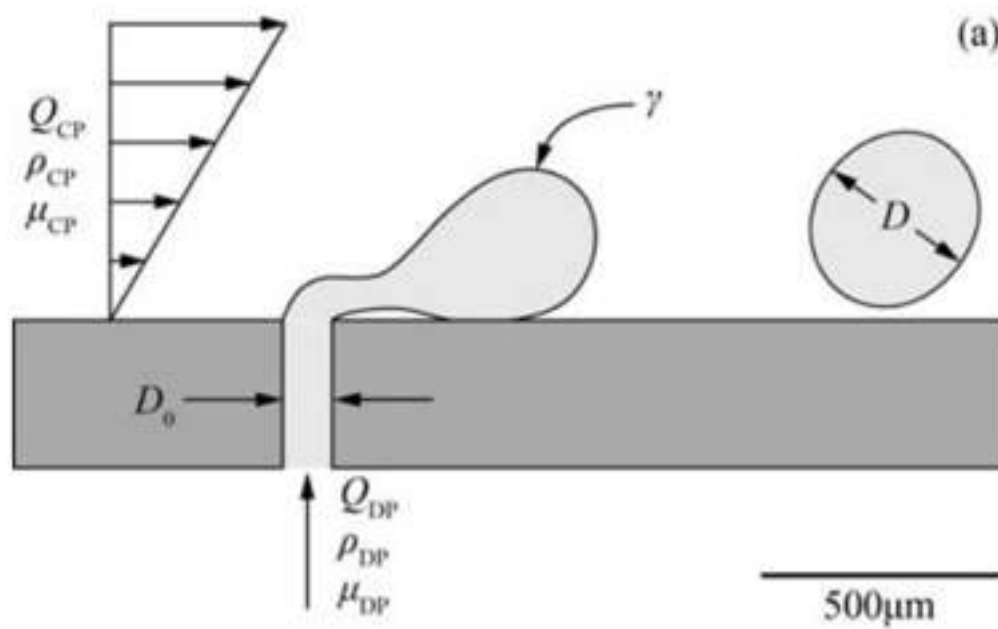


Crossflow-to-jet velocity ratio

$$\lambda = \frac{V_\infty}{V_j}$$

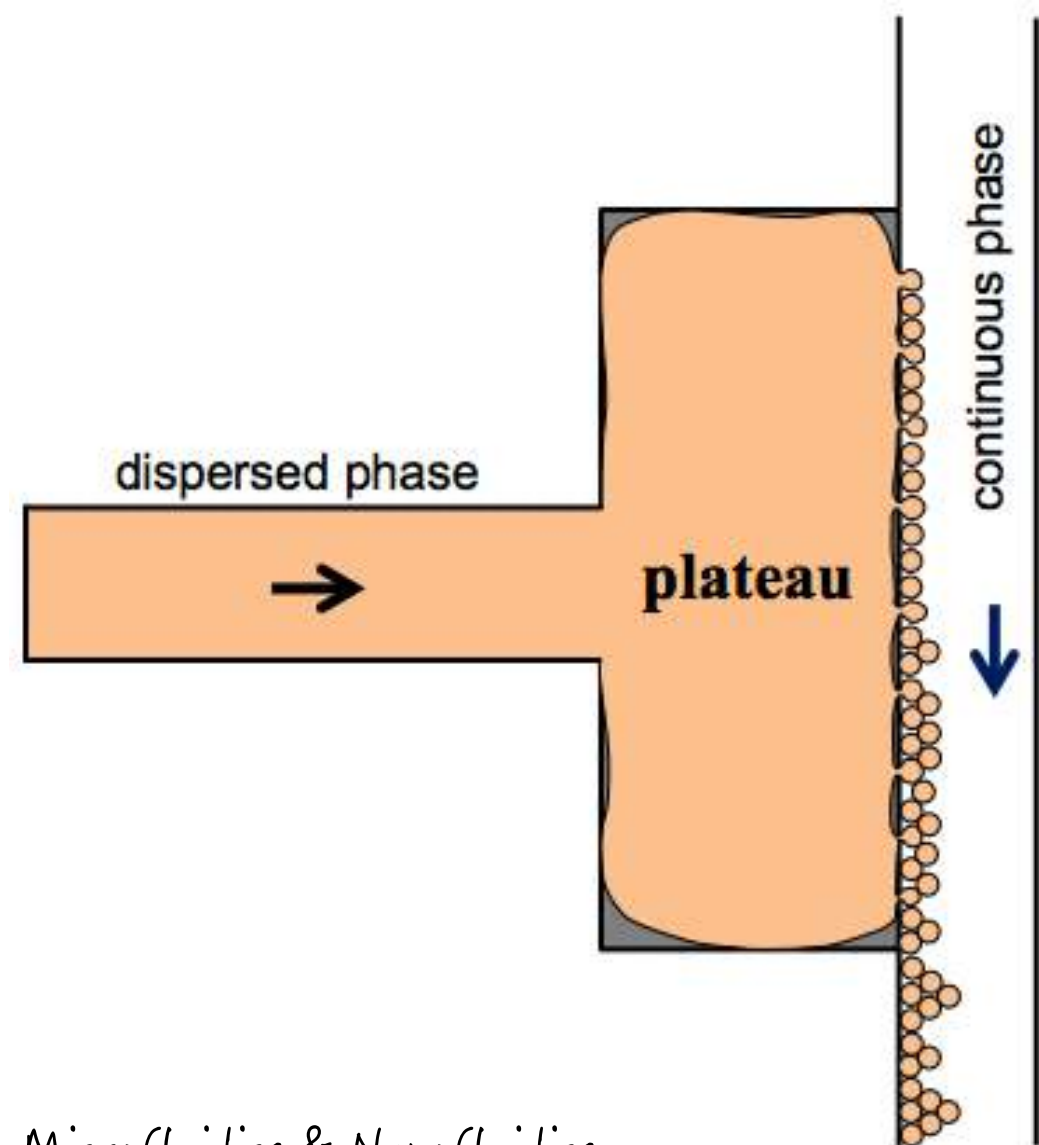
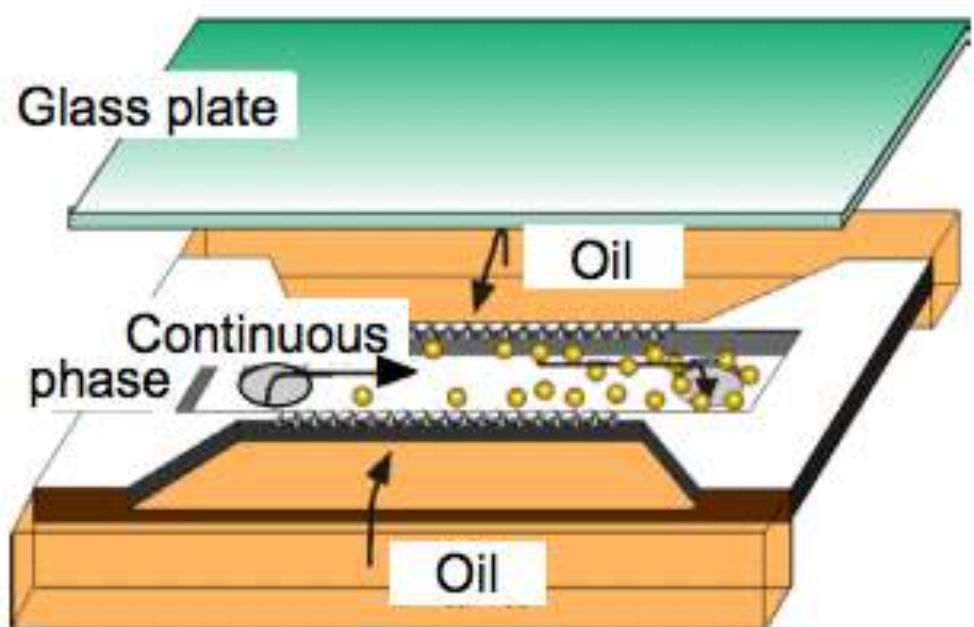
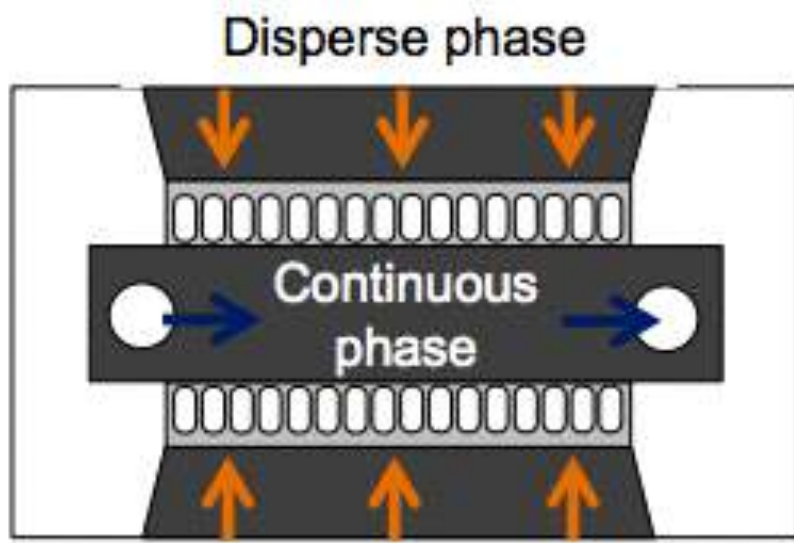
- Liquid-liquid drop interactions in several applications
  - drug delivery;
  - mixing T-junctions;
  - membrane and microchannel emulsification;
  - porous filtration;
  - nanojets and ink-jet printing;
  - molten jets and steelmaking processes;

- Membrane emulsification processes



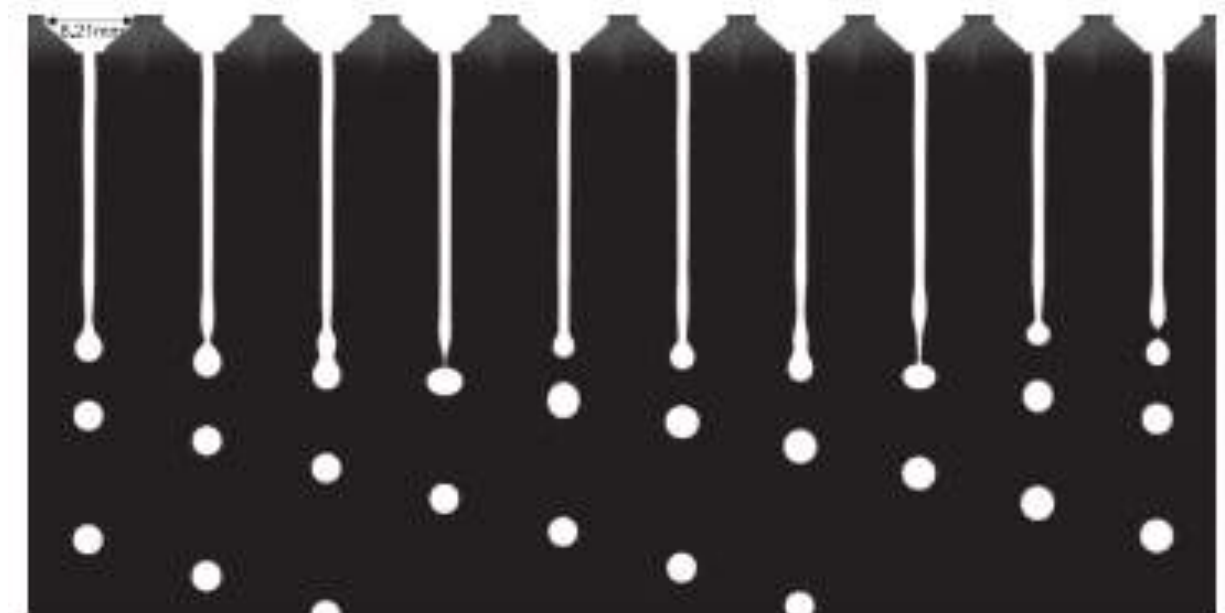
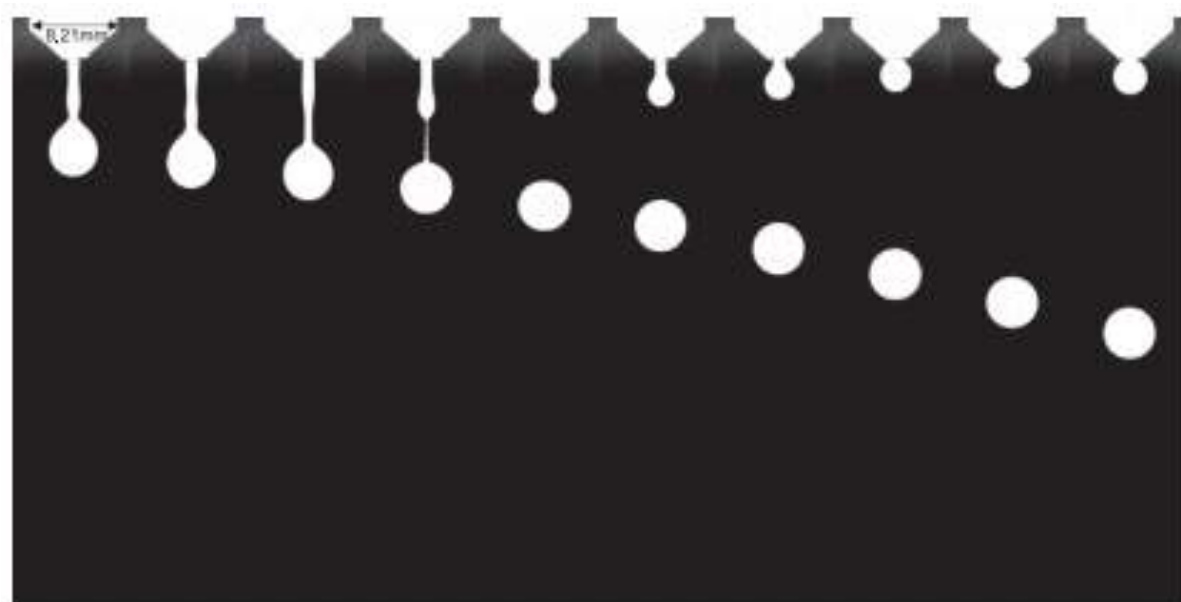
R. Meyer, 2010,  
Ph.D. thesis, PennState

- Microchannel emulsification; droplet generator



Vladisavljevic, Microfluidics & Nanofluidics  
2012, 13:151-178

- Calcia/alumina molten microjets in steelmaking processes



Wegener, Chem. Eng. Sci.  
2014. 105:143-154

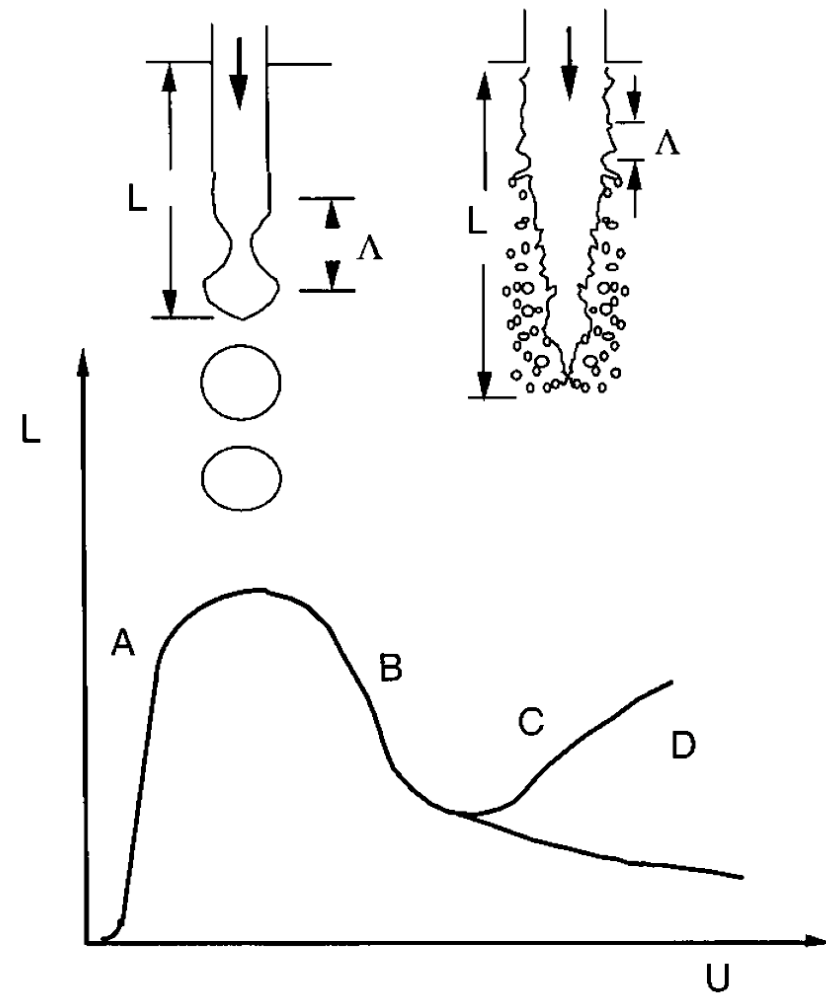
# Supportive arguments

- Drop interaction problems -> modern applications
- CFD/MCFD evolution -> microscale, microfluidics
- Multiphase/multifluid dynamics -> complex flows -> robust simulation tools

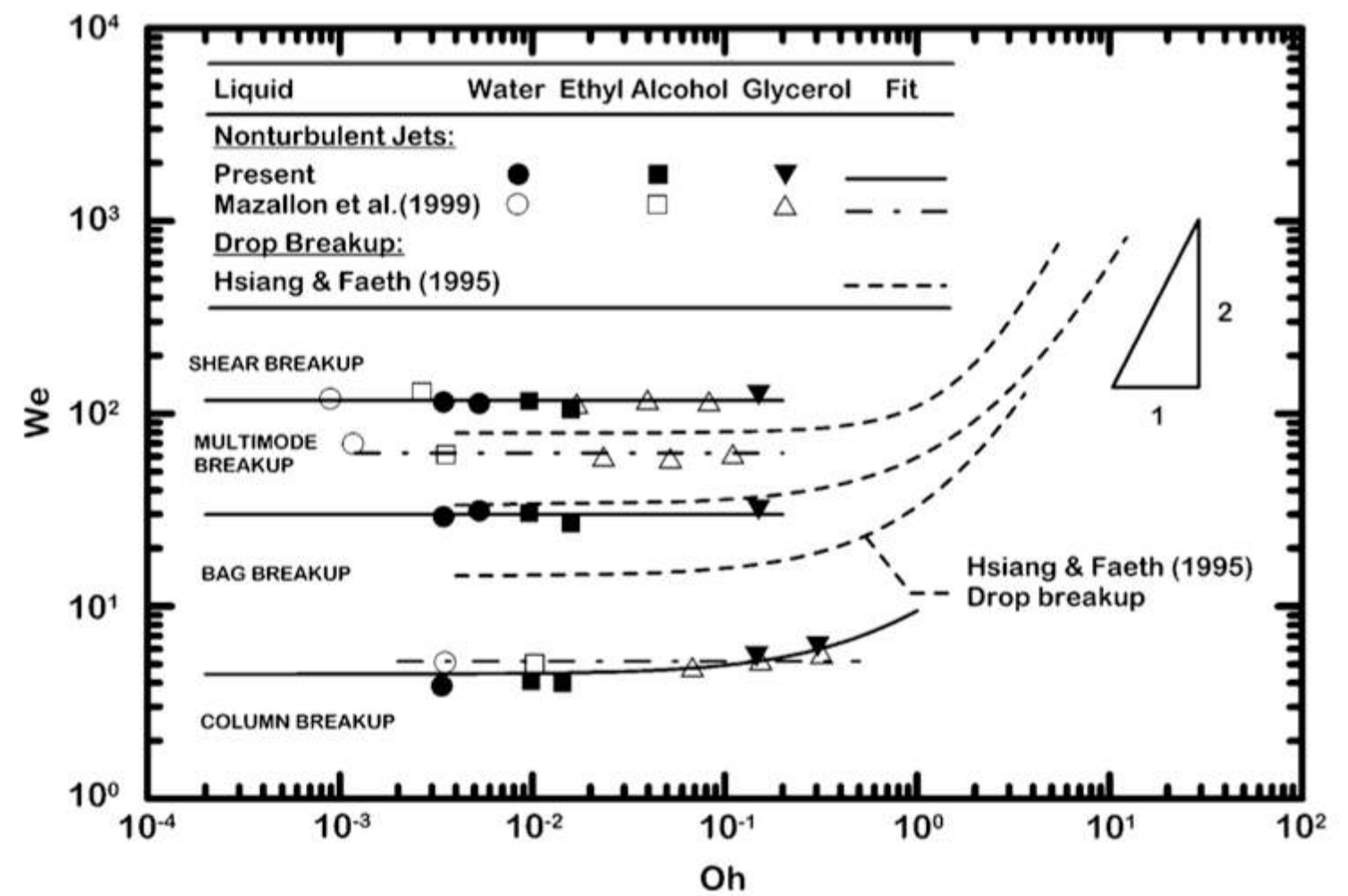
# DJICF to produce knowledge

- ALE/FEM-based studies of DJICF configurations make up a new approach
- Incompressible nonturbulent liquid-liquid dynamics is less known in comparison to its compressible turbulent gas-liquid counterpart
- Cost-effective computational models dealing with topological changes are necessary to capture physical aspects of mobile interfaces

- Where does this thesis come in?



Lin, 2003



Salam et al., AIAA, (42), 2529-2540, 2004

Drop “pinch-off” in the primary breakup zone of nonturbulent jets

# Purposes of this thesis

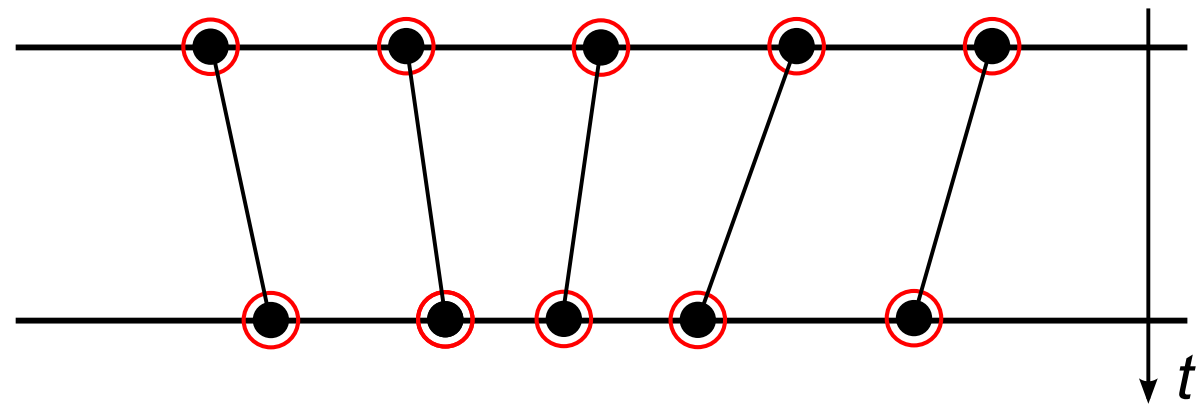
- to use an Arbitrary Lagrangian-Eulerian Finite Element method two-phase flow code to simulate a nonturbulent liquid jet in crossflow by considering surface tension effects
- to apply a unit cell-based model that resorts to periodic boundary conditions along with a moving frame reference technique to follow the jet and reduce computational costs
- to perform an analysis of the flow in the primary breakup zone of drop formation based on experimental liquid-liquid pairs

keypoints

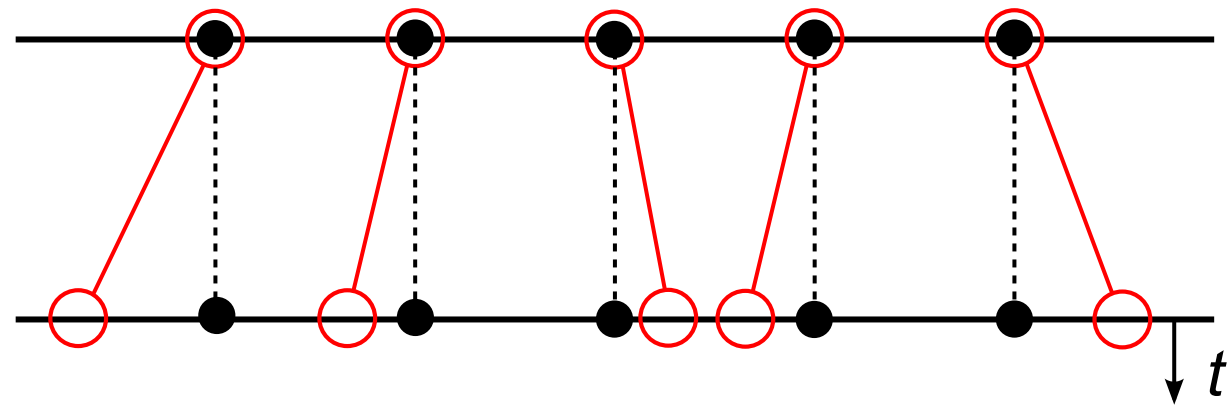
---

# 2. Technicalities & tools

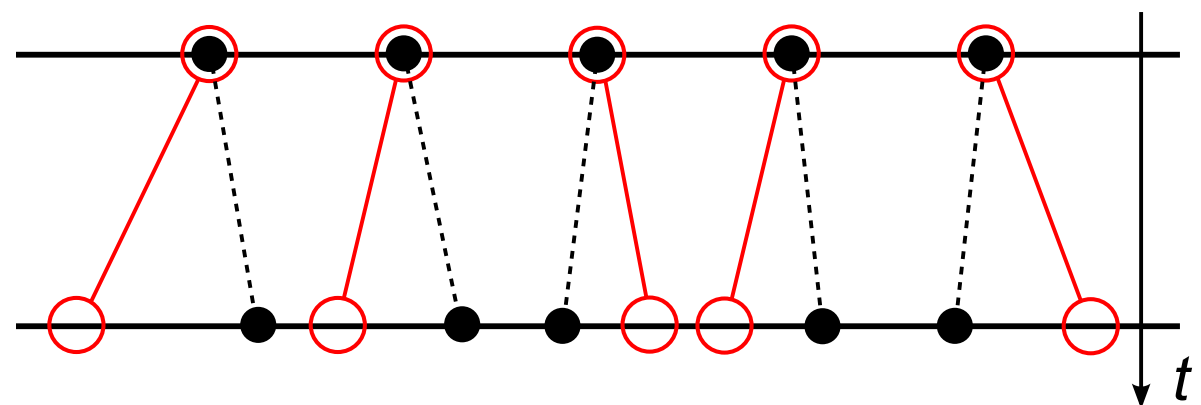
- ALE description of movement



Lagrangian

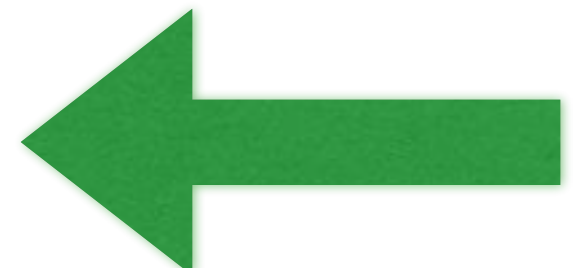


Eulerian



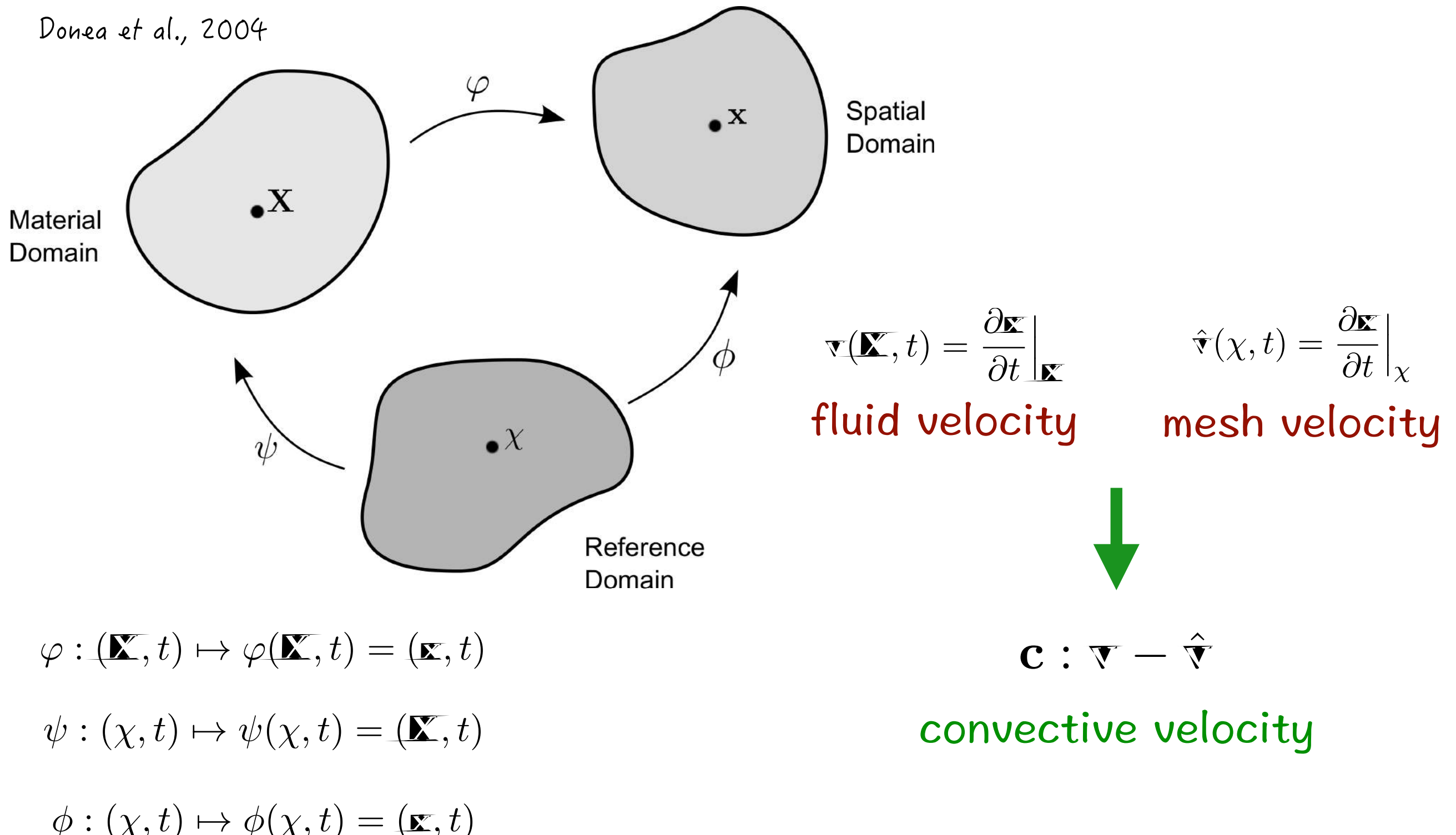
Arbitrary

● mesh nodes  
○ material points



# Motion laws as homeomorphisms

Donea et al., 2004

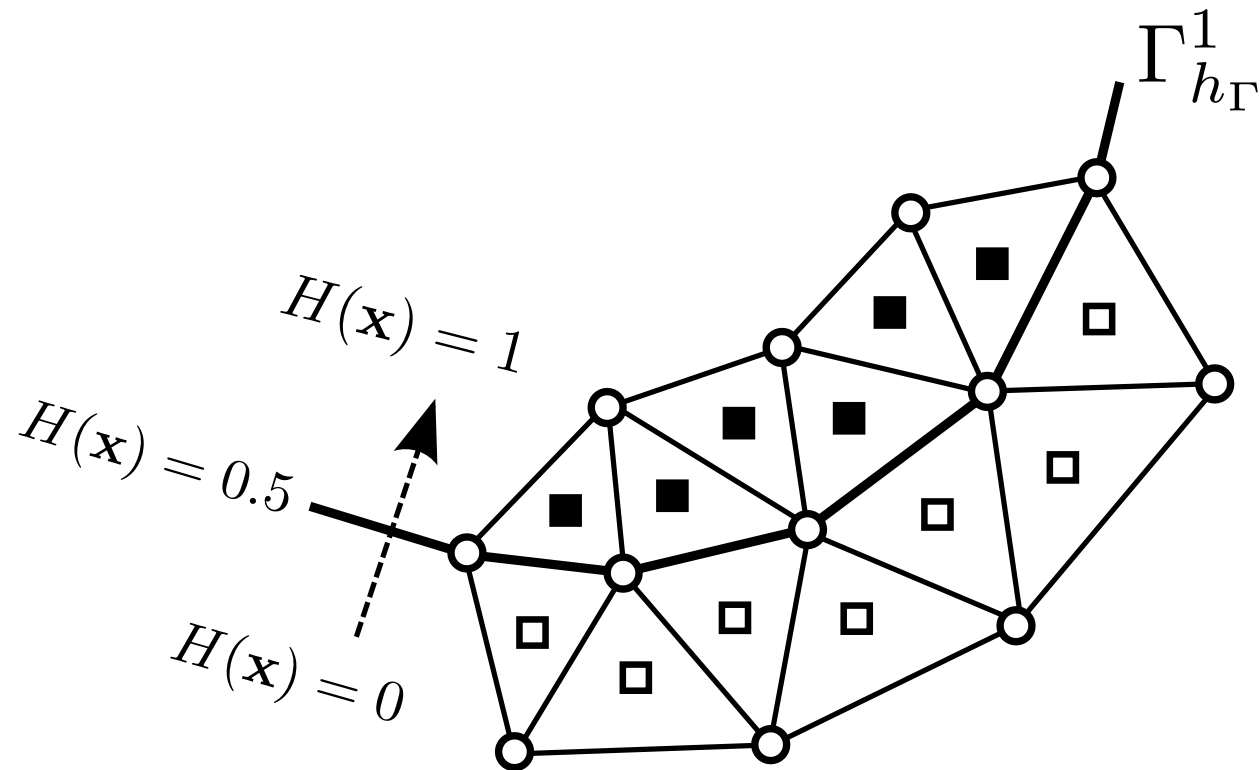


$$\varphi : (\mathbf{X}, t) \mapsto \varphi(\mathbf{X}, t) = (\mathbf{x}, t)$$

$$\psi : (\chi, t) \mapsto \psi(\chi, t) = (\mathbf{X}, t)$$

$$\phi : (\chi, t) \mapsto \phi(\chi, t) = (\mathbf{x}, t)$$

- Mesh generation, tessellation and pre-preprocessing features



marker function:  
Heaviside

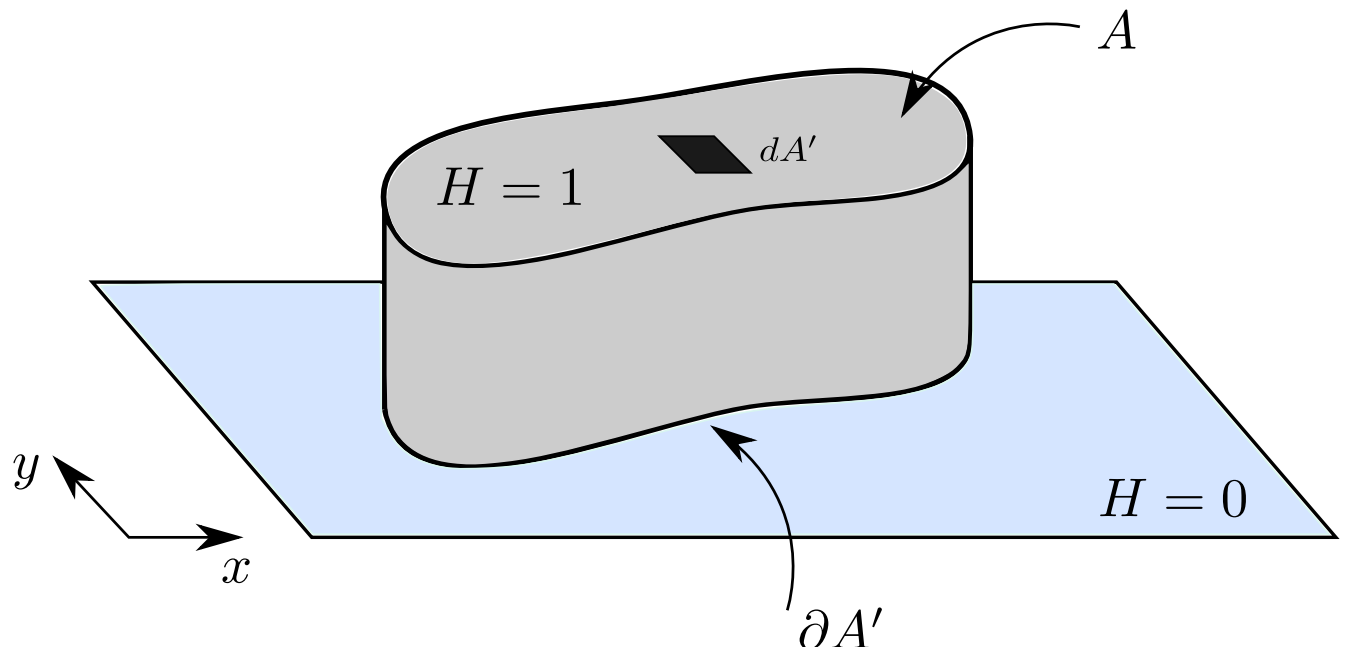
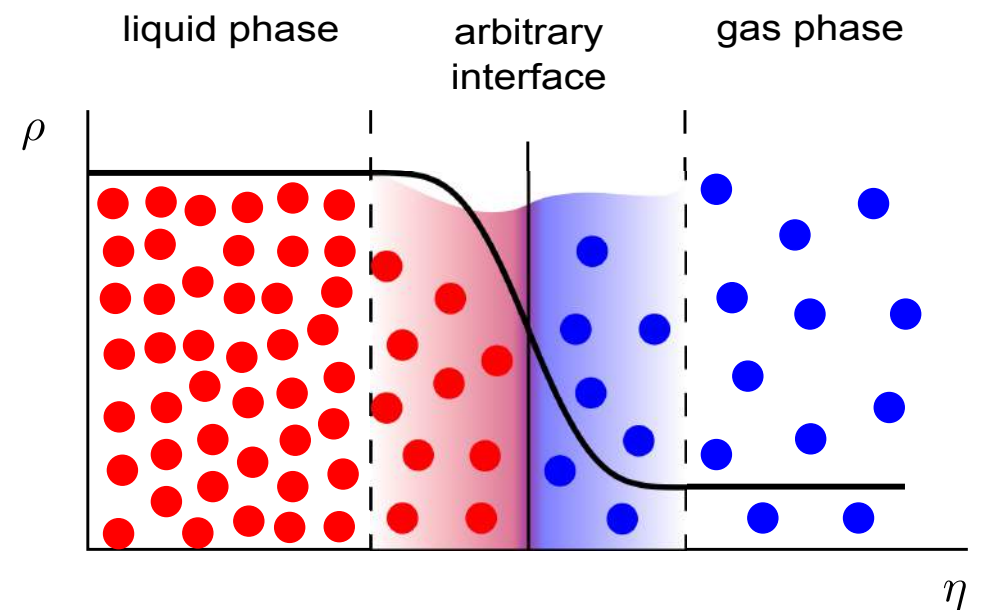
$$H(\mathbf{x}_j) := \begin{cases} 0, & \text{if } \mathbf{x}_j \in \mathcal{T}_h^{\Omega^2} \cup \mathcal{T}_{h_2}^{\Psi^2} \\ 0.5, & \text{if } \mathbf{x}_j \in \mathcal{T}_{h_1}^{\Psi^1} \\ 1, & \text{if } \mathbf{x}_j \in \mathcal{T}_h^{\Omega^1}. \end{cases}$$

two data structures:  
surface mesh + volume mesh

$$\begin{aligned} \mathcal{T}_{h_1}^{\Psi^1} &:= \{T \in \mathcal{T}_h; T \in \text{interface}\}, \\ \mathcal{T}_{h_2}^{\Psi^2} &:= \{T \in \mathcal{T}_h; T \in \text{convex hull}\}, \\ \mathcal{T}_{h_\Psi}^{\Psi} &:= \mathcal{T}_{h_1}^{\Psi^1} \cup \mathcal{T}_{h_2}^{\Psi^2} \\ \mathcal{T}_h^{\Omega^1} &:= \left\{ T \in \mathcal{T}_h; \mathring{T} \subset \Omega^1 \right\}, \quad \rightsquigarrow \blacksquare \text{ (elements)}, \\ \mathcal{T}_h^{\Omega^2} &:= \left\{ T \in \mathcal{T}_h; \mathring{T} \subset \Omega^2 \right\}, \quad \rightsquigarrow \square \text{ (elements)}, \\ \mathcal{T}_h^\Omega &:= \mathcal{T}_h^{\Omega^1} \cup \mathcal{T}_h^{\Omega^2}, \end{aligned}$$

$T$ : triangle or  
tetrahedron

## • Interface representation, tracking and modelling



$$\phi(\mathbf{x}) = \phi^1 H(\mathbf{x}) + \phi^2(1 - H(\mathbf{x})),$$

$$\phi^i = \phi|_{\Omega^i}, i = 1, 2$$

- jump of properties;
- generalised functions;
- no Marangoni effects;

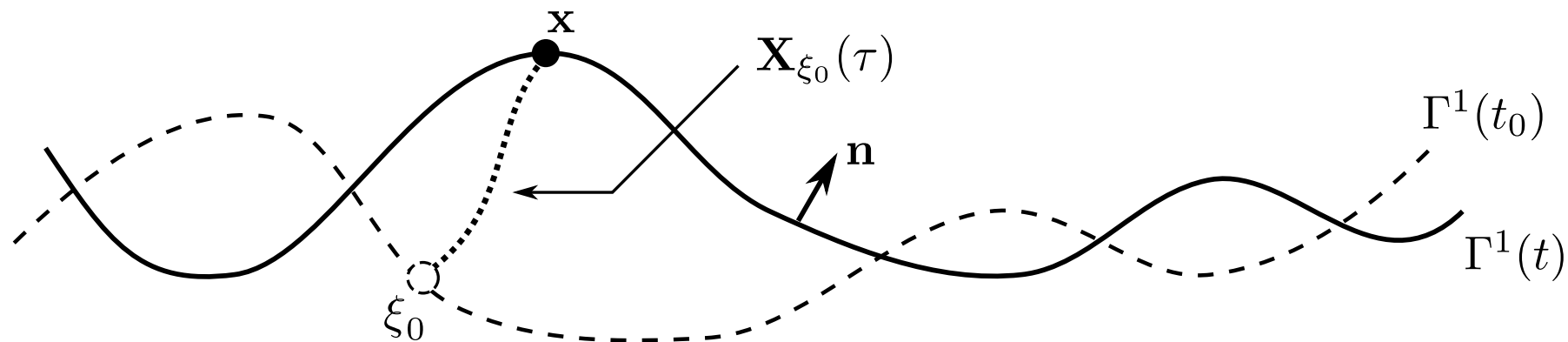
$$\nabla H = - \int_{A_I} \delta(x - x_I) \delta(y - y_I) \mathbf{n}_I dA_I = -\delta(\eta) \mathbf{n},$$

$$\nabla H = -\delta \mathbf{n}$$

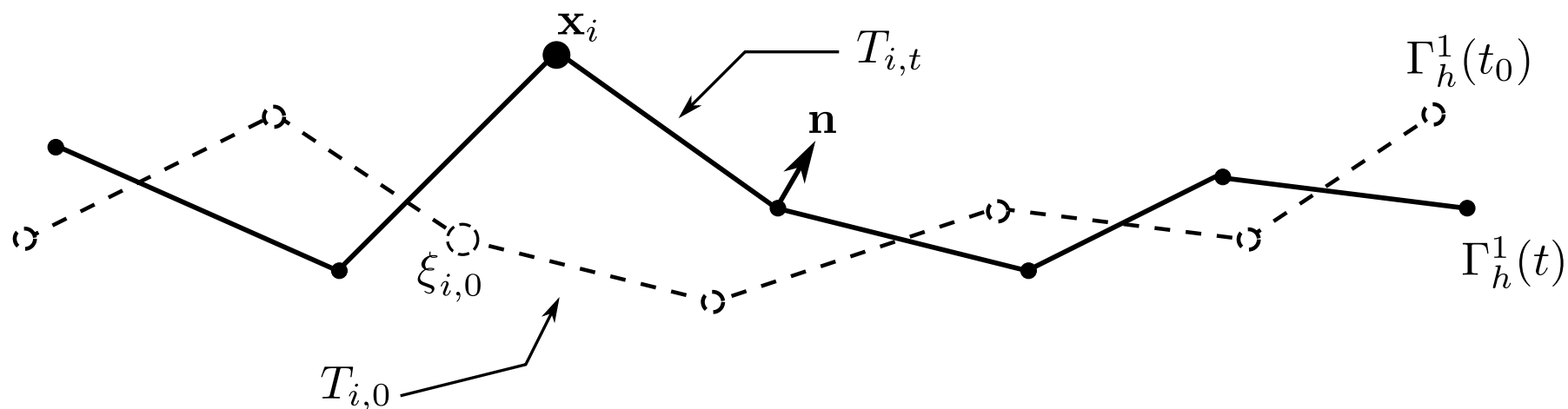
**surface force**  
 $\mathbf{f} = \sigma \kappa \mathbf{n}$

# Front tracking

$$\mathcal{V}_{h_1}^1(\tau) := \{T(\tau) \in \mathcal{T}_h(\tau); \quad K(\mathbf{x}_i) = 0.5\}, \\ i = 1, 2, \dots, \nu, \quad \tau \in [t_0, t]$$



continuous



Reusken, 2011

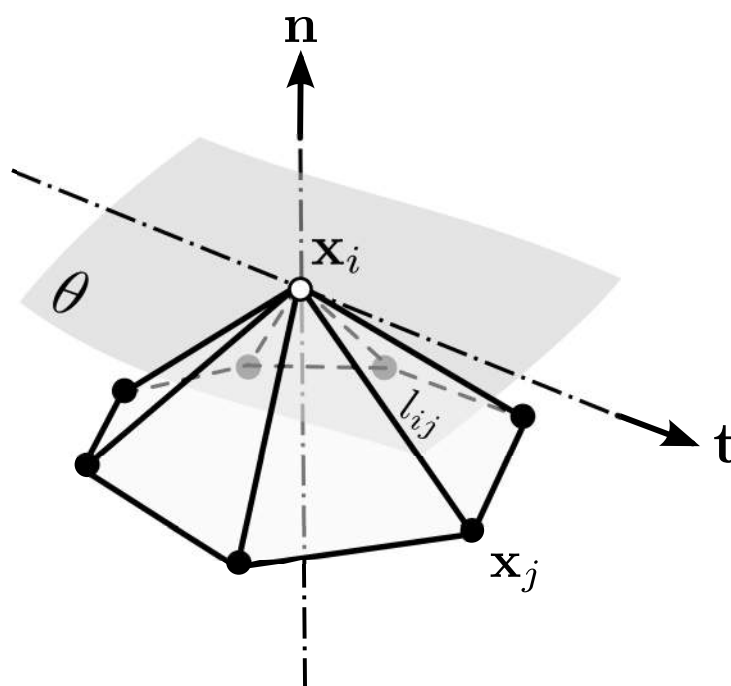
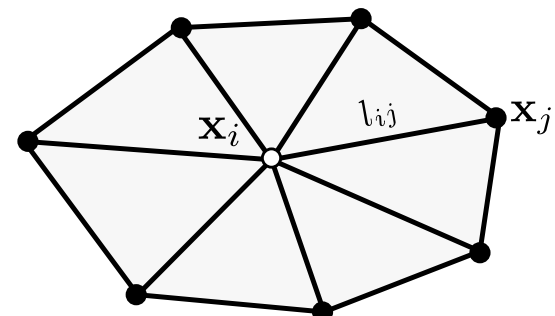
discrete

$$\Gamma(t) \ni \mathbf{x} = \xi_0 + \int_{t_0}^t \hat{\nabla}(\mathbf{X}_{\xi_0}(\tau), \tau) d\tau, \quad \xi_0 \in \Gamma(t_0), \quad t \geq t_0,$$

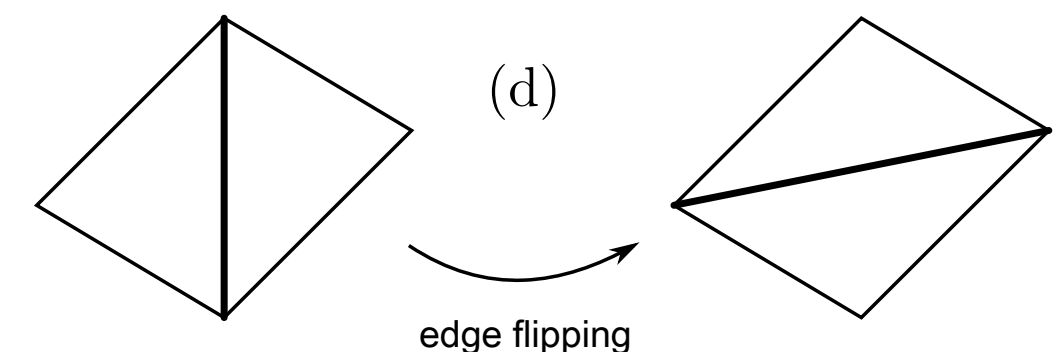
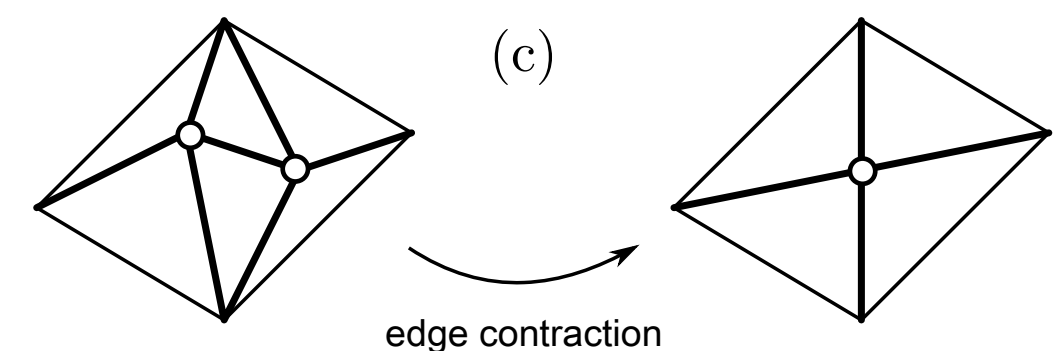
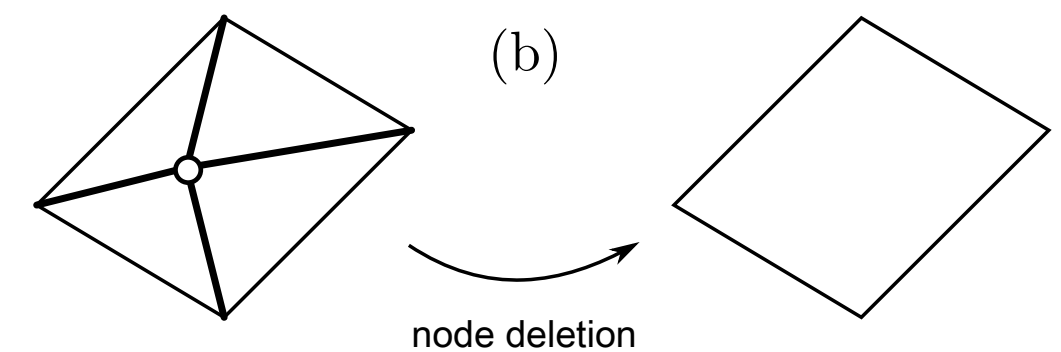
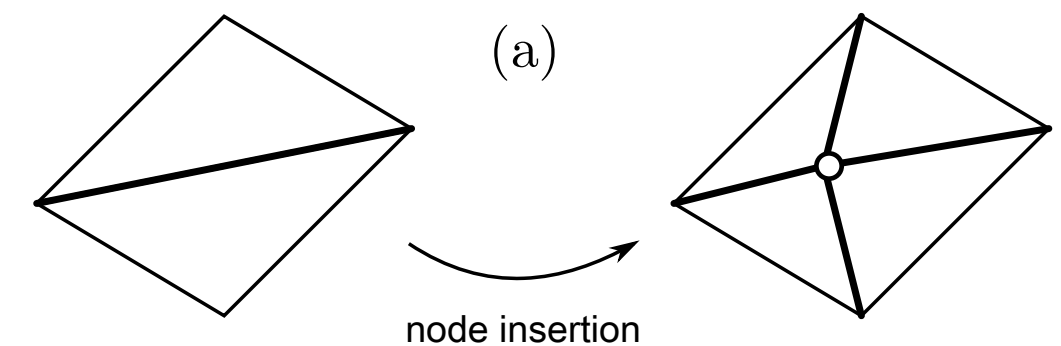
# Dynamic mesh control

## mesh operations

### Laplace smoothing



$$\mathbf{x}_i \rightarrow \hat{\mathbf{x}}_i := \sum_{j \in S(i)}^{S} w_{ij} (\mathbf{x}_j - \mathbf{x}_i), \quad w_{ij} = l_{ij}^{-1},$$



# Generalized ALE mesh motion control

$$\hat{\mathbf{v}}(\mathbf{x}_j) = \begin{cases} \mathbf{v} - \gamma_1(\mathbf{v} \cdot \mathbf{t})\mathbf{t} + \gamma_2(\mathbf{v}_e \cdot \mathbf{t})\mathbf{t} & , \text{ if } \mathbf{x}_j \in \mathcal{T}_{h_1}^{\Gamma^1} \text{ interface} \\ \beta_1\mathbf{v} + \beta_2\mathbf{v}_{I;\epsilon} + \beta_3\mathbf{v}_e & , \text{ otherwise } \text{ volume} \end{cases}$$

Anjos, 2012-2014

$\beta_1$  : pure Lagrangian motion control

$\beta_2$  : neighbourhood-based velocity smoothing

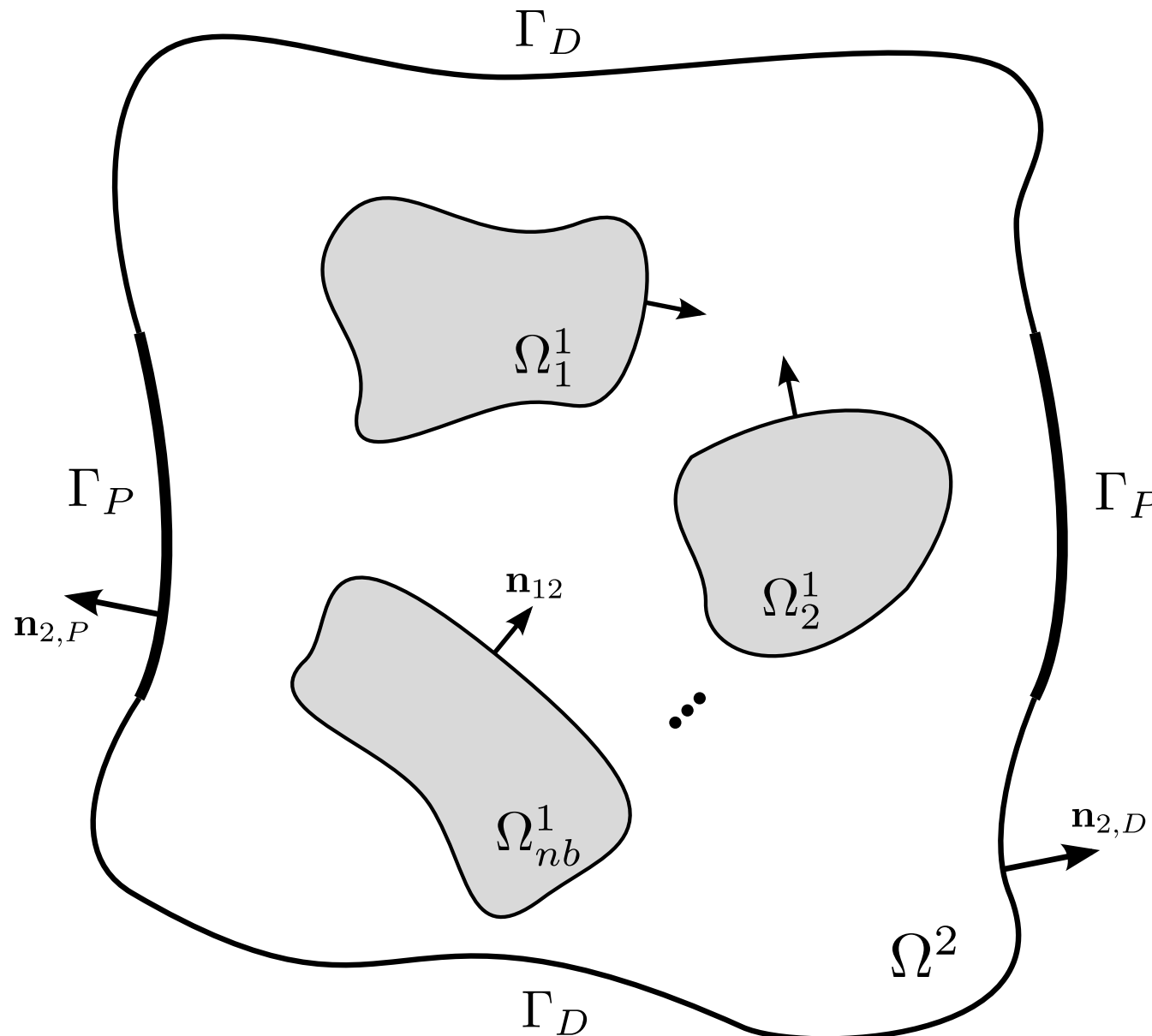
$\beta_3$  : elastic-based velocity Laplacian smoothing

$\gamma_1$  : tangent interface velocity magnitude control

$\gamma_2$  : elastic-based velocity and mesh quality

# 3. ALE/FEM modeling

- Generalized two-phase/two-fluid domain



$$\begin{aligned}\Omega &:= \Omega^1 \cup \Omega^2, \quad \Omega^1 = \bigcup_{g=1}^{nb} \Omega_g^1, \\ \Gamma &:= \Gamma^1 \cup \Gamma^2, \\ \Gamma^1 &= \bigcup_{g=1}^{nb} \Gamma_g^1 \\ \Gamma^2 &= \Gamma_D \cup \Gamma_P\end{aligned}$$

1: dispersed phase

2: continuous phase

- FE spaces

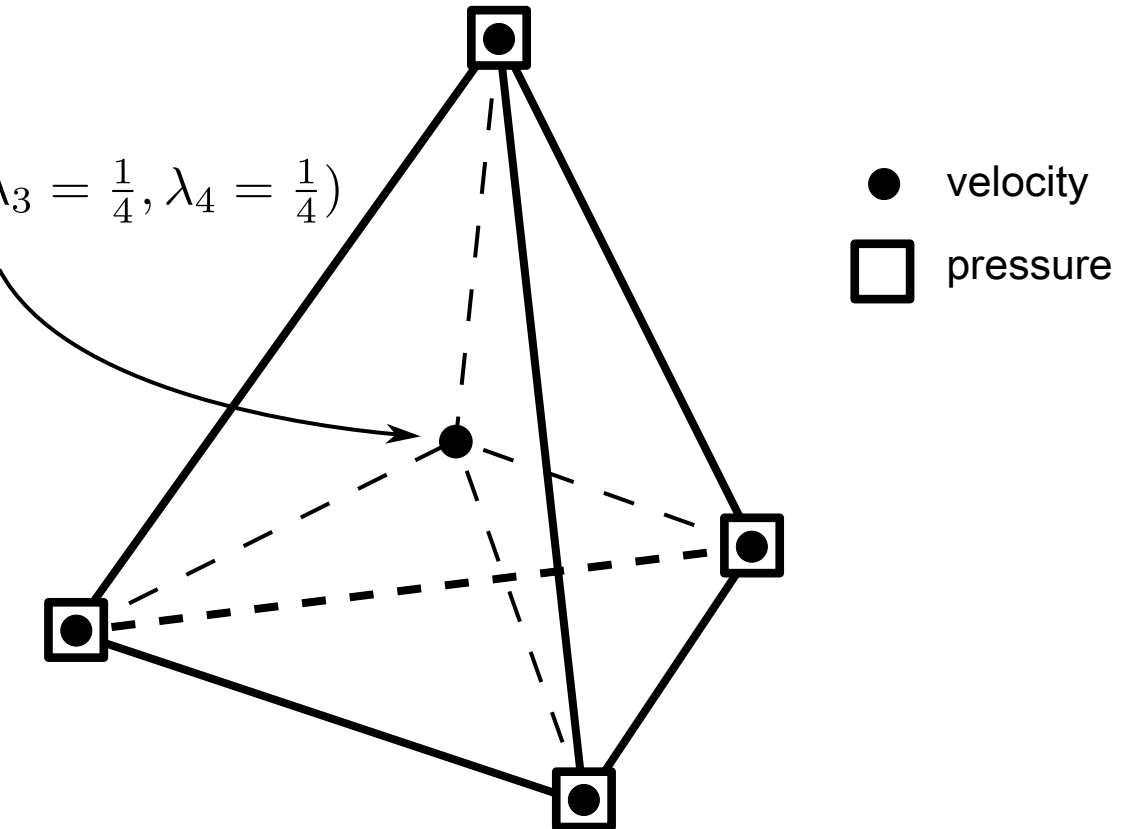
velocity

$$\mathcal{P}(T) = \mathcal{P}_1 \oplus \{\lambda_1 \lambda_2 \lambda_3\}^3$$

pressure

$$\mathcal{P}(T) = \mathcal{P}_1$$

$$(\lambda_1 = \frac{1}{4}, \lambda_2 = \frac{1}{4}, \lambda_3 = \frac{1}{4}, \lambda_4 = \frac{1}{4})$$



Taylor-Hood's MINI element 3D  
LBB-stable

Girault & Raviart, 1986

## • Governing equations

$$\mathbf{f} = \sigma \kappa \nabla H$$

$$\rho \frac{\hat{D}_{\mathbf{v}}}{Dt} + \nabla p - \frac{1}{Re} \nabla \cdot [\mu (\nabla_{\mathbf{v}} + \nabla_{\mathbf{v}}^T)] - \frac{1}{Fr^2} \rho \mathbf{g} - \frac{1}{We} \mathbf{f} = 0$$

$$\nabla \cdot \mathbf{v} = 0$$

$$\frac{D\Psi}{Dt} - \frac{1}{ReSc} \nabla^2 \Psi = 0$$

(decoupled)

$$\hat{D}_{\mathbf{v}} = \left( \frac{\partial_{\mathbf{v}}}{\partial t} + (\mathbf{v} - \hat{\mathbf{v}}) \cdot \nabla_{\mathbf{v}} \right)$$

“one-fluid” formulation

Tryggvason, 2009

- Semi-Lagrangian method

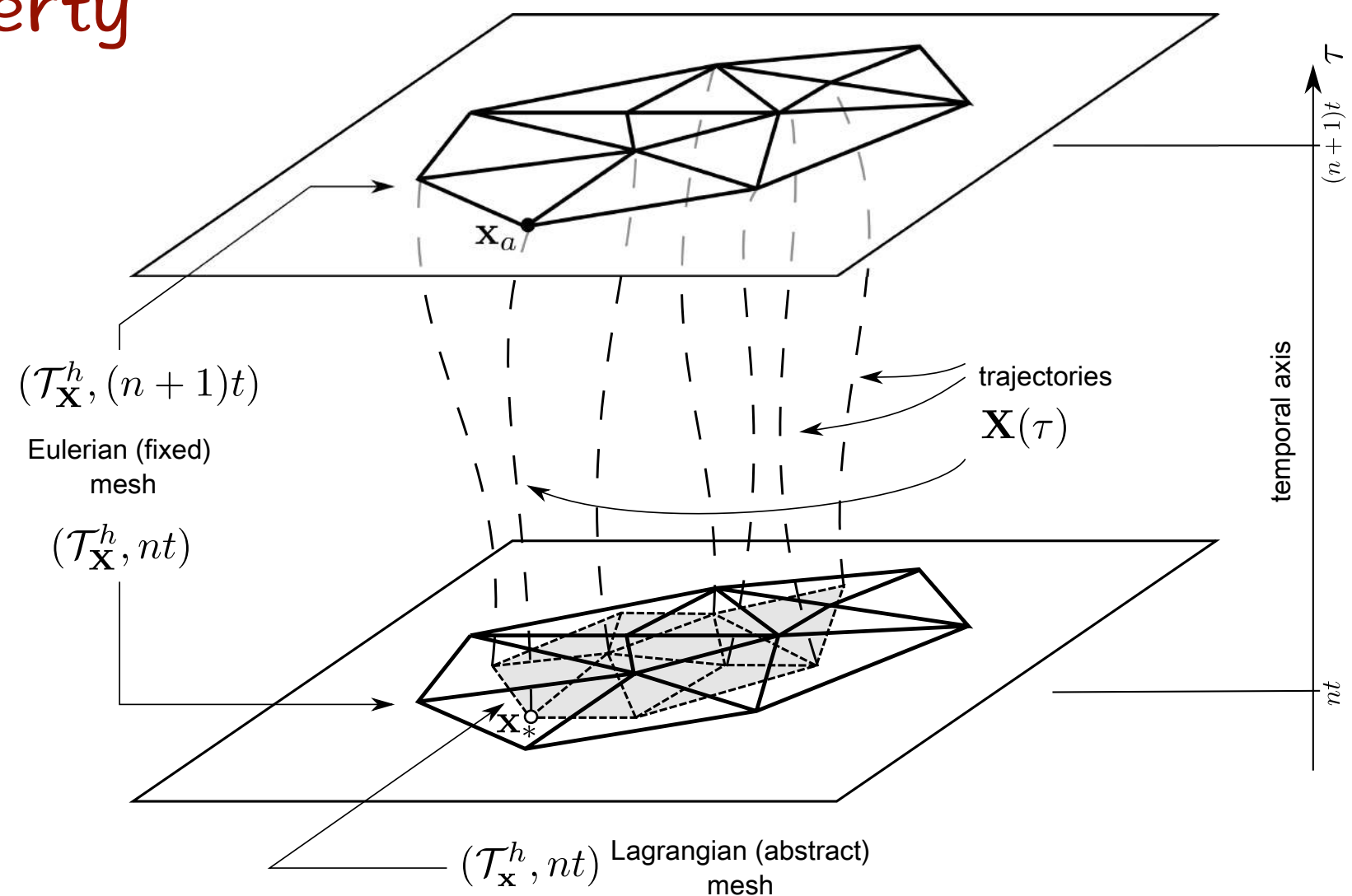
Smolarkiewicz, 1992

$$\frac{D\Phi}{D\tau} = \frac{\partial \Phi}{\partial \tau} + \nabla \cdot \nabla \Phi \approx \frac{\Phi(\mathbf{x}_a, (n+1)t; \tau) - \Phi(\mathbf{x}_d, nt; \tau)}{\Delta t}$$

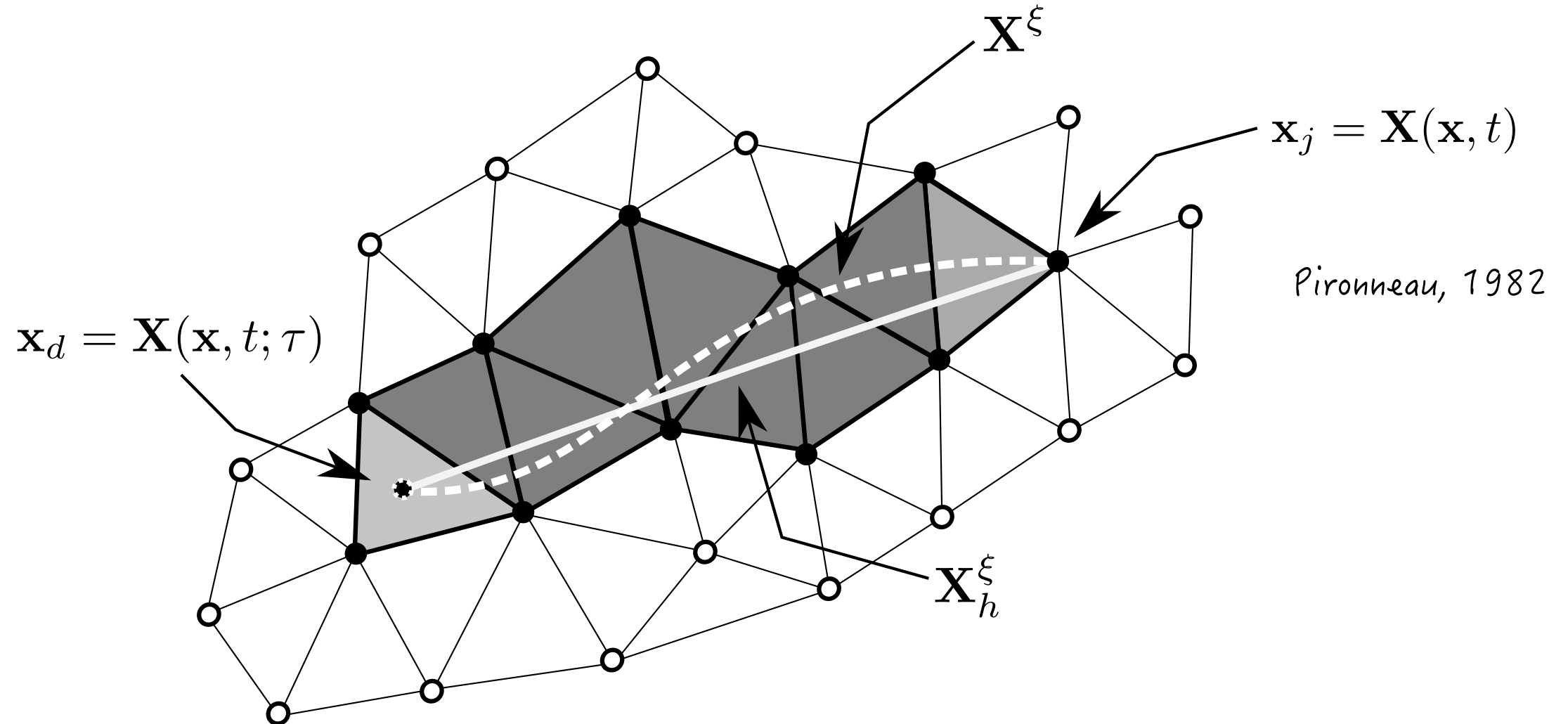
$\Phi$  : advected property

space-time scheme

Kaazempur-Mofrad, 2002



- Departure point search in ALE



Pironneau, 1982

$$(\mathbf{x}_d; \tau) = (\mathbf{x}_j; \tau) - (\mathbf{v} - \hat{\mathbf{v}})(\mathbf{x}_j) \Delta t, \quad \mathbf{x}_j \text{ of } T \in \mathcal{T}_h$$

ALE velocity taken into account for the backward integration

---

# 4. PBC

## (Periodic Boundary Conditions)

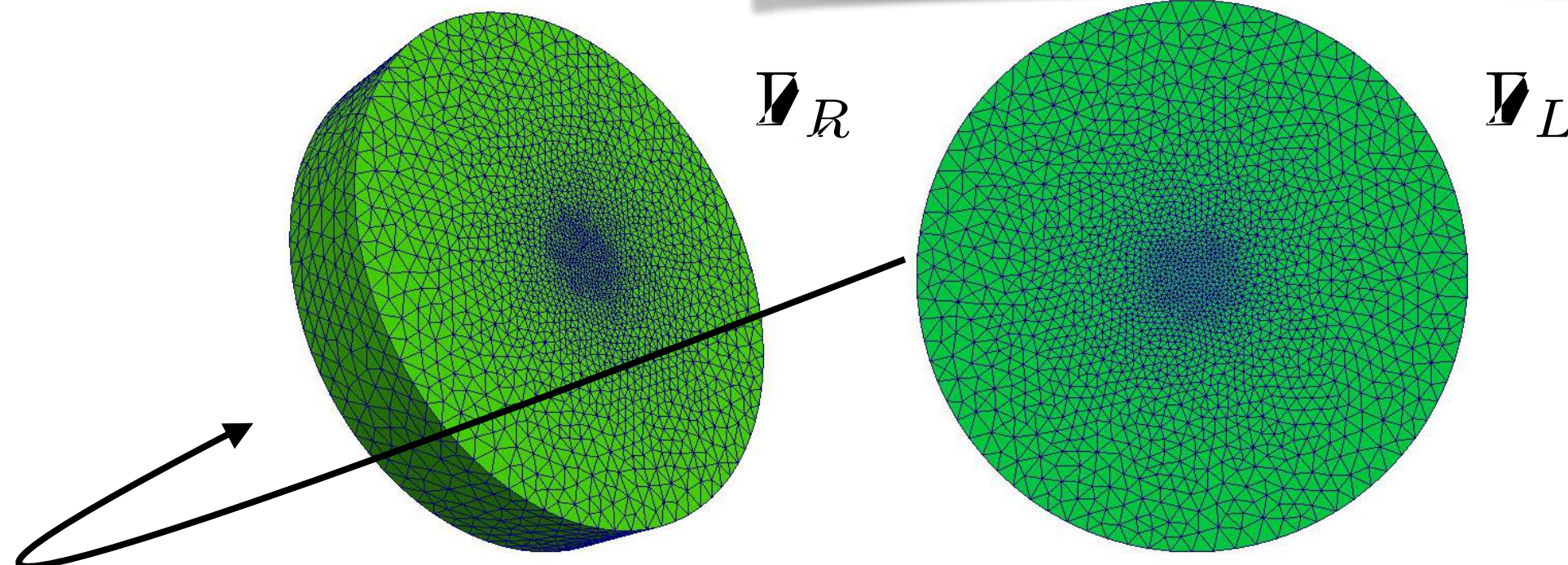
### implementation

# Periodic meshes

## script-based meshes

“master” & “slave” elements

$$\underline{x}_{\text{slave}} = \underline{x}_{\text{master}} + L_P \mathbf{e}_P$$



$$L_R \equiv L_L + \text{translation}$$

Periodic decomposition via the transformed variable approach

hypothesis: fully developed flow

$$\mathbf{v}|_{\Gamma_L} = \mathbf{v}|_{\Gamma_R}$$

$$\frac{\partial p}{\partial(\mathbf{x} \cdot \mathbf{e}_P)} \approx \frac{\Delta p}{L_P} = \frac{p|_{\Gamma_R} - p|_{\Gamma_L}}{L_P} = \beta$$

periodic pressure decomposition (PPD)

Patankar, 1977

Beale, 2007

$$p = -\beta(\mathbf{x} \cdot \mathbf{e}_P) + \tilde{p} \Rightarrow \tilde{p}|_{\Gamma_L} = \tilde{p}|_{\Gamma_R}$$

dimensionless form (dependent on the problem) Lahbabi, 1986

$$\beta^* = \frac{\beta L_{ref}}{\rho_{ref} U_{ref}^2} = \left( \frac{\beta}{\rho_{ref} U_{ref}^2} \right) L_{ref}$$

$\beta^* := Eu_{\beta^*}$  Euler  
modified

Oliveira &  
Mangiavacchi, 2013

# Variational formulation of the periodic forms

**strong form**

$$\left\{ \begin{array}{l} B_{1,P}(\mathbf{v}, \tilde{p}, \mathbf{f}; \hat{\mathbf{v}}, \rho, \mu, \mathbf{g}) = 0 \\ B_2(\mathbf{v}) = 0 \\ B_3(\Psi) = 0. \end{array} \right.$$

**unknowns:**  $(\mathbf{v}, \tilde{p}, \Psi)$  in  $\Omega \times \tau$

**PBC: Dirichlet & Neumann**

$$\mathbf{v}|_{\Gamma_L} = \mathbf{v}|_{\Gamma_R}$$

$$\mathbf{n}_L \cdot \nabla \mathbf{v}|_{\Gamma_L} = -\mathbf{n}_R \cdot \nabla \mathbf{v}|_{\Gamma_R}$$

$$\tilde{p}|_{\Gamma_L} = \tilde{p}|_{\Gamma_R}$$

$$\mathbf{n}_L \cdot \nabla \tilde{p}|_{\Gamma_L} = -\mathbf{n}_R \cdot \nabla \tilde{p}|_{\Gamma_R}$$

**PPD + INS**

$$B_{1,P}(\mathbf{v}, \tilde{p}, \mathbf{f}; \hat{\mathbf{v}}, \rho, \mu, \mathbf{g}) := \rho \left( \frac{\partial \mathbf{v}}{\partial t} + (\mathbf{v} - \hat{\mathbf{v}}) \cdot \nabla \mathbf{v} \right) - Eu_\beta \mathbf{e}_1 + \nabla \tilde{p} - \frac{1}{Re} \nabla \cdot [\mu (\nabla \mathbf{v} + \nabla \mathbf{v}^T)] - \frac{1}{Fr^2} \rho \mathbf{g} - \frac{1}{We} \mathbf{f} = \mathbf{0}$$

# periodic weight function spaces      Glowinski, 2006

$\mathcal{V}_P := \{\mathbf{w} \in \mathcal{H}_P^1(\Omega); \nabla \cdot \mathbf{v} = 0, \mathbf{v}(\mathbf{x}) = \mathbf{v}(\mathbf{x} + L_P \mathbf{e}_P), \mathbf{x} \in \Gamma_L\}$       velocity

$\mathcal{Q}_P := \{q \in \mathcal{L}_P^2(\Omega); q(\mathbf{x}) = q(\mathbf{x} + L_P \mathbf{e}_P), \mathbf{x} \in \Gamma_L\}$       pressure

$\mathcal{R}_P := \{r \in \mathcal{L}_P^2(\Omega); r(\mathbf{x}) = r(\mathbf{x} + L_P \mathbf{e}_P), \mathbf{x} \in \Gamma_L\}.$       scalar

## weak form

$$\left\{ \begin{array}{l} \int_{\Omega} \mathsf{B}_{1,P}(\mathbf{v}_P, \tilde{p}, \mathbf{f}; \hat{\mathbf{v}}, \rho, \mu, \mathbf{g}) \cdot \mathbf{w}_P d\Omega = 0 \\ \int_{\Omega} \mathsf{B}_{2,P}(\mathbf{v}_P) \cdot q_P d\Omega = 0 \quad (\mathbf{v}_P, q_P, r_P) \in (\mathcal{V}_P, \mathcal{Q}_P, \mathcal{R}_P) \\ \int_{\Omega} \mathsf{B}_{3,P}(\Psi_P) \cdot r_P d\Omega = 0 \end{array} \right.$$

bilinear forms + Galerkin + space-time discretization +  
backward-in-time semi-lagrangian

$$m_{\rho,P}(\rho; \mathbf{v}_{h,P}^{n+1}, \mathbf{w}_{h,P}) + \frac{\Delta t}{Re^{1/2}} k_P(\mu; \nabla \mathbf{v}_{h,P}^{n+1}, \nabla \mathbf{w}_h) + \Delta t g_P(\tilde{p}_h^{n+1}, \nabla \cdot \mathbf{w}_{h,P}) = \Delta t \mathbf{r}_{h,P}^n$$

$$d_P(\mathbf{v}_{h,P}^{n+1}, \nabla \cdot q_{h,P}) = 0$$

with  $\mathbf{r}_{h,P}^n = m_{\rho,P}(\rho; \mathbf{v}_{h,d,P}^n, \mathbf{w}_{h,P}) + m_{\rho,P}(\rho; \mathbf{g}_h^n, \mathbf{w}_{h,P}) +$

$$+ \lambda Eu\beta m_P(\varphi_{h,P}^n \mathbf{e}_P, \mathbf{w}_{h,P}) + \boxed{\frac{1}{We} (\mathbf{f}_{\sigma h}^n, \mathbf{w}_{h,P})}$$

$$\psi_{h,P}^n \mathbf{e}_P, \mathbf{v}_h, \mathbf{w}_h \in \mathcal{V}_P^h \subset \mathcal{V}_P \text{ and } \tilde{p}_h, q_{h,P} \in \mathcal{Q}_P^h \subset \mathcal{Q}_P$$

NS equations

.....

$$m_{\Psi,P}(\Psi_{h,P}^{n+1}, r_{h,P}) + \frac{\Delta t}{ReSc} k_{\Psi,P}(\varrho; \nabla \Psi_{h,P}^{n+1}, \nabla r_{h,P}) = \Delta t m_{\Psi,P}(\Psi_{h,d,P}^n, r_{h,P})$$

$$\Psi_{h,P}, r_{h,P} \in \mathcal{R}_P^h \subset \mathcal{R}_P$$

advection-diffusion

cf.  
CSF  
model  
Brackbill, 1992

## Discrete matricial equations - ODE

$$\mathbf{M}_{\rho,P} \mathbf{v}_P^{n+1} + \frac{\Delta t}{Re} \mathbf{K}_P \mathbf{v}_P^{n+1}$$

$$+ \Delta t \mathbf{G}_P \tilde{\mathbf{p}}^{n+1} = \Delta t \left[ \mathbf{M}_{\rho,P} \mathbf{v}_{d,P}^n + \mathbf{M}_P \mathbf{b}^n + \frac{1}{Fr^2} \mathbf{M}_{\rho,P} \mathbf{g}^n + \frac{1}{We} \mathbf{M}_P \mathbf{f}^n \right]$$

$$\mathbf{D}_P \mathbf{v}_P^{n+1} = \mathbf{0}$$

$$\mathbf{M}_{\Psi,P} \Psi_P^{n+1} + \frac{\Delta t}{ReSc} \mathbf{K}_{\Psi,P} \Psi_P^{n+1} = \Delta t \mathbf{M}_{\Psi,P} \Psi_{d,P}^n$$

compact form

$$\left\{ \begin{array}{l} \mathbf{B}_P \mathbf{v}_P^{n+1} + \Delta t \mathbf{G}_P \tilde{\mathbf{p}}^{n+1} = \mathbf{b}_{1,P} \\ \mathbf{D}_P \mathbf{v}_P^{n+1} = \mathbf{b}_{2,P} \\ \mathbf{B}_{\Psi,P} \Psi_P^{n+1} = \mathbf{b}_{3,P} \end{array} \right. \quad n = 0, 1, 2, \dots, N$$

# Computational implementation on matrices

## FE model-matrix assembled à la Neumann

$$\mathcal{A}(i, j; m)[\cdot] = \begin{bmatrix} \ddots & | & \vdots & | & \vdots & | & \vdots & | & \vdots \\ \hline - & b_{(i+mv, i+mv)} & - & 0 & - & \star & - & 0 & - & ibL \\ \vdots & | & \ddots & | & \vdots & | & \vdots & | & \vdots \\ \hline - & 0 & - & b_{(j+mv, j+mv)} & - & 0 & - & \bullet & - & ibR \\ \vdots & | & \vdots & | & \ddots & | & \vdots & | & \vdots \\ \hline - & \star & - & 0 & - & \triangle & - & 0 & - & ibL_N \\ \vdots & | & \vdots & | & \vdots & | & \ddots & | & \vdots \\ \hline - & 0 & - & \bullet & - & 0 & - & \diamond & - & ibR_N \\ \vdots & | & \vdots & | & \vdots & | & \vdots & | & \ddots \end{bmatrix}$$

## overloading rows/columns in the model-matrix

$$\mathcal{A}_P(i, j; m)[\cdot] = \begin{bmatrix} \ddots & | & \vdots & | & \vdots & | & \vdots & | & \vdots \\ - & 1 & - & 0 & - & 0 & - & 0 & - & ibL \\ \vdots & | & \ddots & | & \vdots & | & \vdots & | & \vdots \\ - & 0 & - & \Sigma_P(i, j; m) & - & \star & - & \bullet & - & ibR \\ \vdots & | & \vdots & | & \ddots & | & \vdots & | & \vdots \\ - & 0 & - & \star & - & \Delta & - & 0 & - & ibL_N \\ \vdots & | & \vdots & | & \vdots & | & \ddots & | & \vdots \\ - & 0 & - & \bullet & - & 0 & - & \diamond & - & ibR_N \\ \vdots & | & \vdots & | & \vdots & | & \vdots & | & \ddots \end{bmatrix}$$

$$\Sigma_P(i, j; m) = b_{(i+mv, i+mv)} + b_{(j+mv, j+mv)}, \quad i, j = ibL, ibR; \quad m = 0, 1, 2.$$

## Computational implementation on vectors

FE model-vector loading B.Cs. and previous-time values

$$\mathcal{U}(i, j; m)[\cdot] = \begin{bmatrix} \vdots \\ c_{(i+mv)} \\ | \\ c_{(j+mv)} \\ \vdots \\ \square \\ | \\ * \\ \vdots \end{bmatrix} \quad \begin{array}{l} ibL \\ ibR \\ \dots \\ ibL_N \\ ibR_N \end{array} \quad m = 0, 1, 2,$$

## overloading rows in the model-vector

$$\mathcal{U}(i, j; m)[\cdot] = \begin{bmatrix} \vdots & \\ 0 & ibL \\ | & \\ \Sigma_P(i, j; m) & ibR \\ \vdots & \\ \square & ibL_N \\ | & \\ * & ibR_N \\ \vdots & \end{bmatrix} \quad m = 0, 1, 2,$$

$$\Sigma_P(i, j; m) = c_{(i+mv)} + c_{(j+mv)}, \quad i, j = ibL, ibR; \quad m = 0, 1, 2,$$

Leads to “eliminated” equations

elimination: overload + extra contribution

$$ibL: [1] \times [0] = [0]$$

$$ibR: [\mathbf{B}_{(ibL, ibL); P, x} + \mathbf{B}_{(ibR, ibR); P, x}] \times [\mathbf{v}_{ibL; P, x} + \mathbf{v}_{ibR; P, x}] + [\star_x] \times [\square_x] + [\bullet_x] \times [*_x]$$

remark: example for x-component

# Solution through projection method

NS global system

$$\mathbf{M}_{NS} \mathbf{v}_{NS} = \mathbf{b}_{NS}$$

$$\mathbf{M}_{NS} = \begin{bmatrix} \mathbf{B} & -\Delta t \mathbf{G} \\ \mathbf{D} & \mathbf{0} \end{bmatrix}; \quad \mathbf{v}_{NS} = \begin{bmatrix} \mathbf{v}^{n+1} \\ \mathbf{p}^{n+1} \end{bmatrix}; \quad \mathbf{b}_{NS} = \begin{bmatrix} \mathbf{r}^n \\ \mathbf{0} \end{bmatrix} + \begin{bmatrix} \mathbf{bc}_1 \\ \mathbf{bc}_2 \end{bmatrix}$$

.....

$$\begin{bmatrix} \mathbf{B} & \mathbf{0} \\ \mathbf{D} & \Delta t \mathbf{D} \mathbf{M}_{\rho,L}^{-1} \mathbf{G} \end{bmatrix} \begin{bmatrix} \mathbf{I} & -\Delta t \mathbf{M}_{\rho,L}^{-1} \mathbf{G} \\ \mathbf{0} & \mathbf{I} \end{bmatrix} \begin{bmatrix} \mathbf{v}^{n+1} \\ \mathbf{p}^{n+1} \end{bmatrix} = \begin{bmatrix} \mathbf{r}^n \\ \mathbf{0} \end{bmatrix} + \begin{bmatrix} \mathbf{bc}_1 \\ \mathbf{bc}_2 \end{bmatrix}$$

LU factorization

Chang, 2002

$$\begin{bmatrix} \mathbf{B} & \mathbf{0} \\ \mathbf{D} & \Delta t \mathbf{D} \mathbf{M}_{\rho,L}^{-1} \mathbf{G} \end{bmatrix} \begin{bmatrix} \mathbf{v}^\# \\ \mathbf{p}^{n+1} \end{bmatrix} = \begin{bmatrix} \tilde{\mathbf{b}}_1 \\ \mathbf{bc}_2 \end{bmatrix}; \quad \tilde{\mathbf{b}}_1 = \mathbf{r}^n + \mathbf{bc}_1$$

.....  
splitting of forces

$$\begin{bmatrix} \mathbf{I} & -\Delta t \mathbf{M}_{\rho,L}^{-1} \mathbf{G} \\ \mathbf{0} & \mathbf{I} \end{bmatrix} \begin{bmatrix} \mathbf{v}^{n+1} \\ \mathbf{p}^{n+1} \end{bmatrix} = \begin{bmatrix} \mathbf{v}^\# \\ \mathbf{p}^{n+1} \end{bmatrix}$$

Solve  $\mathbf{Bv}^\# = \tilde{\mathbf{b}}_1$ ;

$$\mathbf{v}_{corr}^\# = \mathbf{v}^\# + \Delta t e(\mathbf{g}, \mathbf{f}, Fr, We)$$

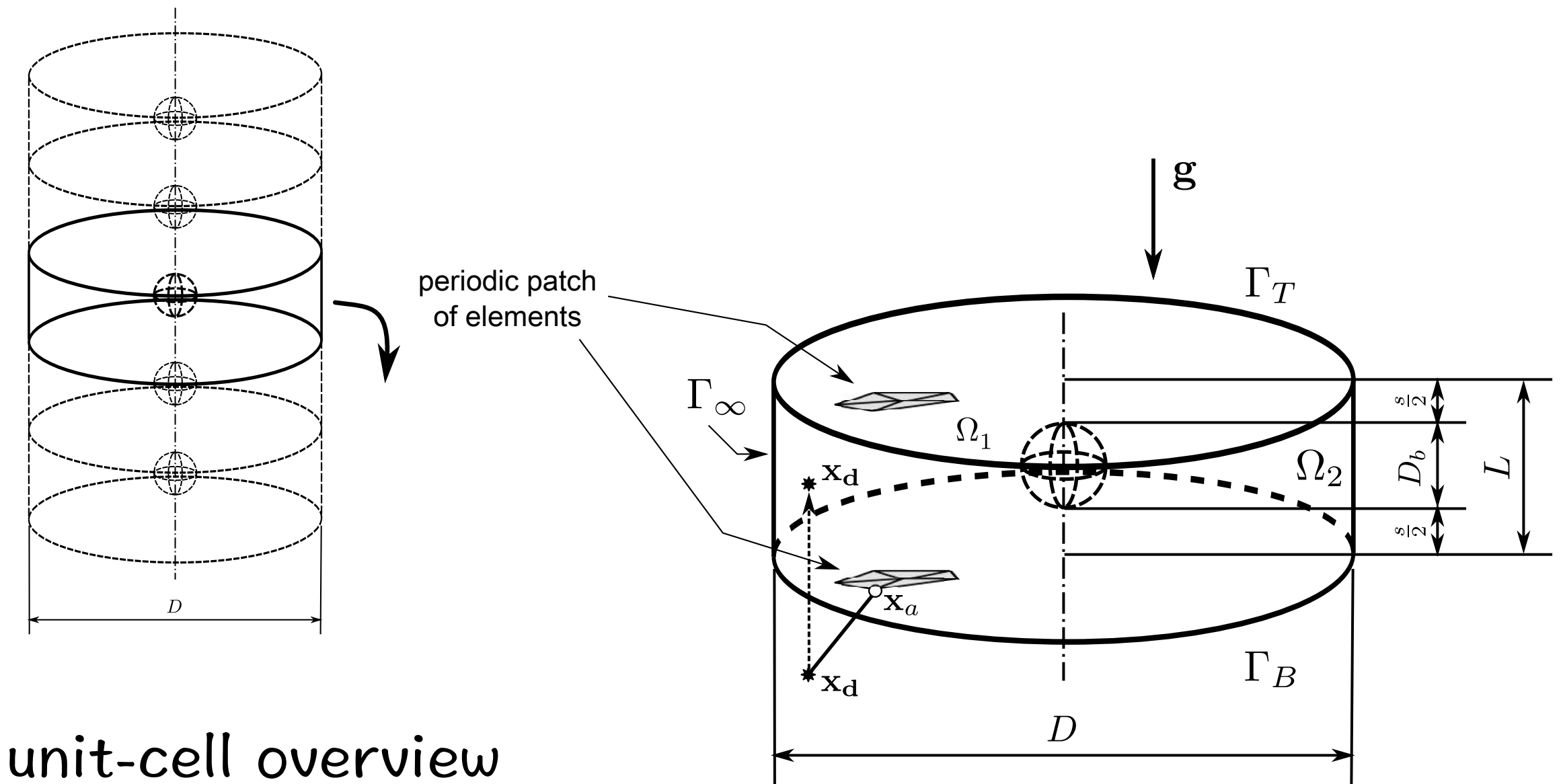
Solve  $\tilde{\mathbf{E}} \mathbf{p}^{n+1} = \tilde{\mathbf{b}}_2$ ; with  $\tilde{\mathbf{E}} = \Delta t \mathbf{D} \mathbf{M}_{\rho}^{-1} \mathbf{G}$ ;  $\tilde{\mathbf{b}}_2 = \tilde{\mathbf{b}}_2 - \mathbf{D} \mathbf{v}^\#$ ;

Correct  $\mathbf{v}^{n+1} = \mathbf{v}^\# + \Delta t \mathbf{M}_{\rho}^{-1} \mathbf{G} \mathbf{p}^{n+1}$ .

---

# 5. Validation of the methodology

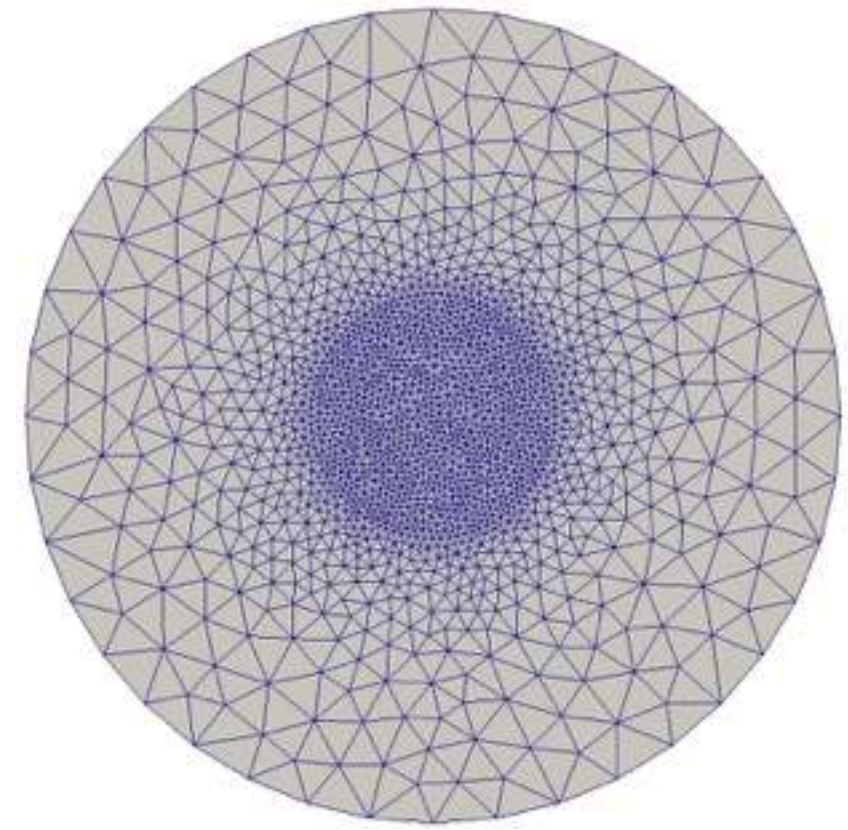
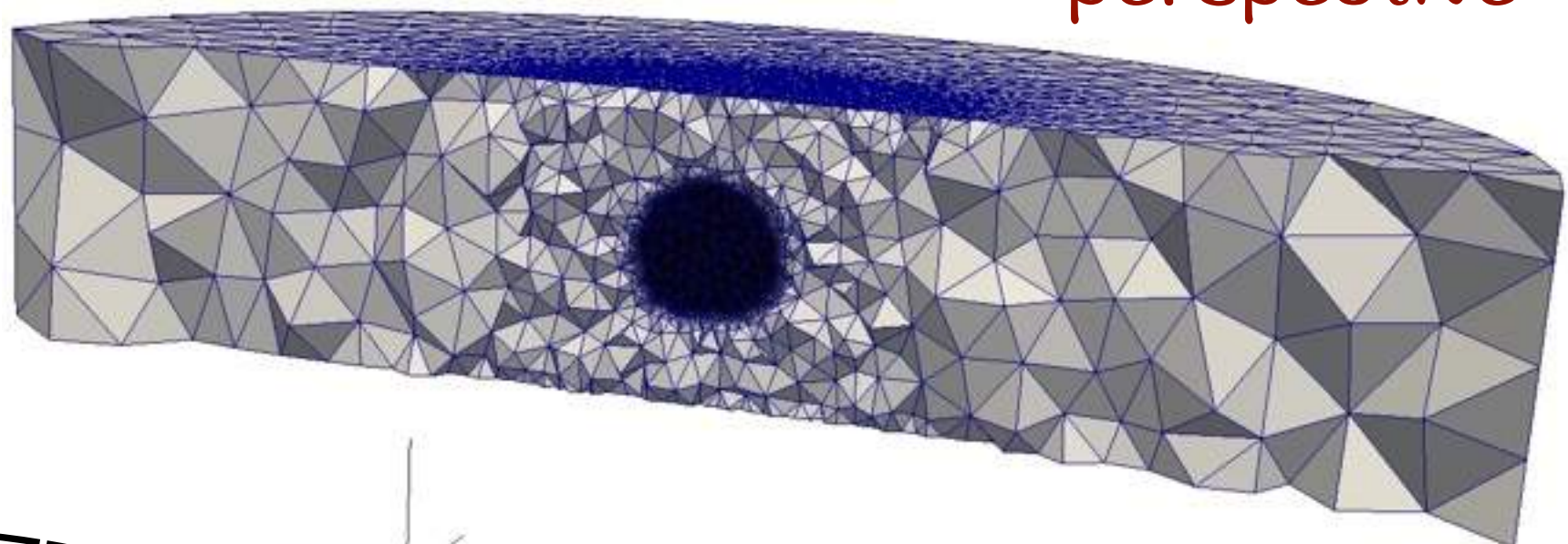
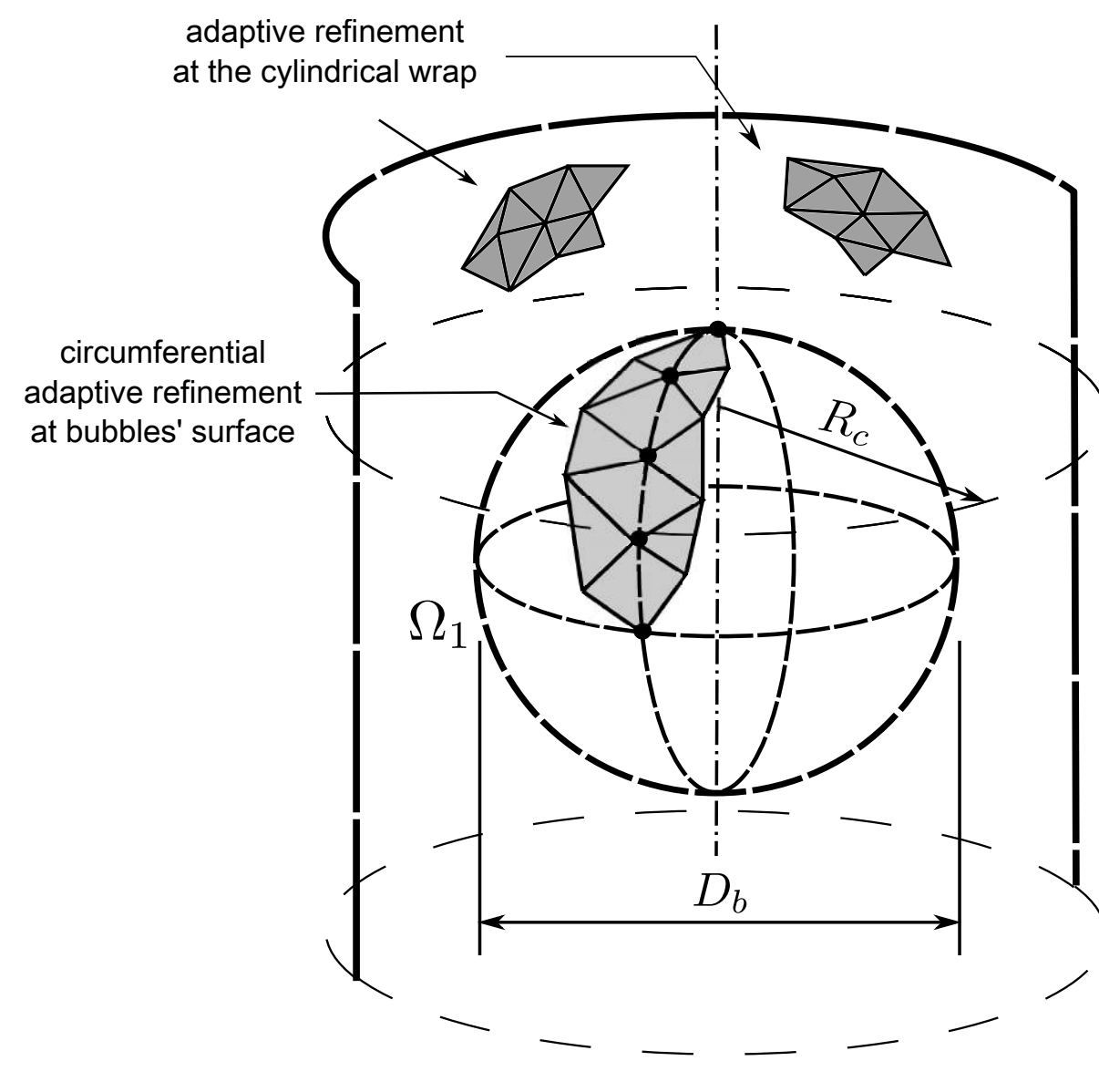
- Air bubble plume in pool of quiescent water (to appear on JBSME)



- Periodic cell mesh

perspective

adaptive  
refinement



top view

## • Model

Archimedes

$$\rho \frac{\hat{D}\mathbf{u}}{Dt} = \lambda Eu_\beta \mathbf{e}_P - \nabla \tilde{p} + \frac{1}{Ar^{1/2}} \nabla \cdot [\mu (\nabla \mathbf{u} + \nabla \mathbf{u}^T)] + \rho \mathbf{g} + \frac{1}{Eo} \mathbf{f}_\sigma$$

$$\nabla \cdot \mathbf{u} = 0, \quad \text{in } \Omega \times t,$$

Eotvos

$$p = -\lambda Eu_\beta (\mathbf{x} \cdot \mathbf{e}) + \tilde{p} \quad \text{ppd}$$

b.c.

$$\mathbf{u}|_{\Gamma_B} = \mathbf{u}|_{\Gamma^T} \quad \text{in } (0, t_{max}]$$

$$Eu_\beta = \frac{\beta_{ref}}{\rho_{ref} g_{ref}} \quad \text{Euler modified}$$

$$\mathbf{n} \cdot \nabla \mathbf{u}|_{\Gamma_B} = -\mathbf{n} \cdot \nabla \mathbf{u}|_{\Gamma^T} \quad \text{in } (0, t_{max}]$$

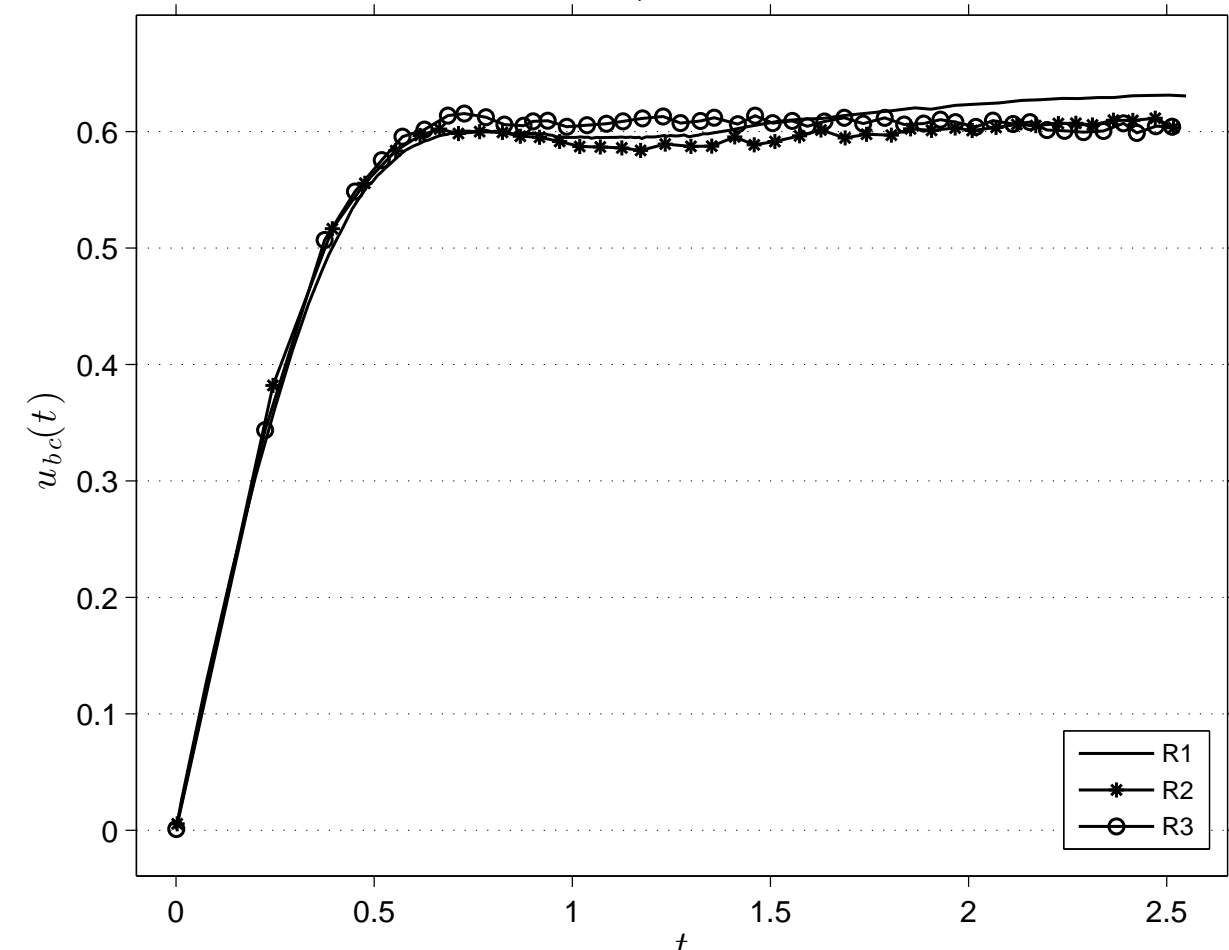
$$\tilde{p}|_{\Gamma_B} = \tilde{p}|_{\Gamma^T} \quad \text{in } (0, t_{max}]$$

$$\mathbf{n} \cdot \nabla \tilde{p}|_{\Gamma_B} = -\mathbf{n} \cdot \nabla \tilde{p}|_{\Gamma^T} \quad \text{in } (0, t_{max}]$$

$$\lambda = \frac{L_{ref}}{D_b} \quad \text{cell aspect ratio}$$

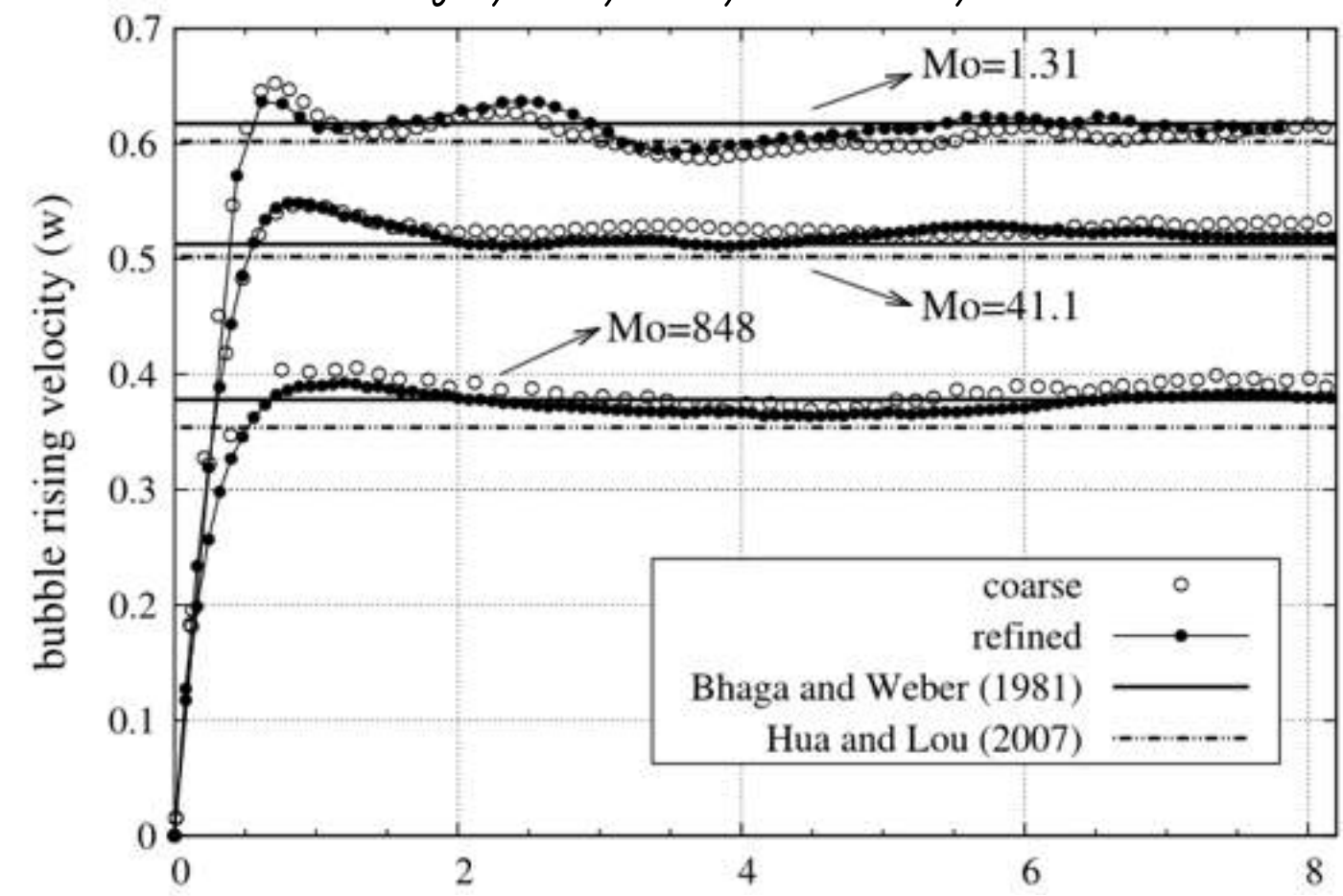
## Rising velocities

Oliveira, JBSME 2015



Data					
$\mu^1, \mu^2$	$\rho^1, \rho^2$	$\sigma$	$D_b$	$Ar$	$Eo$
1.78e-5, 0.54	1.22, 1350	7.8e-2	2.61e-2	1092	116

Anjos, JCP, 270, 366-377, 2014



$$\mathcal{E}_{Rj,R1} = \frac{100\%}{t_{max}} \left( \frac{v_{bc,j}(t) - v_{bc,1}(t)}{v_{bc,1}(t)} \right), \quad j = 2, 3, \text{ with}$$

$$v_{bc,i}(t) = \int_0^{t_{max}} u_{bc,i}(t) dt, \quad i = 1, 2, 3,$$

test R1: free rising + no-slip walls

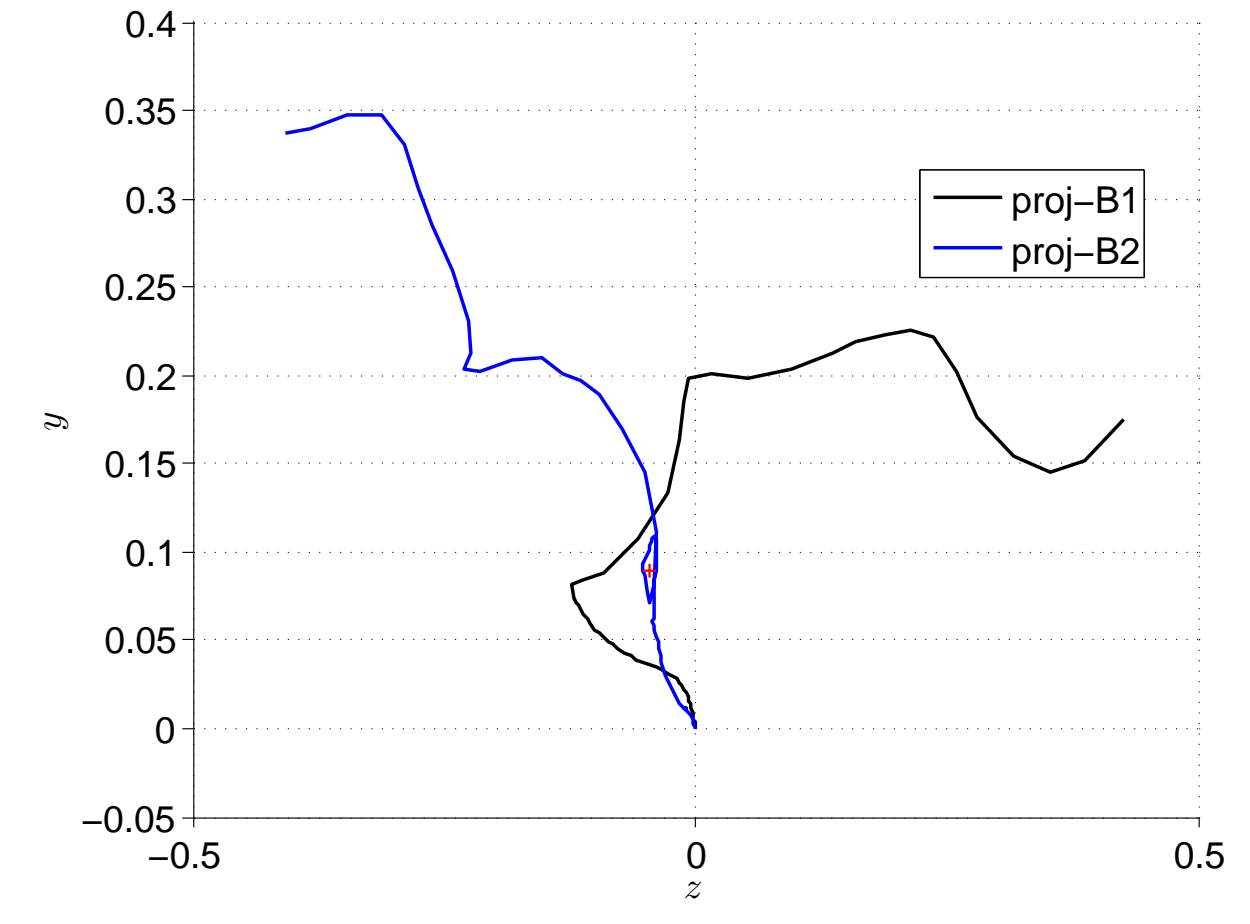
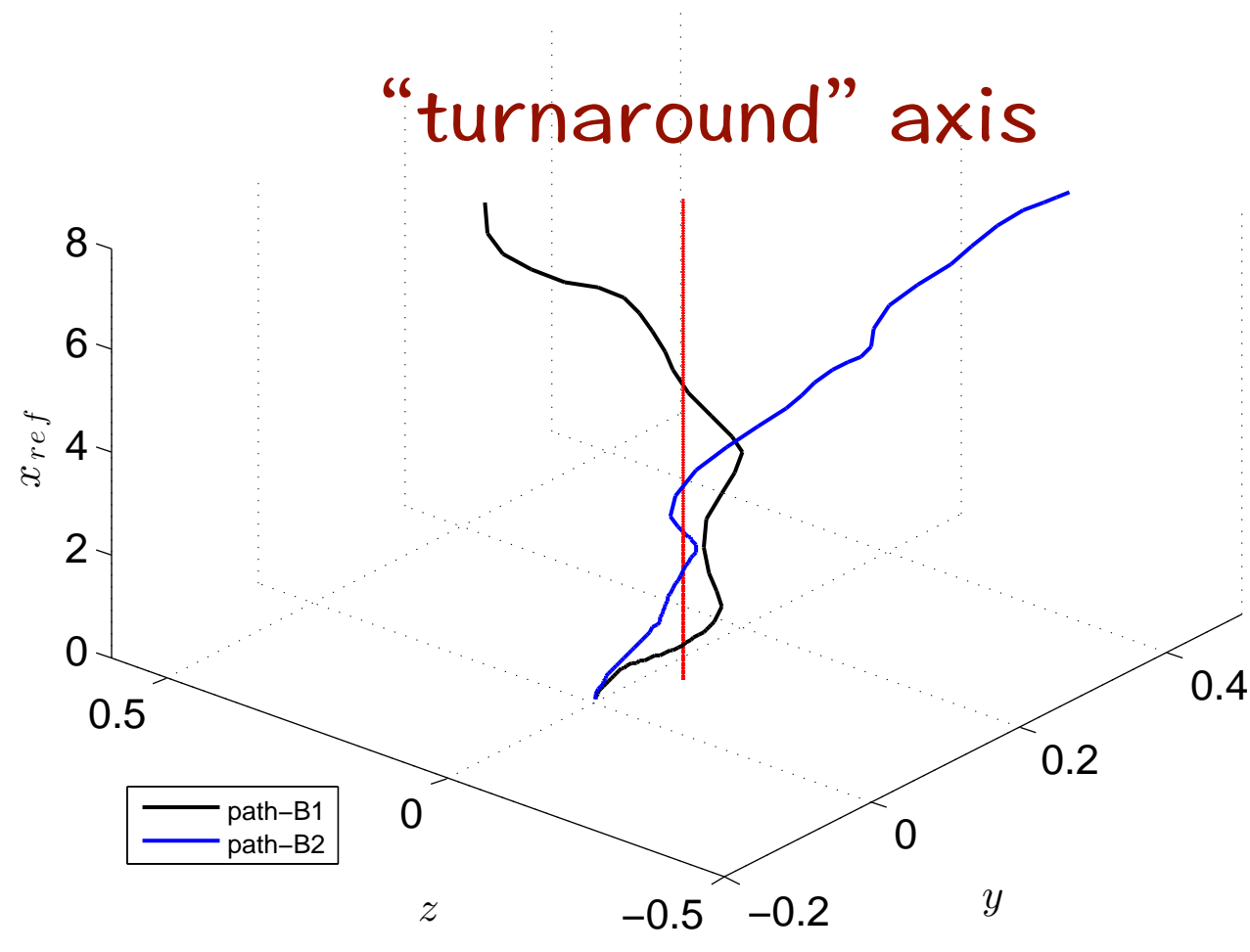
test R2: OBC (top/bottom) + gravity + Eu

test R3: moving-frame + PBC + gravity + Eu

$$\mathcal{E}_{R2,R1} = 3.97\%$$

$$\mathcal{E}_{R3,R1} = 3.51\%$$

- Path oscillation

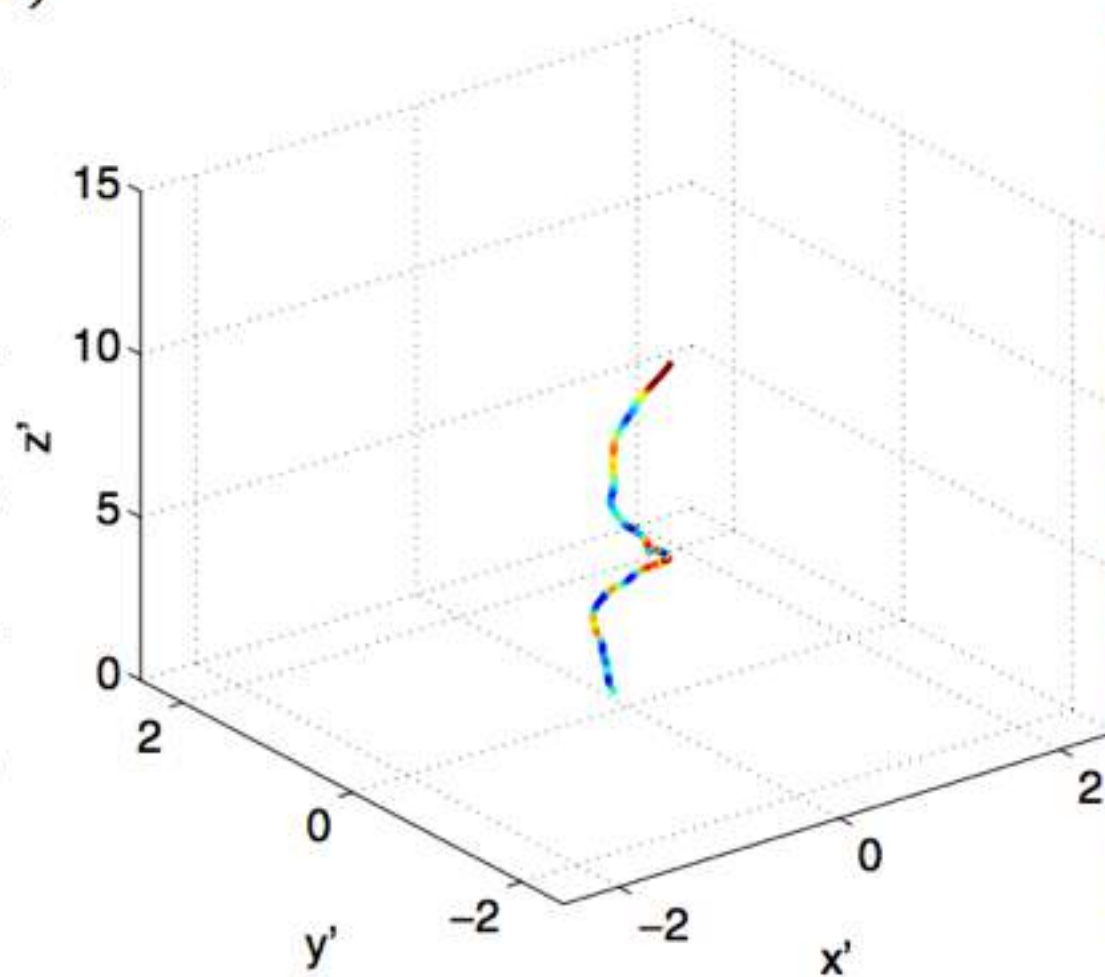


Case	$\mu^1, \mu^2$	$\rho^1, \rho^2$	$\sigma$	$D_b$	$Ar^{1/2}$	$Eo$
B1	18.2e-6, 958.08e-6	1.205, 998	0.0728	4e-3	824.96	2.15
B2	idem	idem	idem	5.2e-3	1222.8	3.63

Oliveira, 2014

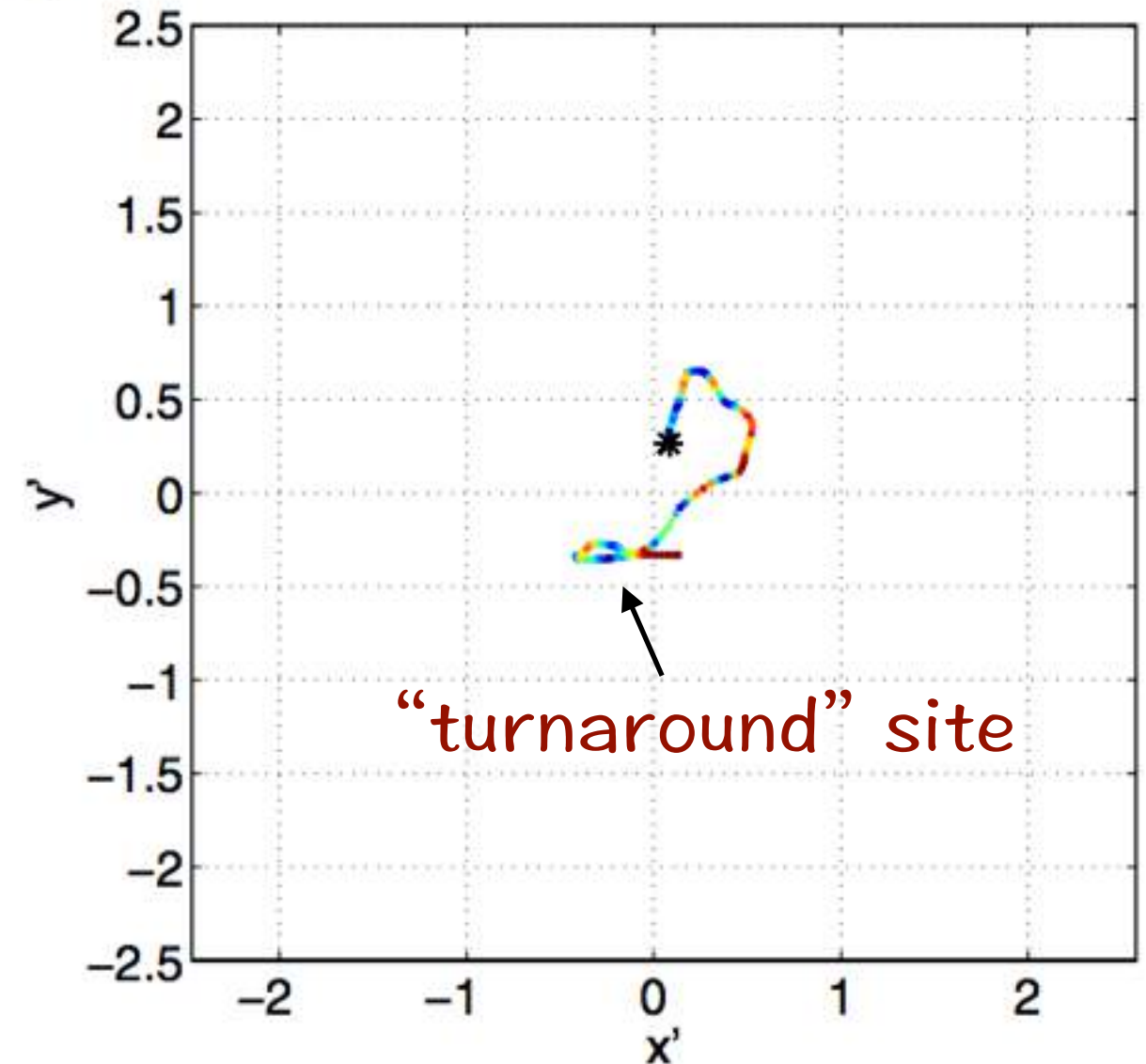
- Qualitative comparison

f)



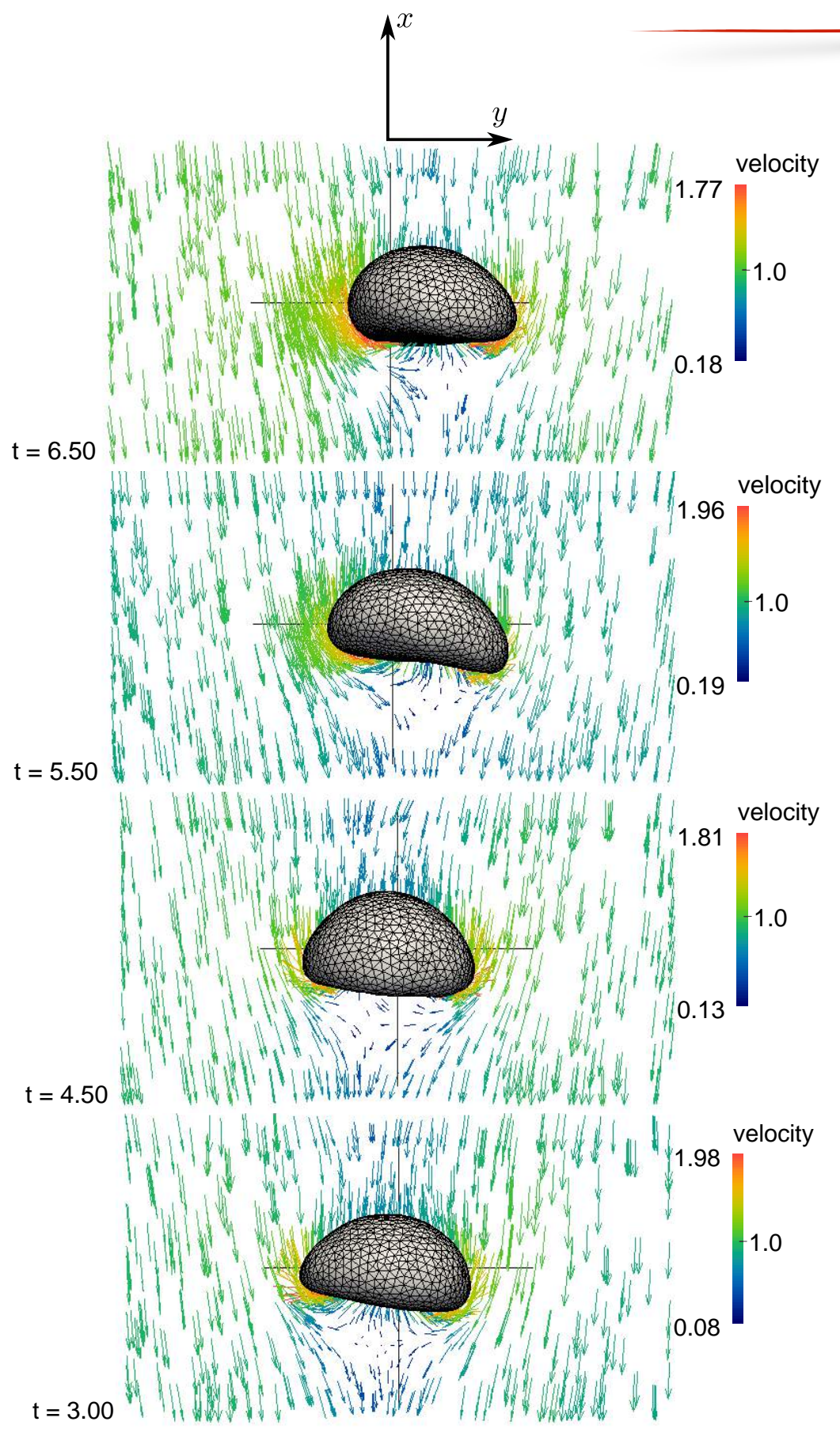
spatial path

f)

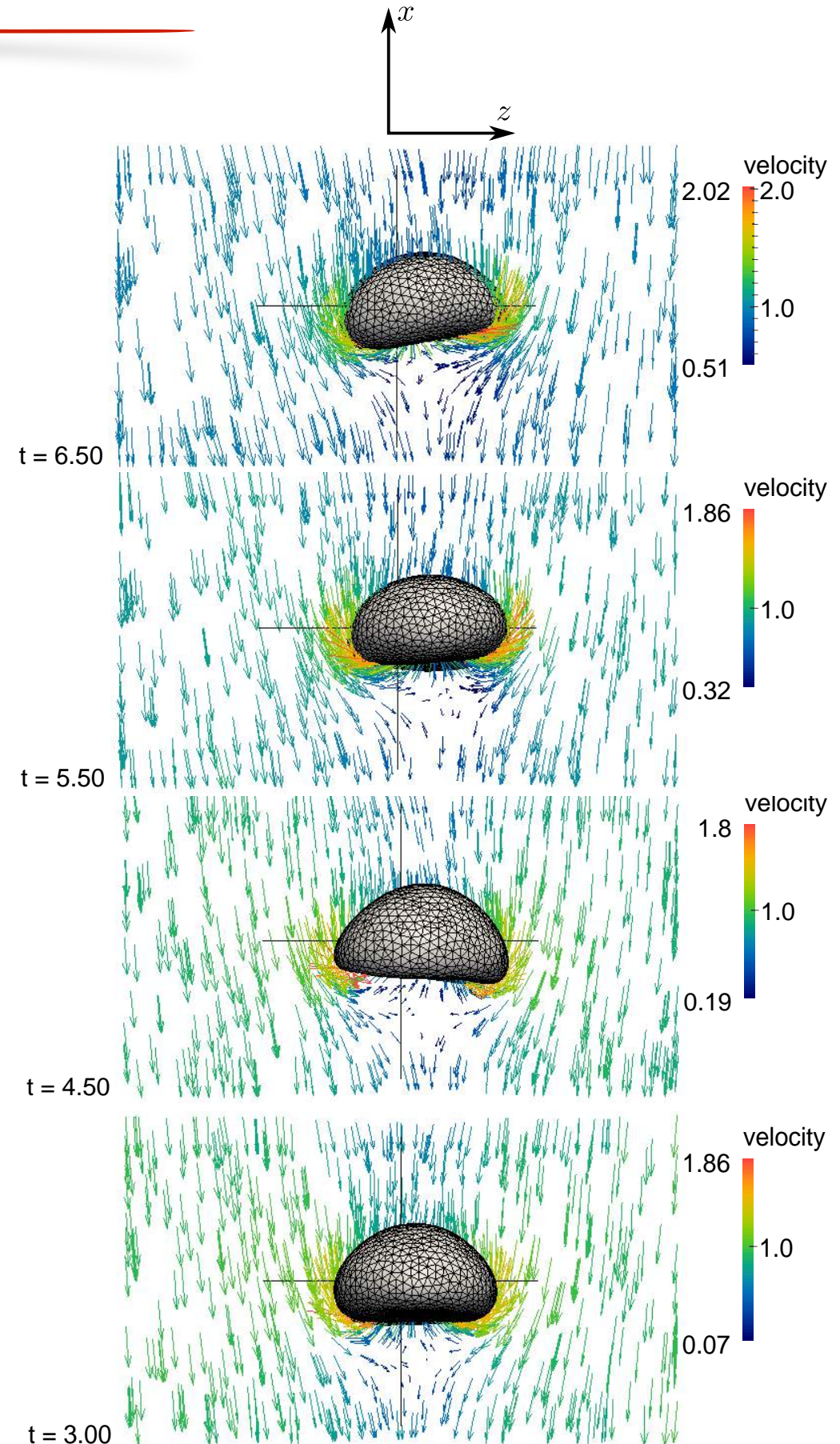


path projection

Veldhuis, 2008



## Hydrodynamics Test B1 - projection planes



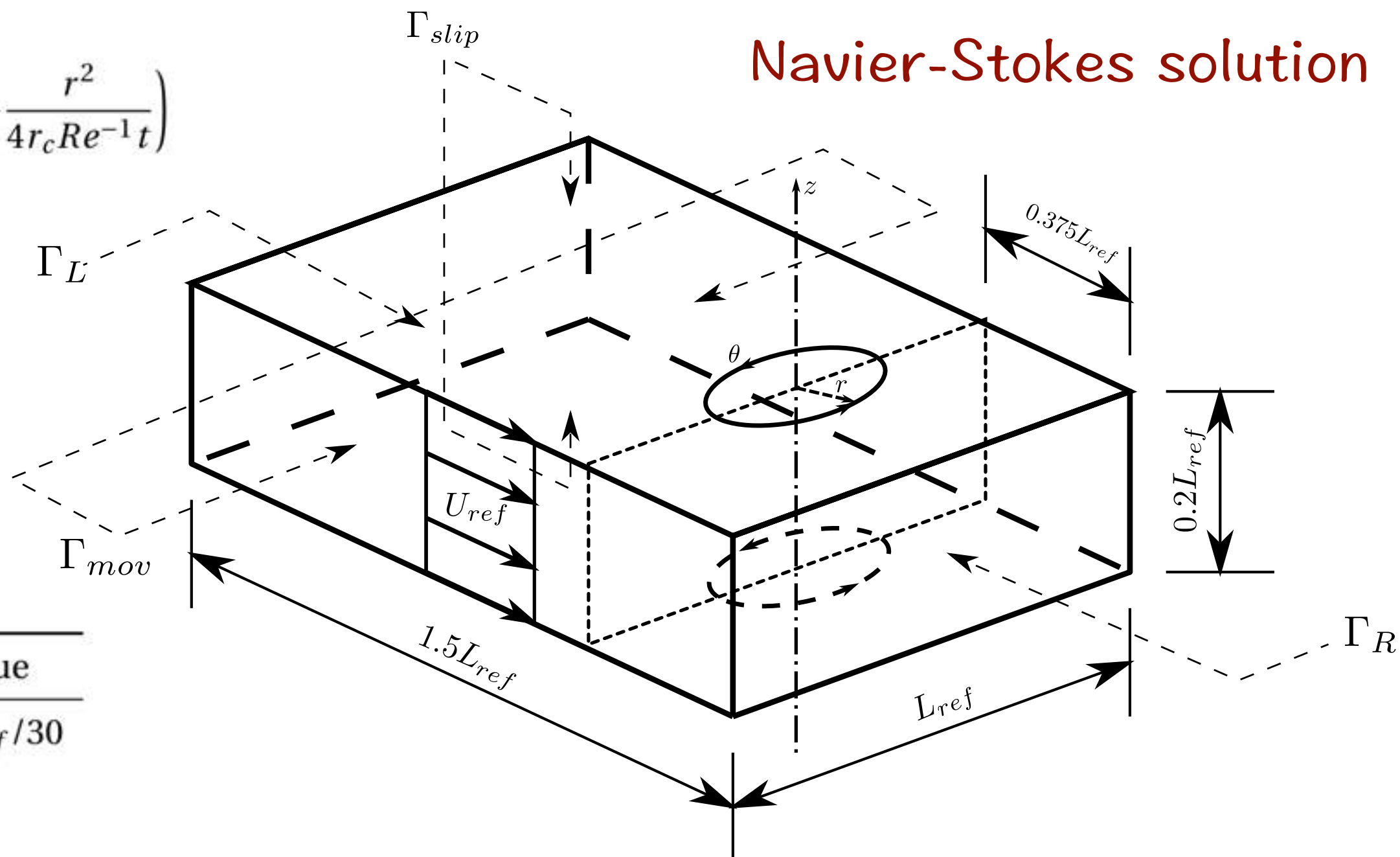
# Taylor's vortex: transport and scalar advection

$$v_r(t) = 0$$

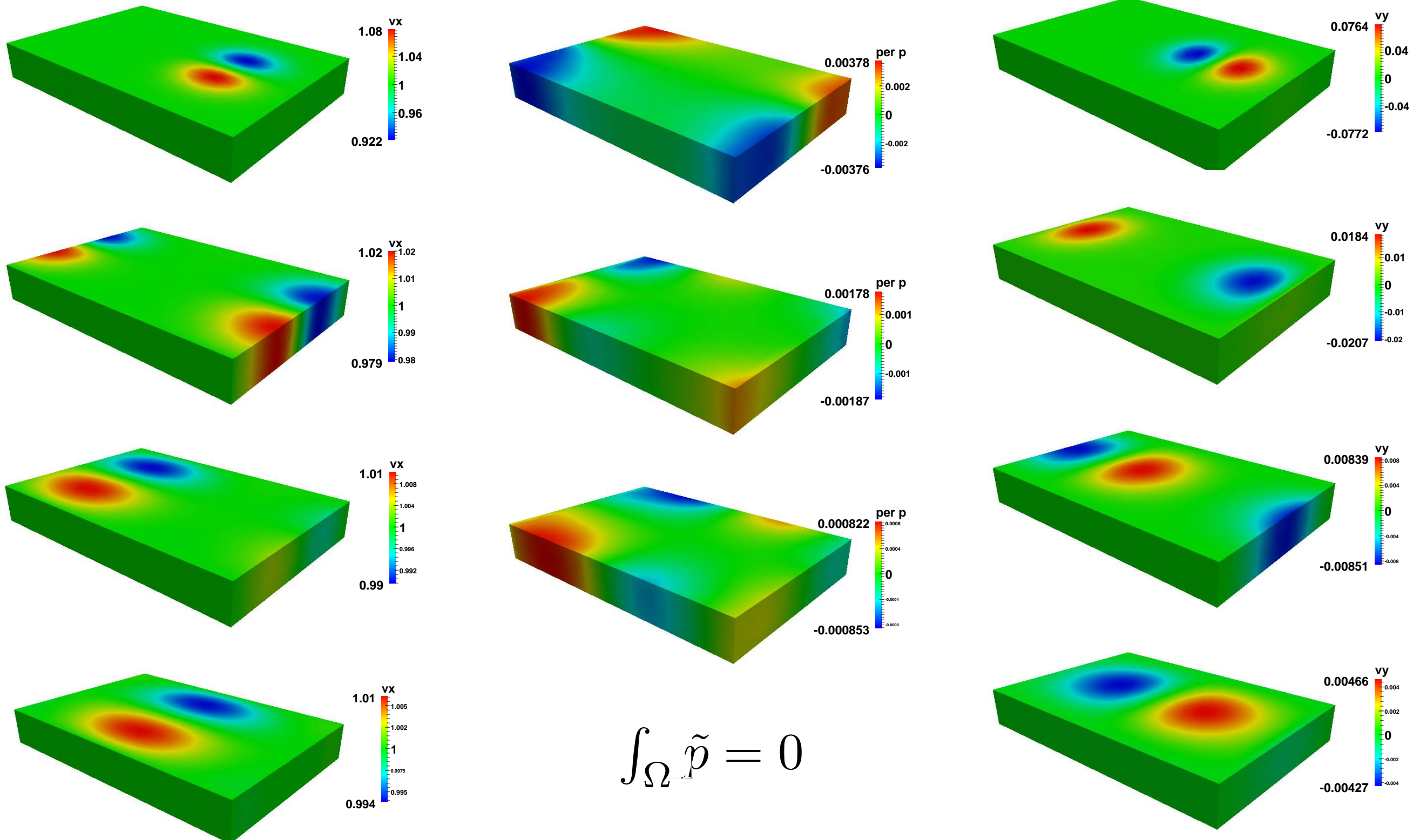
$$v_\theta(t) = \bar{\omega}r \exp\left(-\frac{r^2}{4r_c Re^{-1}t}\right)$$

$$v_z(t) = 0$$

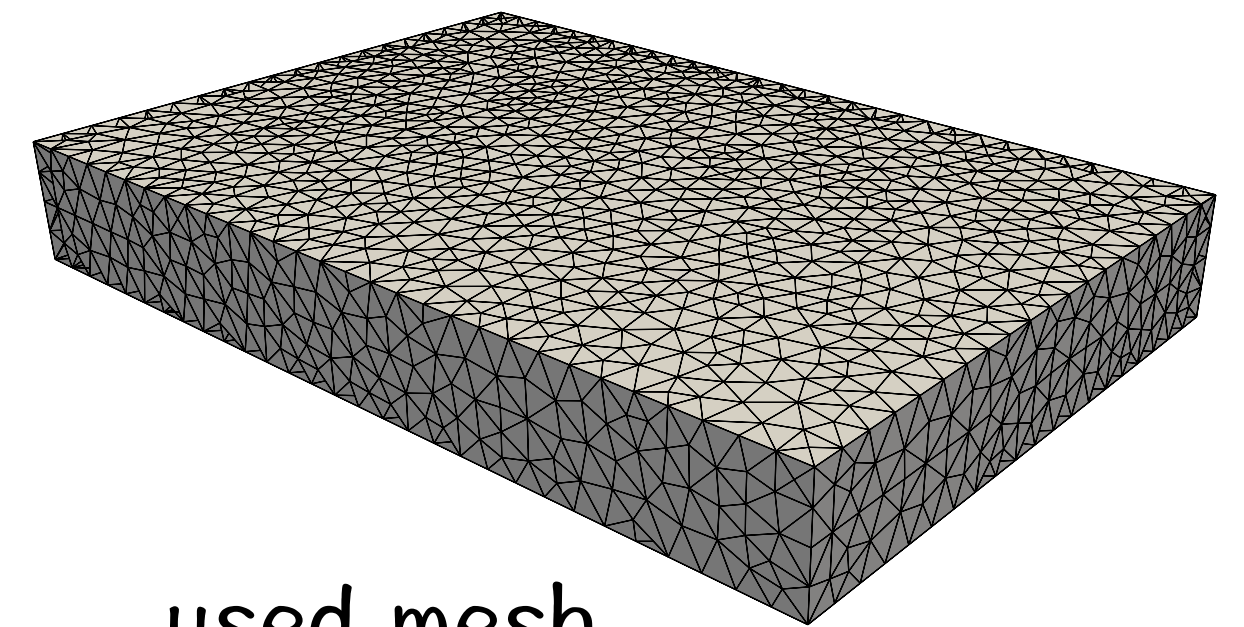
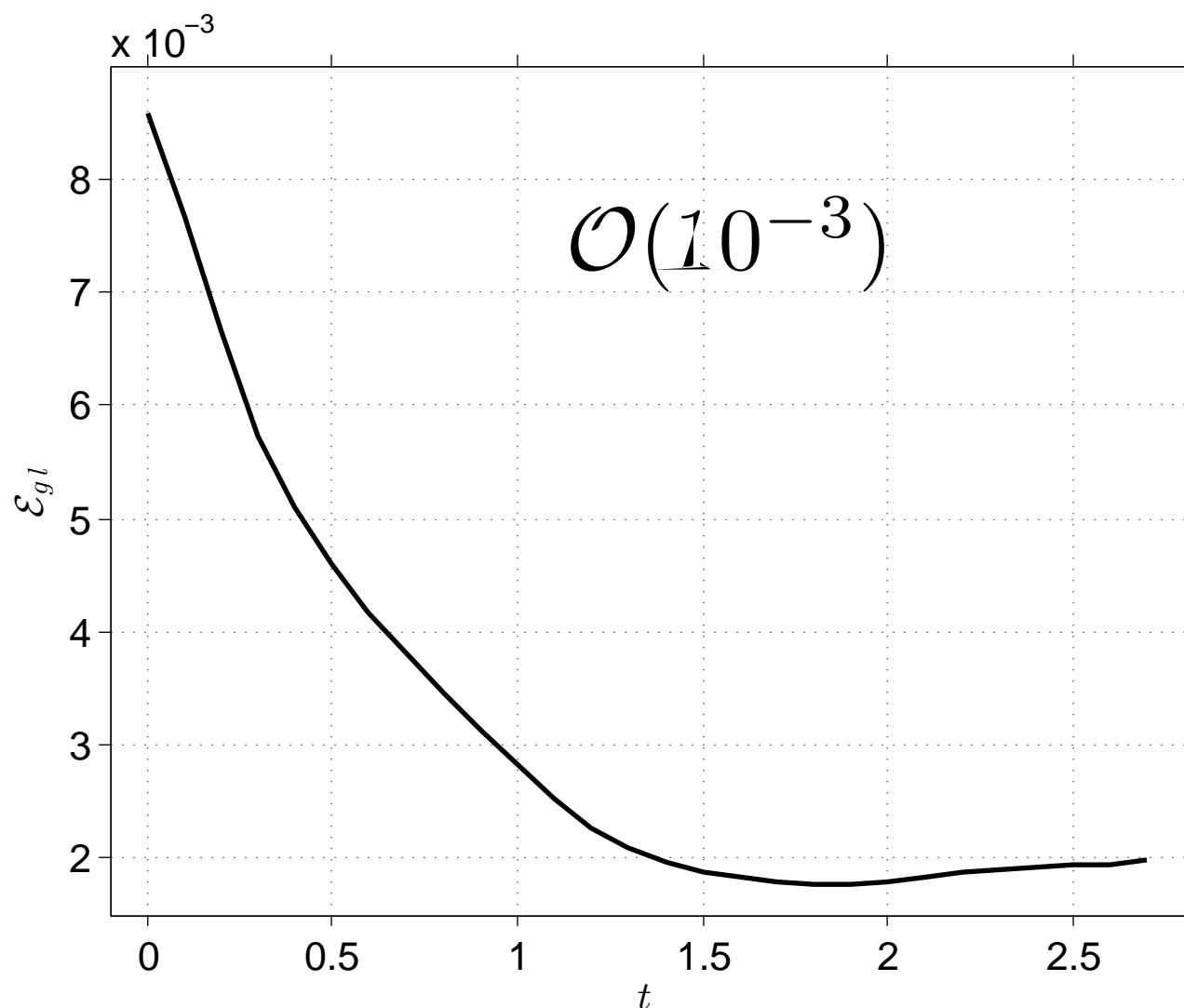
Parameter	Value
$r_c$	$L_{ref}/30$
$U_{ref}$	1
$\bar{\omega}$	1
$Re$	35
$Sc$	650
$\Delta t$	0.1



# Simulations



# Relative error



$$\mathbf{e}_{rel} = \left\{ \int_{\Omega} \frac{(\mathbf{v} - \mathbf{v}_h)^2}{\mathbf{v}_h^2} \right\}^{\frac{1}{2}}$$

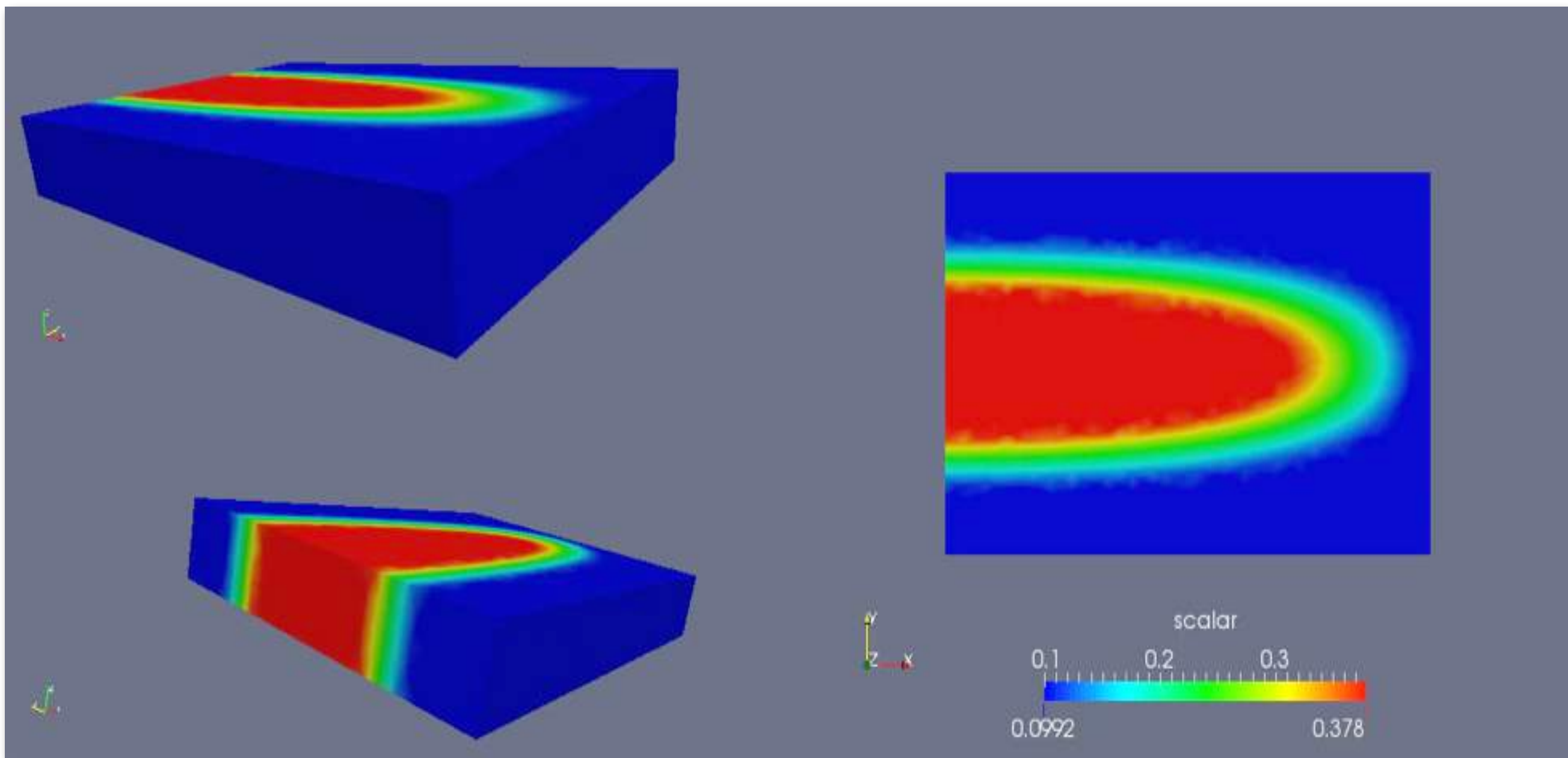
$\mathcal{L}_2$  – norm

# Scalar transport

$$\phi|_{\Gamma_L} = \phi|_{\Gamma_R}$$

$$\phi(\mathbf{x}) = a \exp \left[ -\frac{(\mathbf{x} \cdot \mathbf{e}_2 - \mathbf{x}_m)^2}{2b^2} \right] \cos(\mathbf{x} \cdot \mathbf{e}_1), \quad b = \frac{1}{2\pi}$$

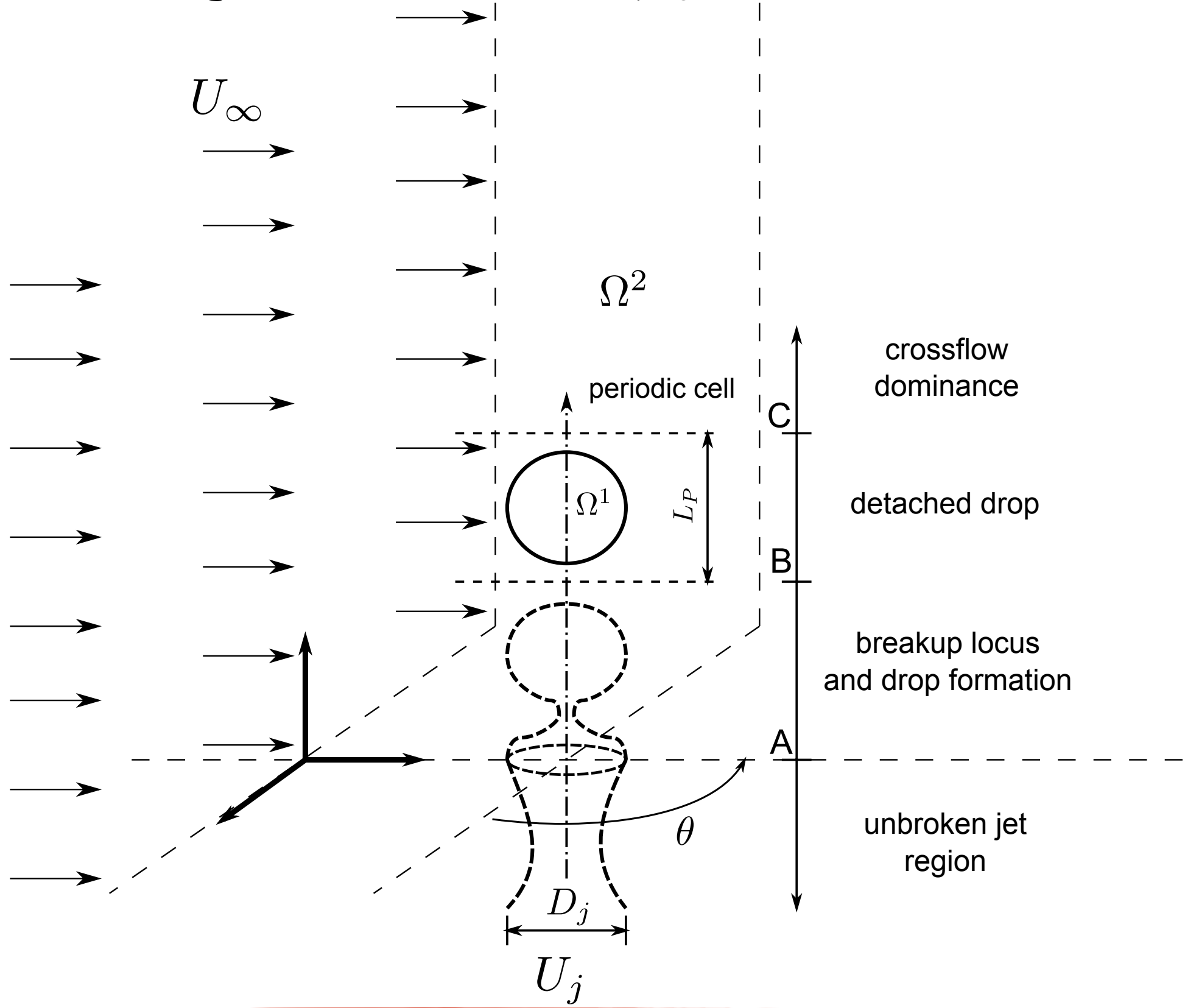
pulsating Gaussian profile



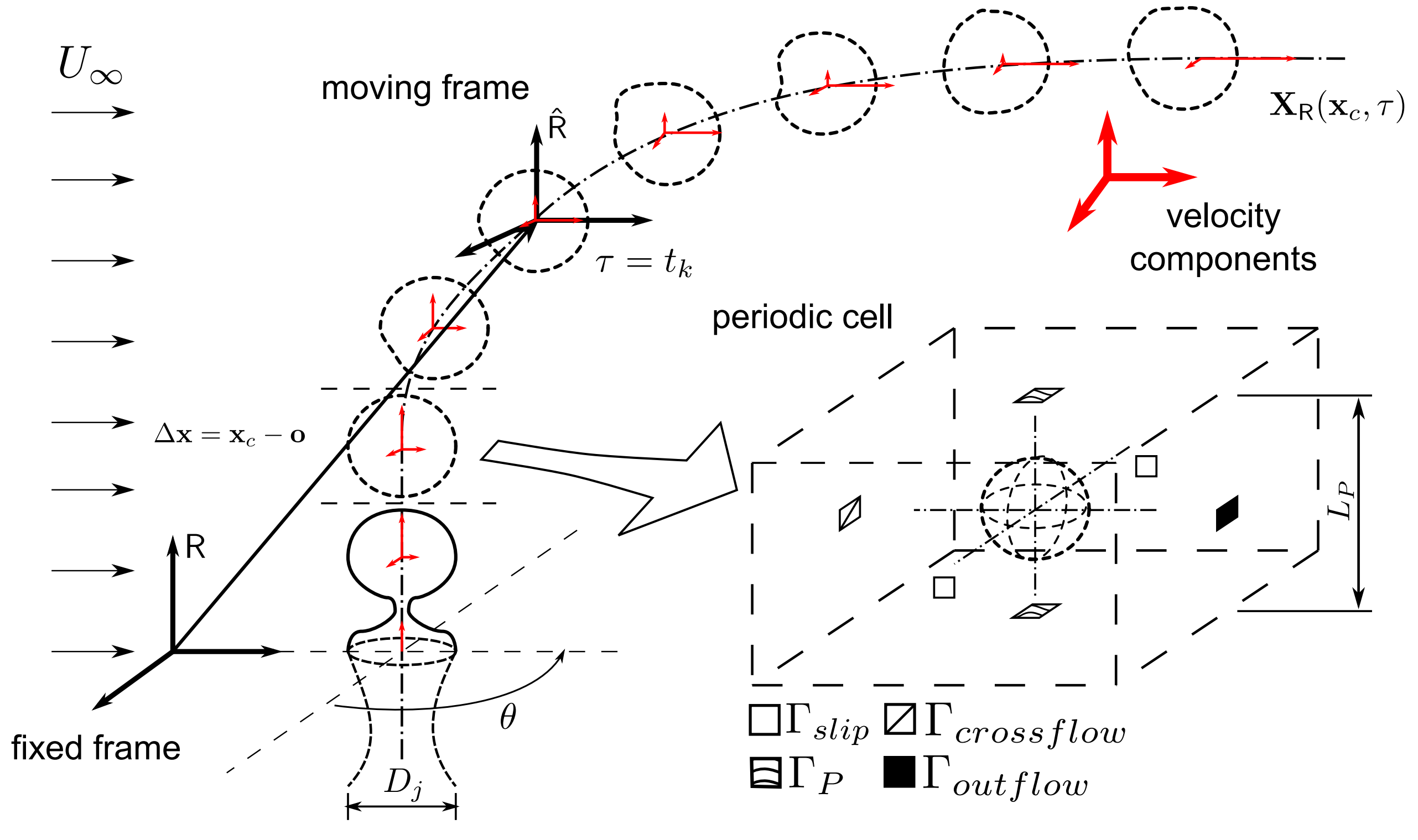
---

# 6. The DJICF problem and results

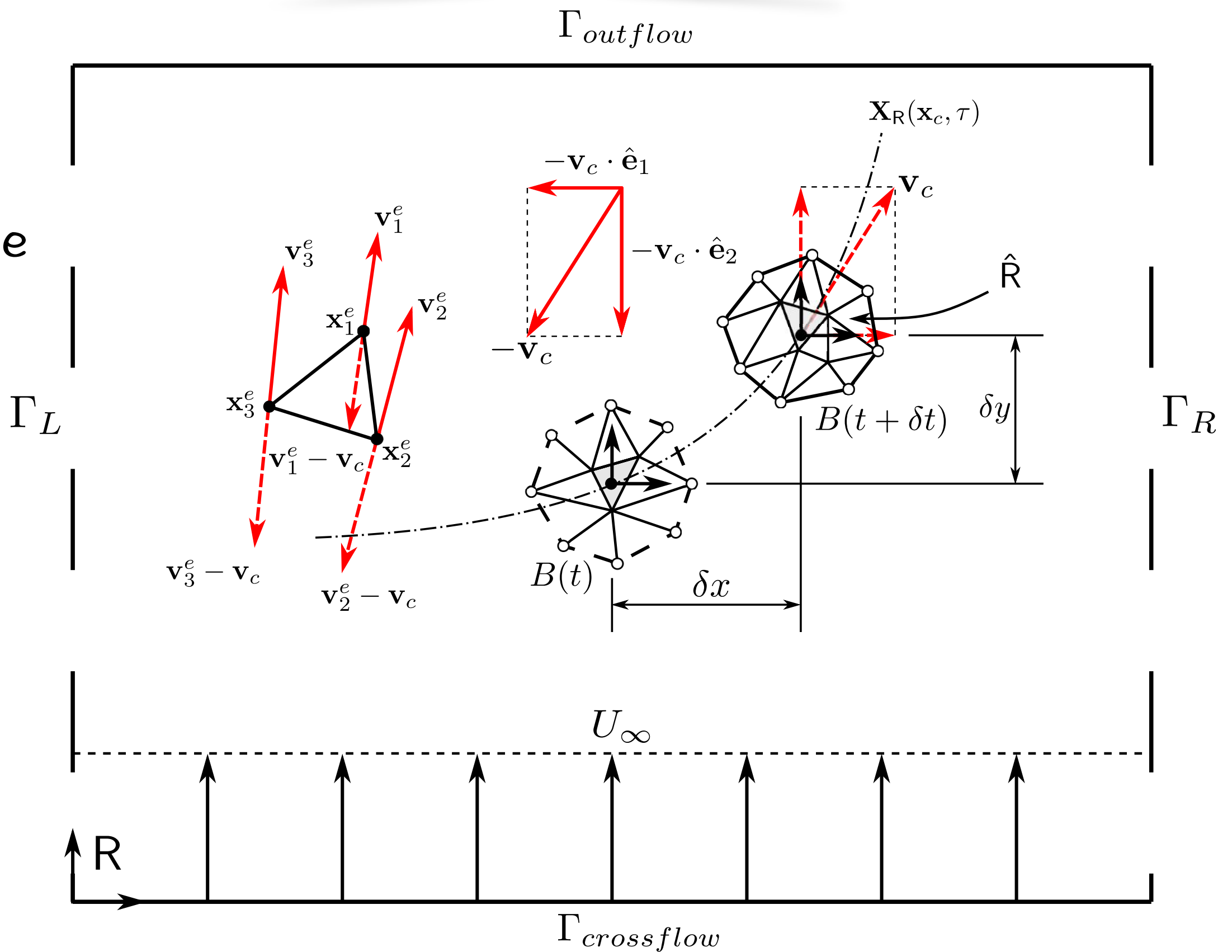
# The problem: arrangement of the drop jet



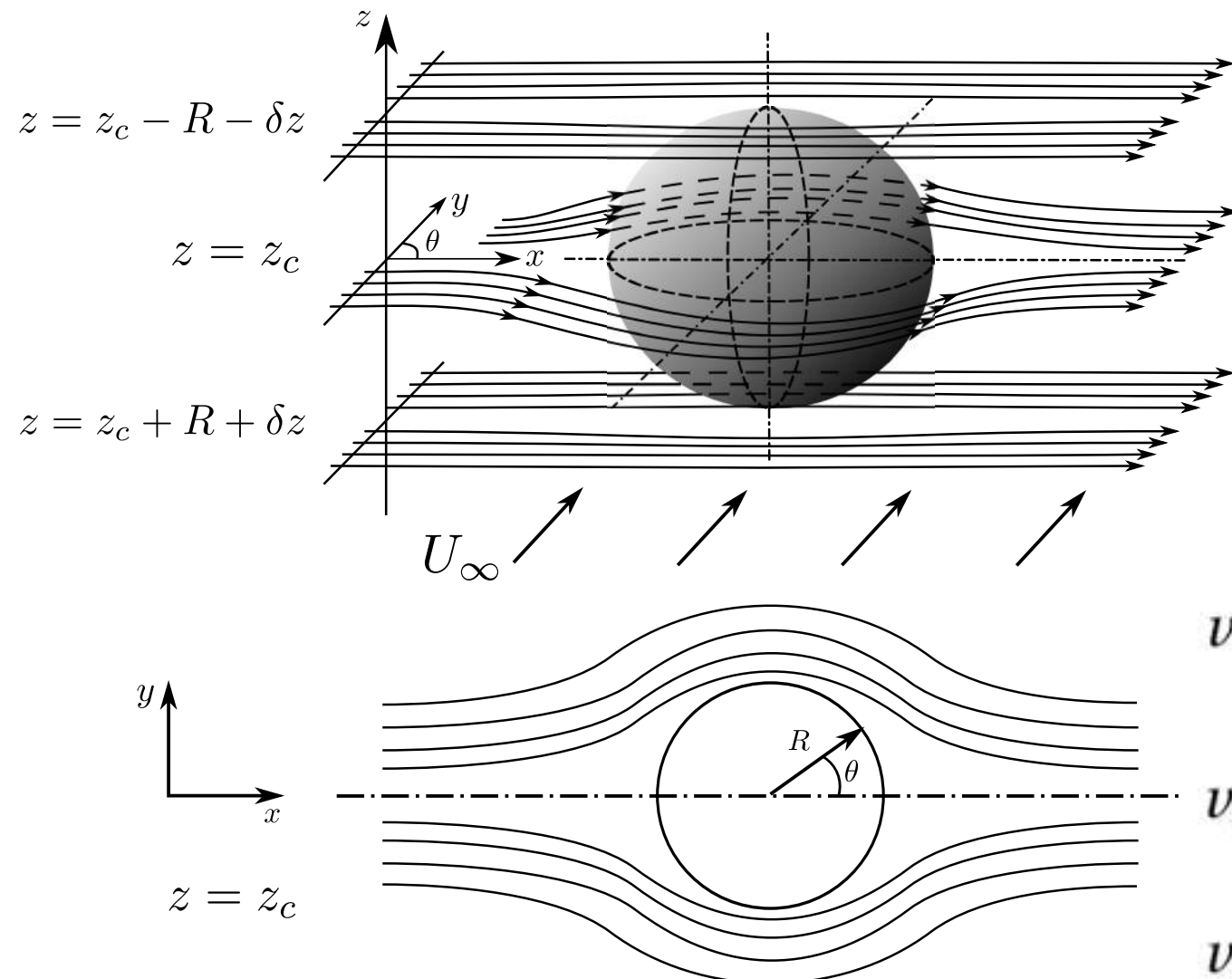
# Moving-frame technique



MFR  
2D  
scheme



- Initial condition



$$v_r = (U_j \cos(\theta) + U_\infty \sin(\theta)) \left[ 1 - \left( \frac{R}{r} \right)^2 \right] + U_{added}$$

$$v_\theta = (-U_j \sin(\theta) + U_\infty \cos(\theta)) \left[ 1 + \left( \frac{R}{r} \right)^2 \right]$$

$$v_z = 0,$$

# Study of cases

- Pair silicone oil/  
water-glycerine solution  
  
Webster & Longmire,  
book: Manipulation and Control of JICF, 2001
- Pair water-glycerine/  
n-heptane solution  
  
Meister & Scheele (Richards)  
AIChE Journ. 15:689-699, 1969 (1994)

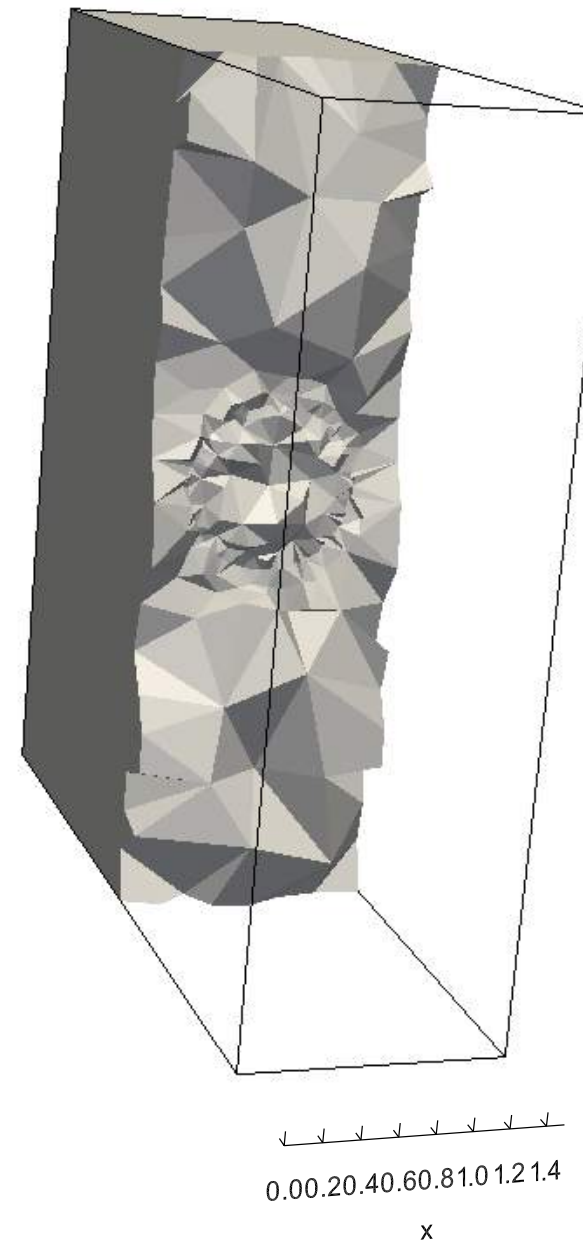
Data				
$\mu$	$\rho$	$D_j$	$Re$	$We$
2.43	1.45	0.68	1851	2.20

Data				
$\mu$	$\rho$	$Oh$	$Re$	$We^*$
0.15	1.18	0.013	50	0.80

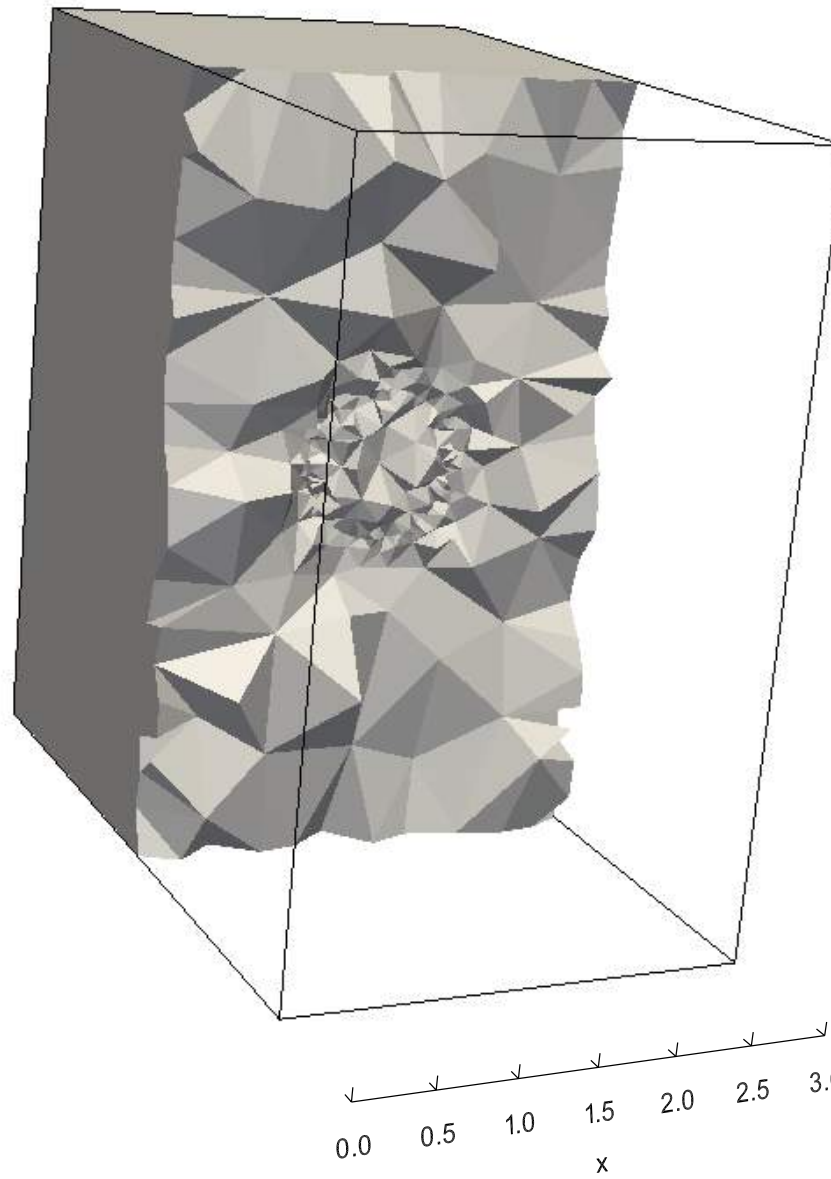
## configurations

$(Ref, L_P, \lambda)$ , for  $Ref = MS, WL$ ;  $L_P = 1.5, 3.0, 5.0$  and  $\lambda = 1.0, 1.5, 2.0$ .

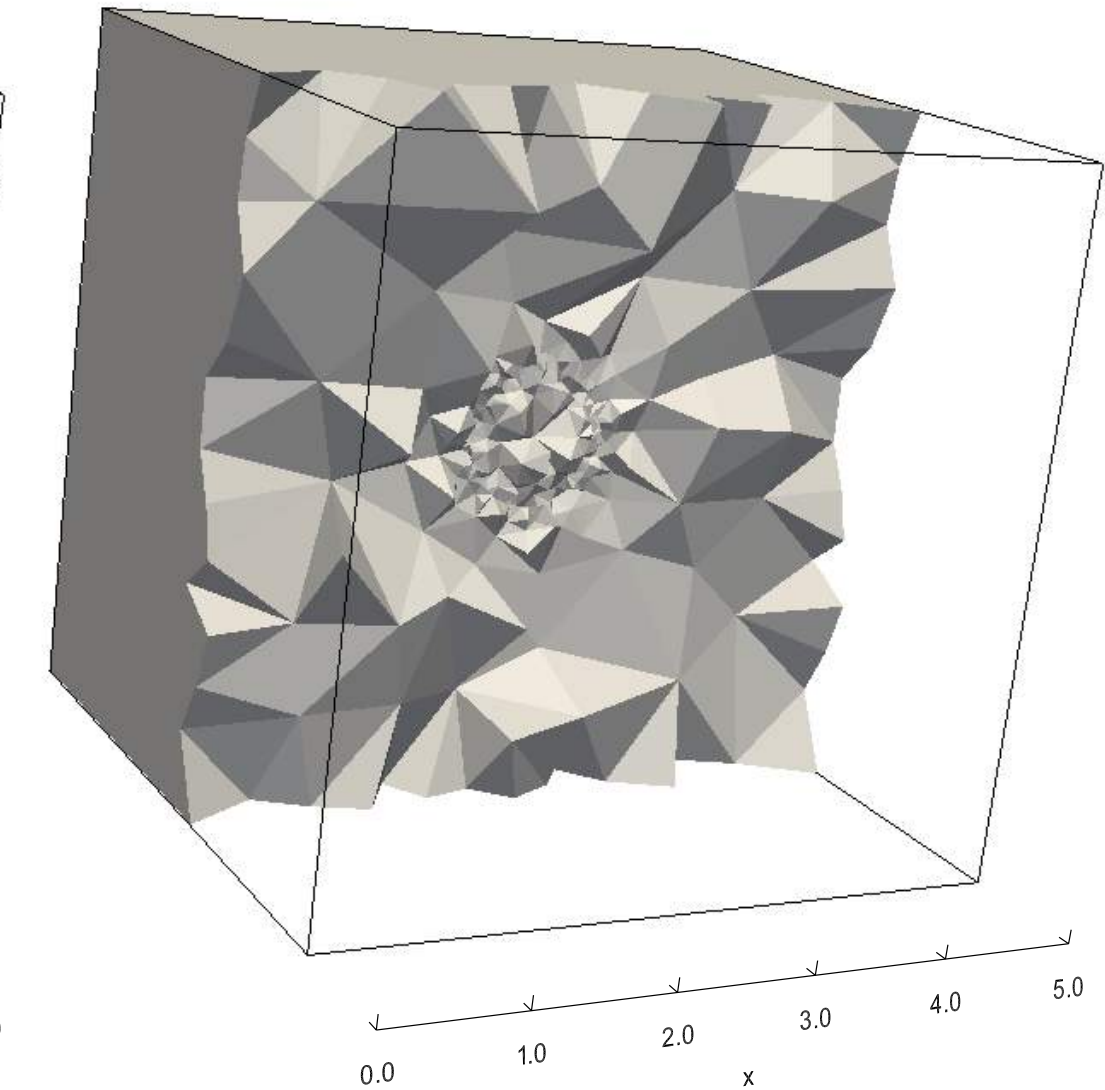
# Simulation meshes



$$L_P = 1.5$$



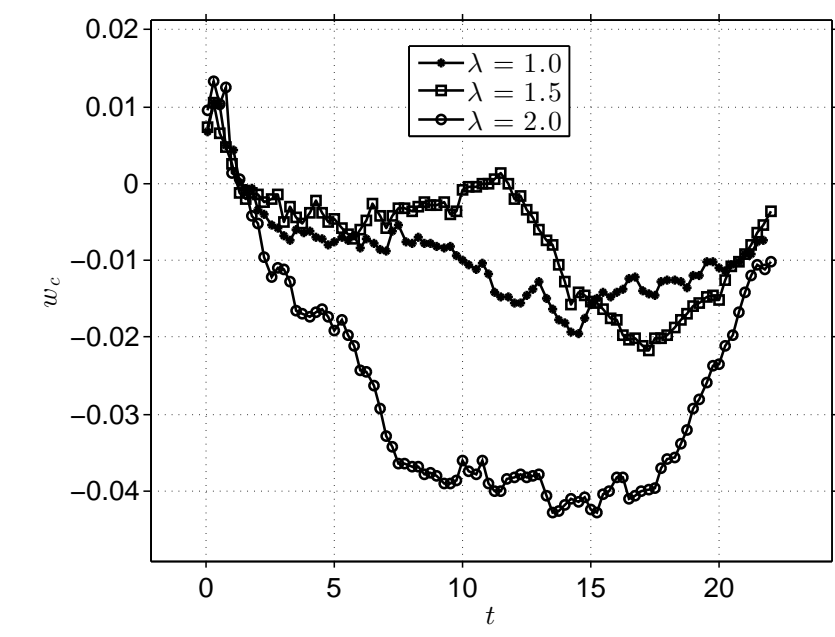
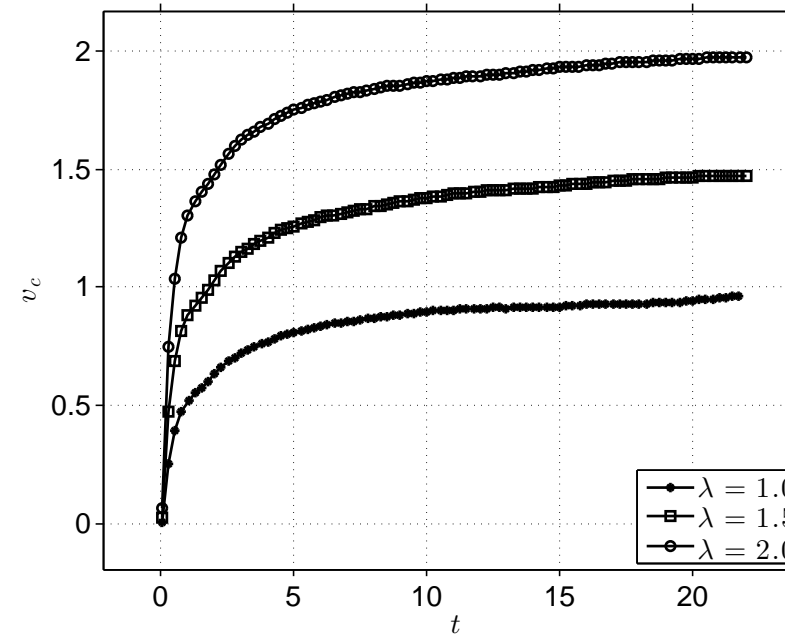
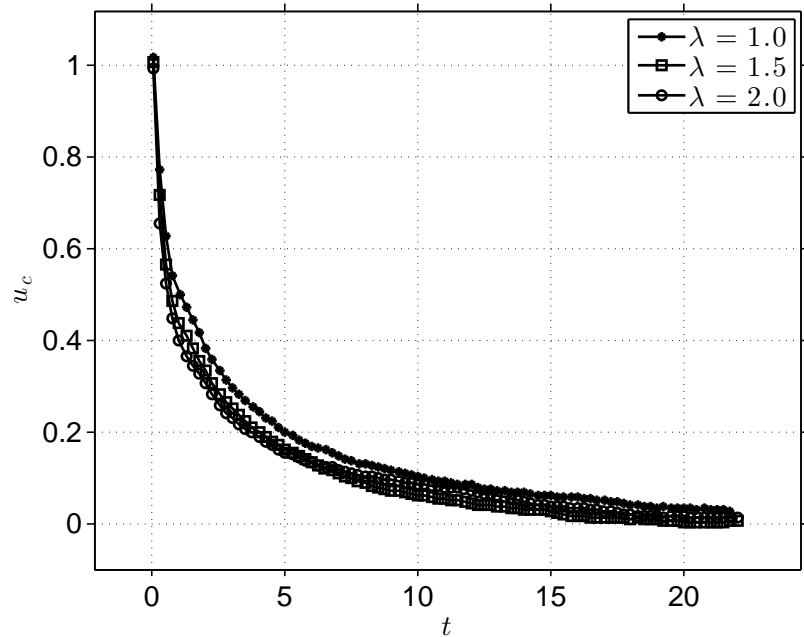
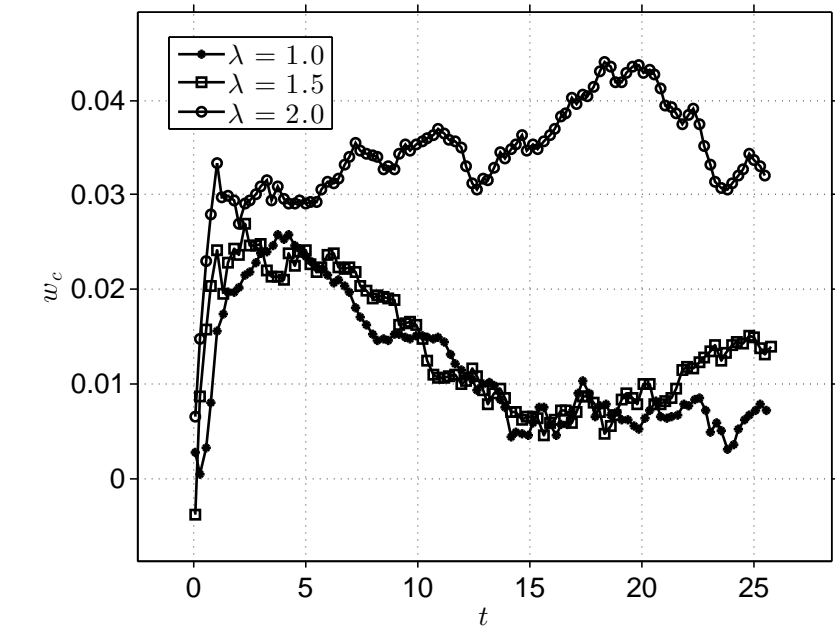
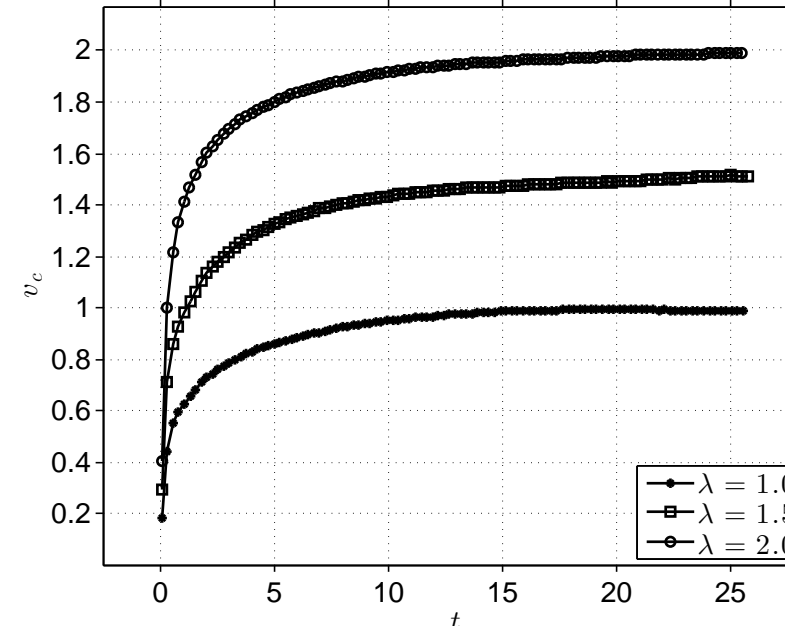
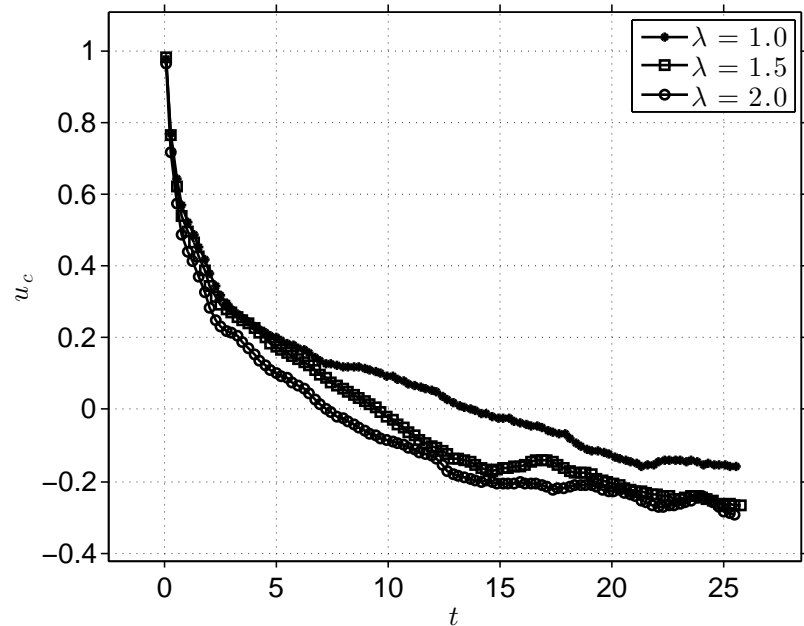
$$L_P = 3.0$$



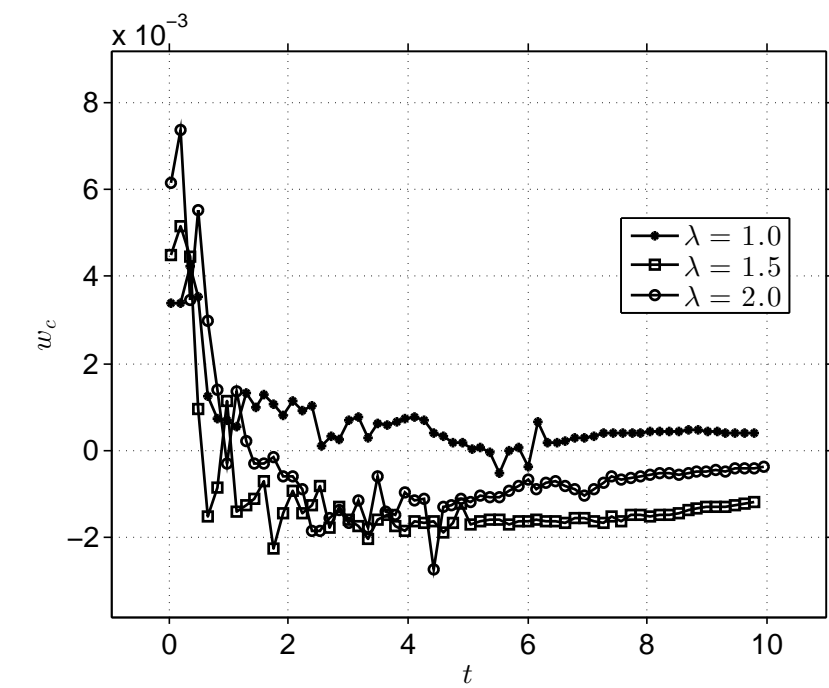
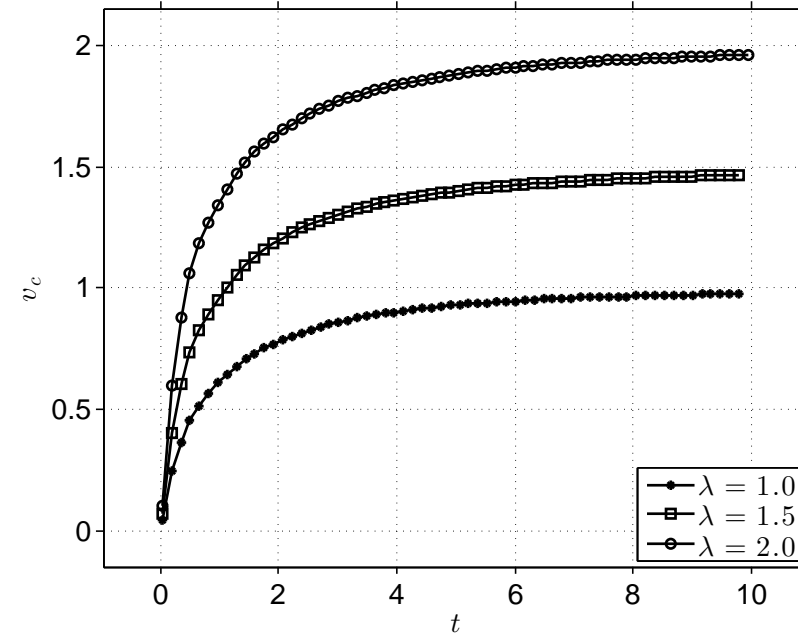
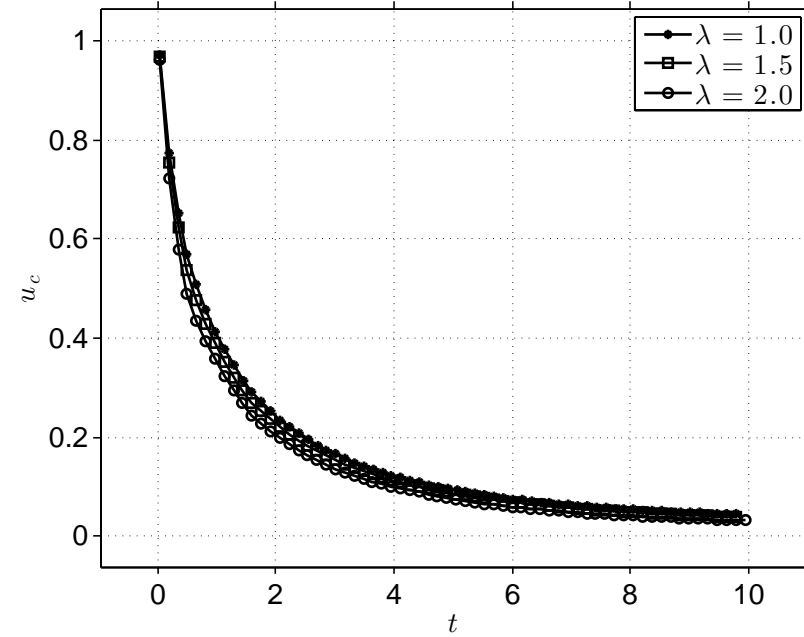
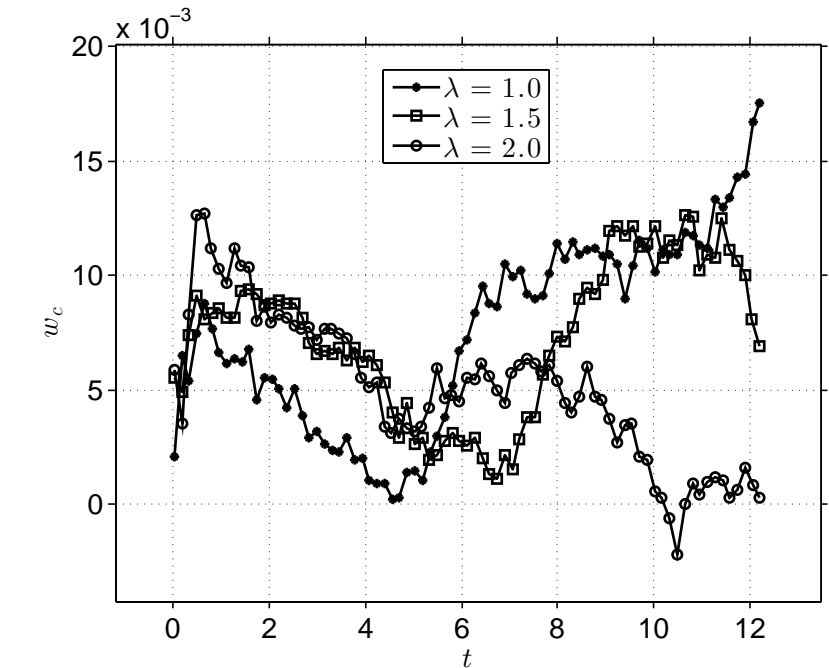
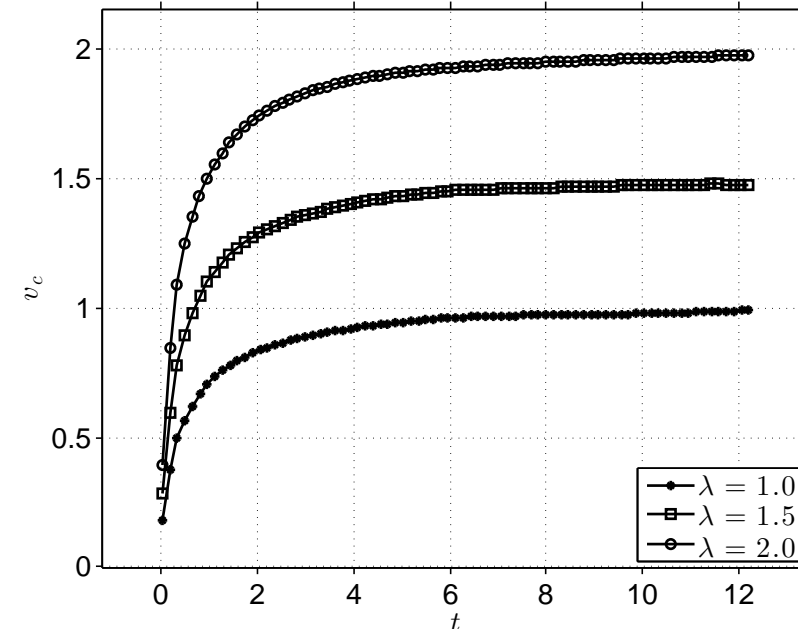
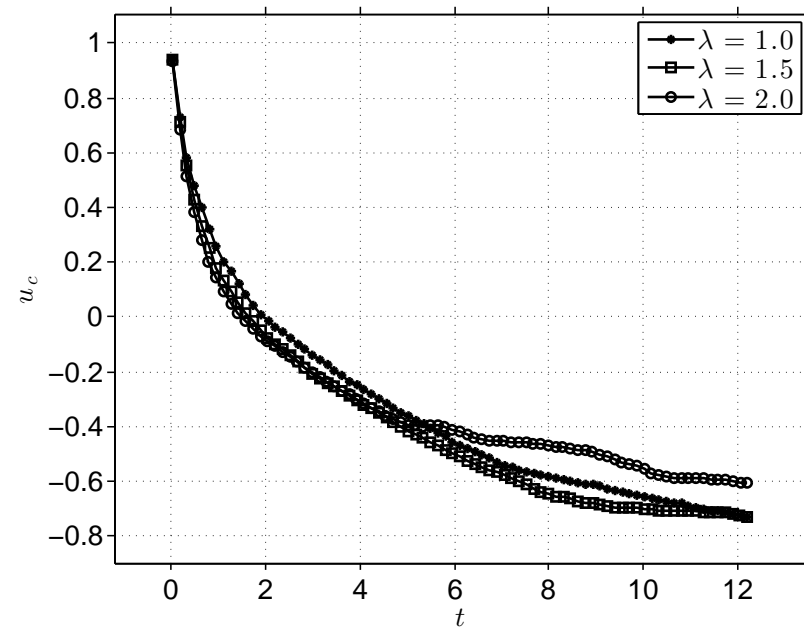
$$L_P = 5.0$$

# Velocity profiles

$$\nabla : (MS, \cdot, L_P = 1.5, 3.0)$$

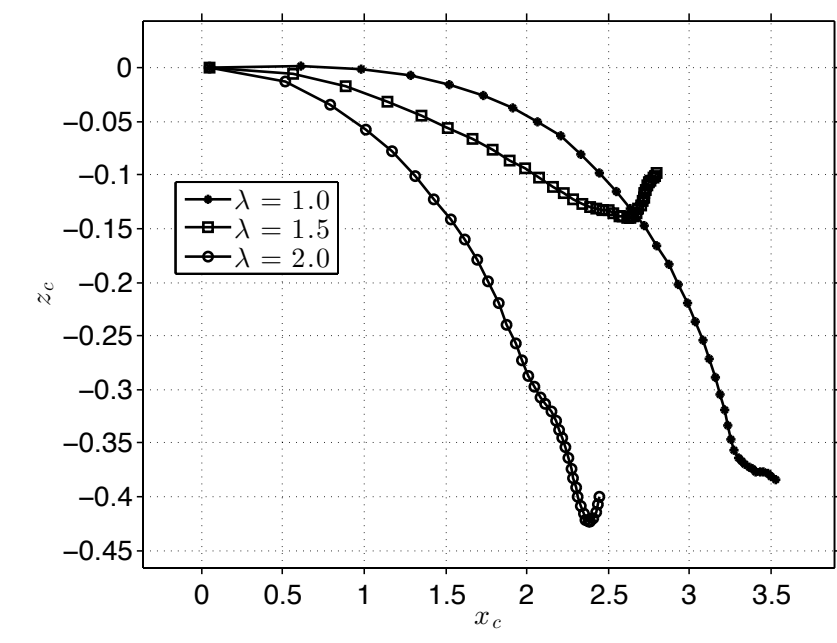
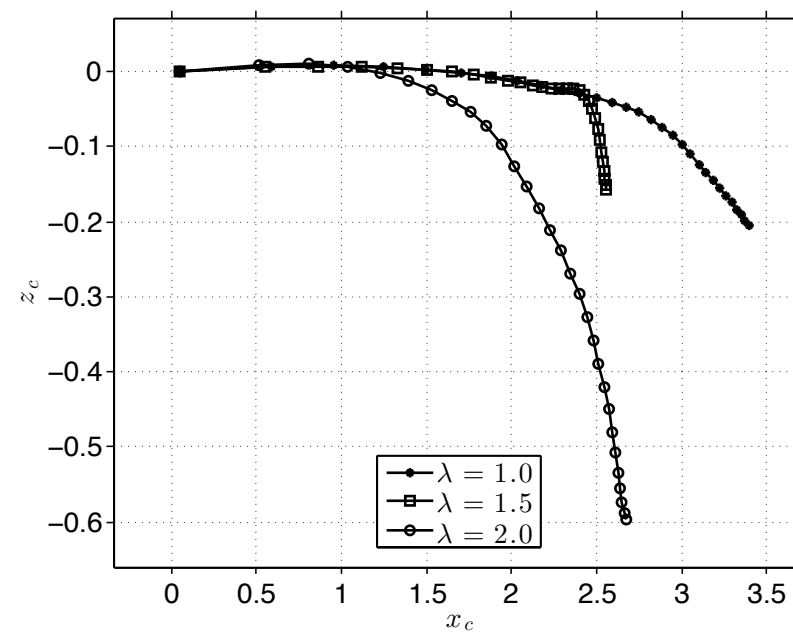
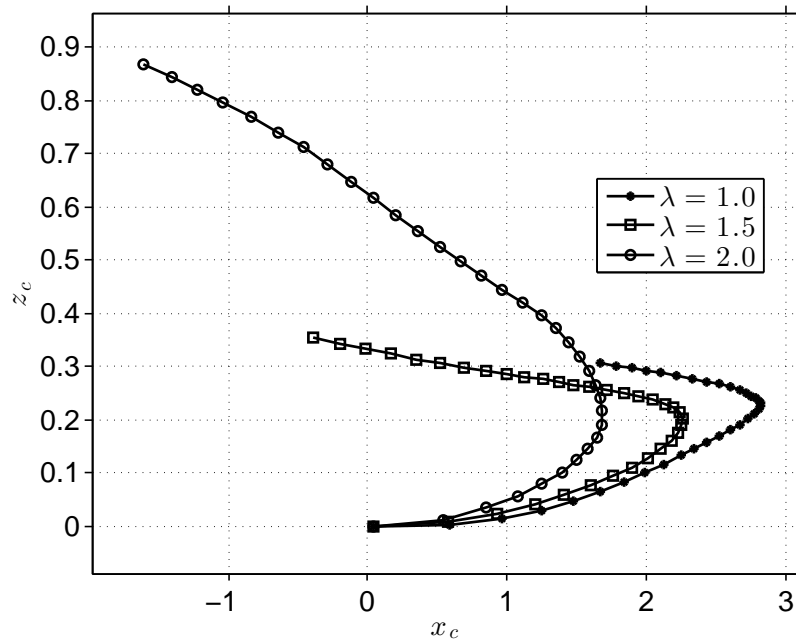
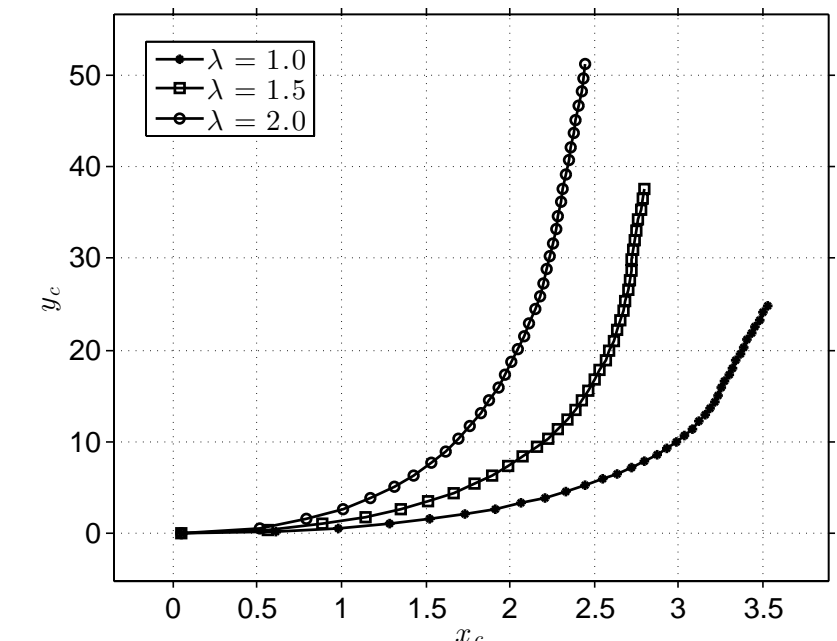
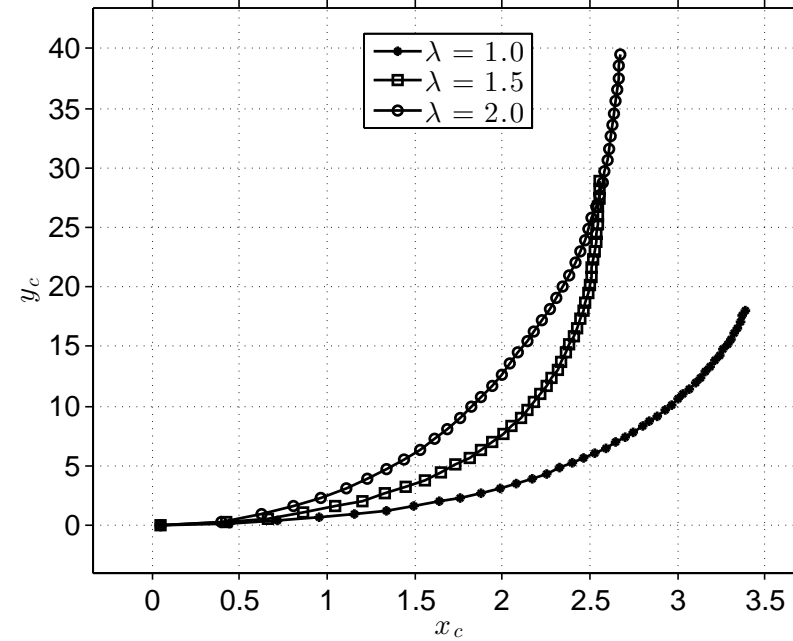
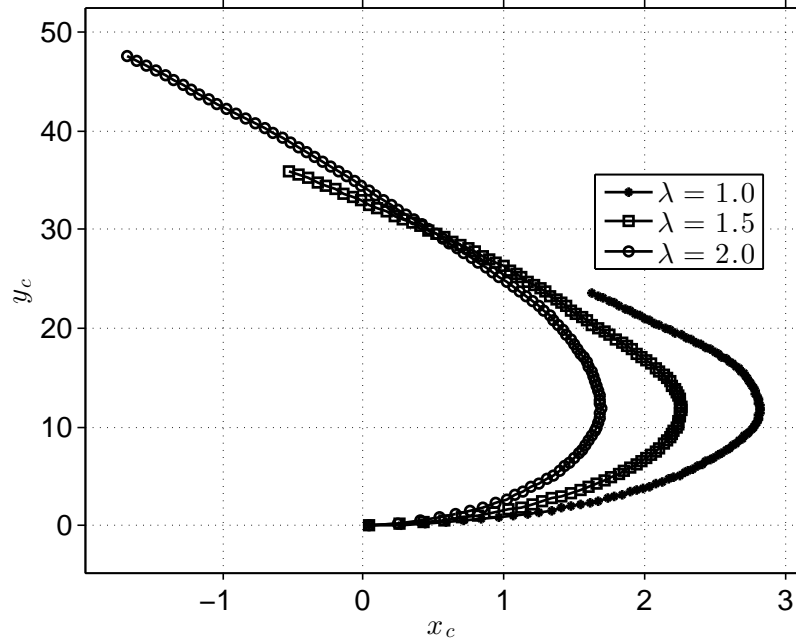


$$\nabla : (\mathbb{W}L, \cdot, L_P = 1.5, 3.0)$$

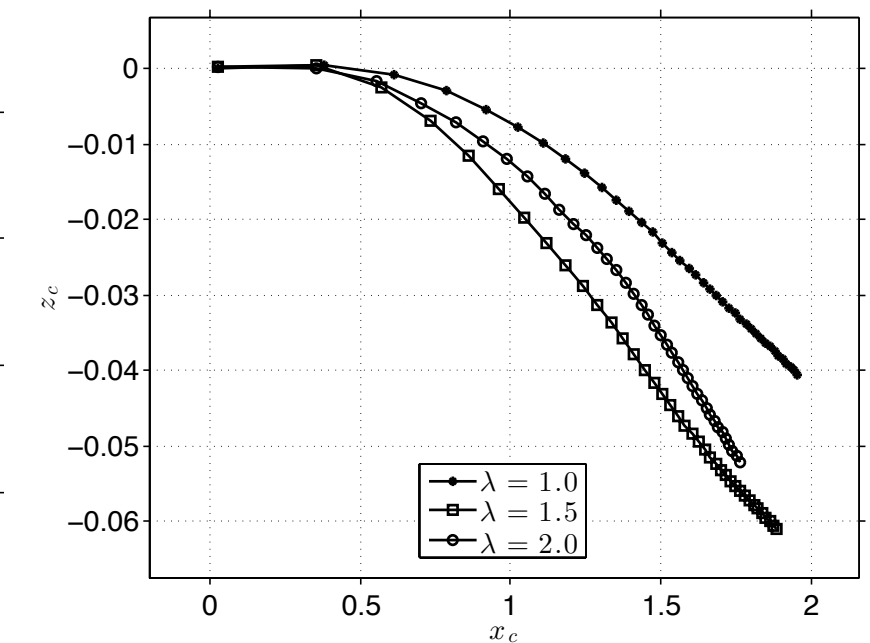
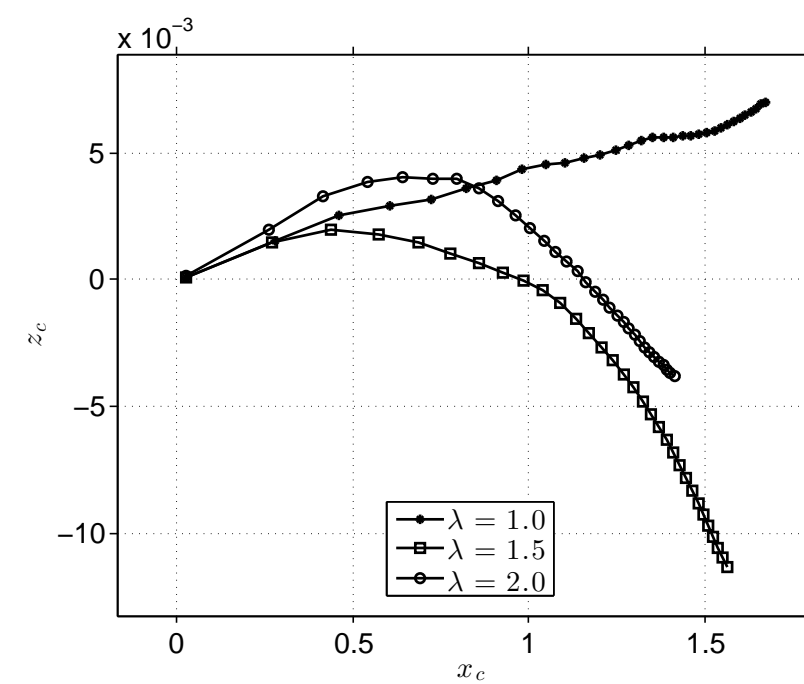
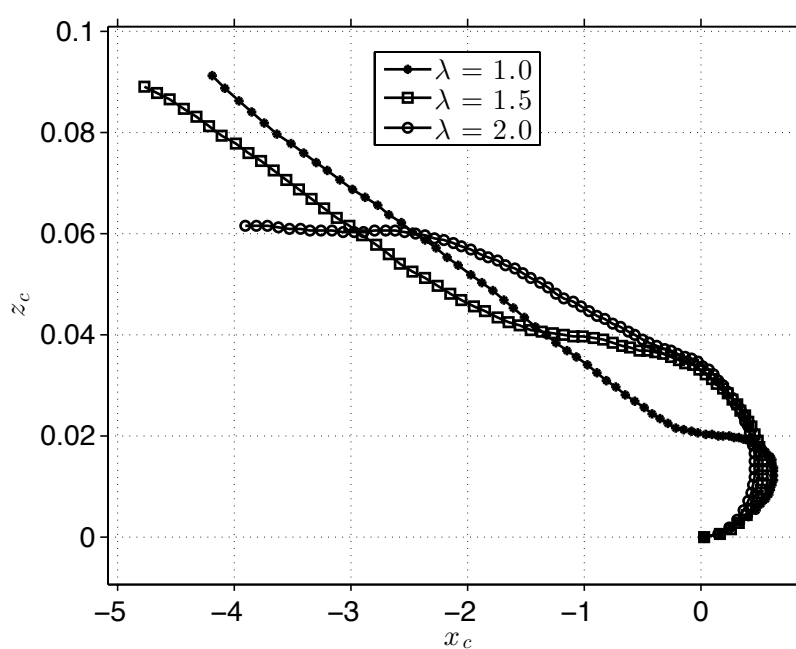
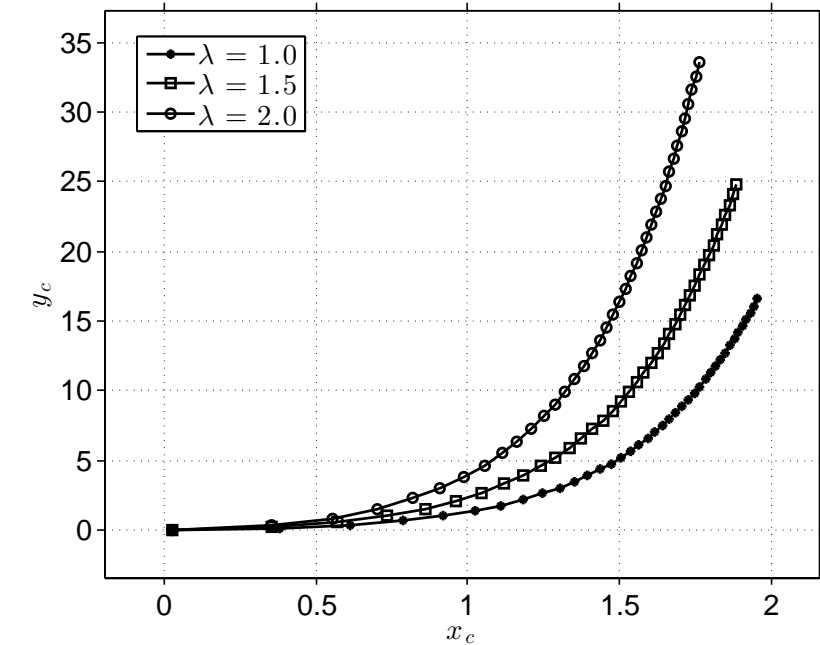
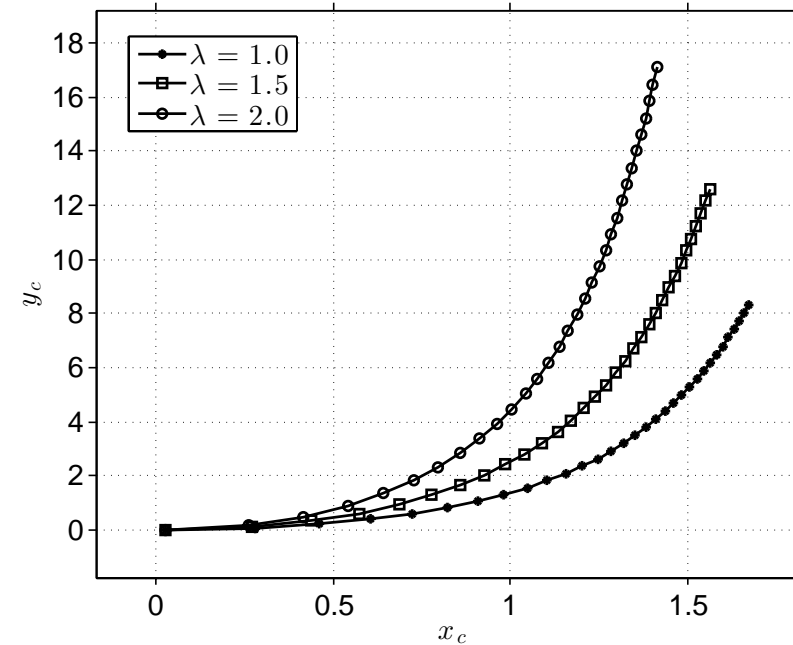
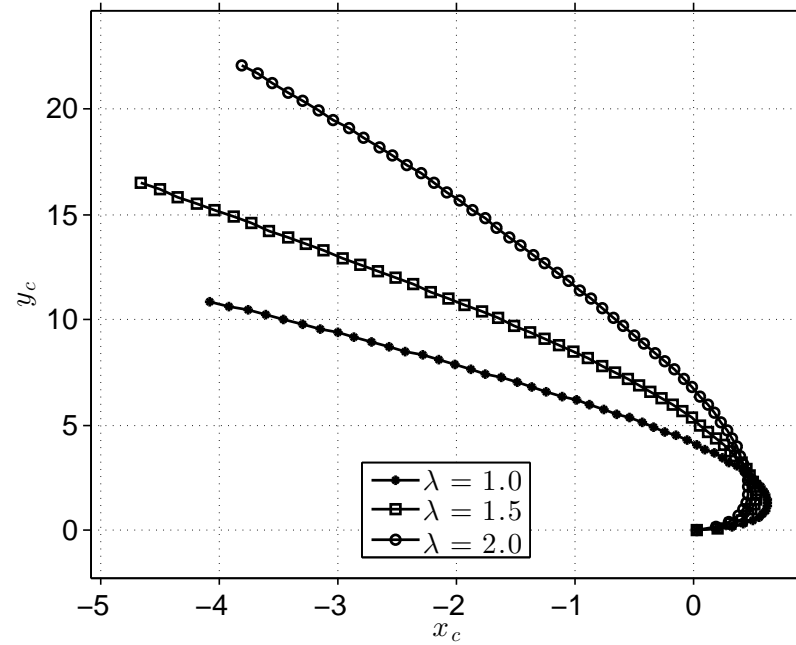


# Trajectory curves

$$\mathbf{x}(\mathbf{X}, t) : (MS, \cdot, L_P = 1.5, 3.0)$$

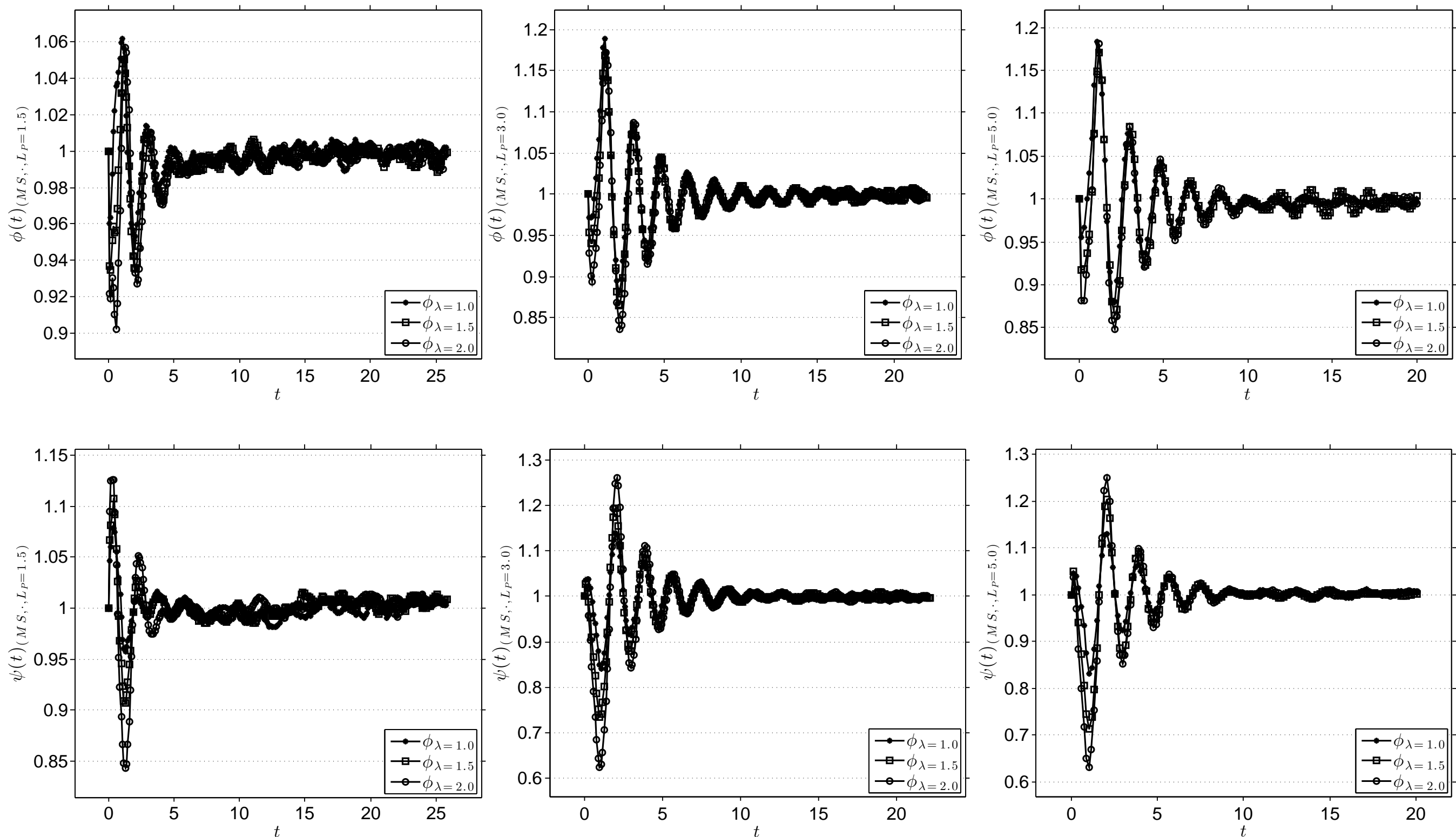


$$\mathbf{x}(\mathbf{X}, t) : (\mathbb{W}L, \cdot, L_P = 1.5, 3.0)$$

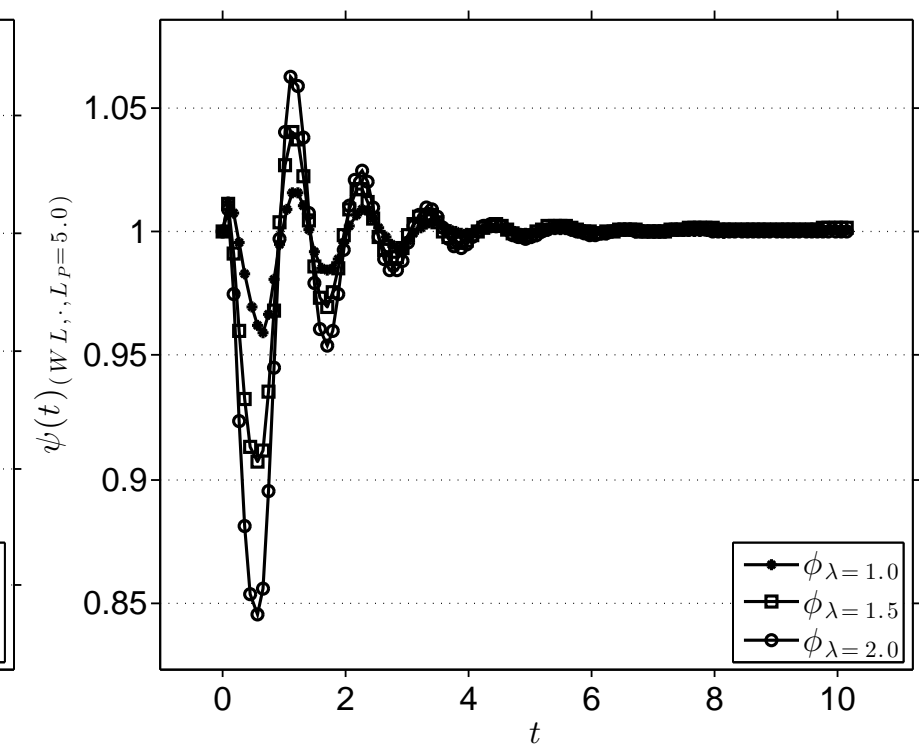
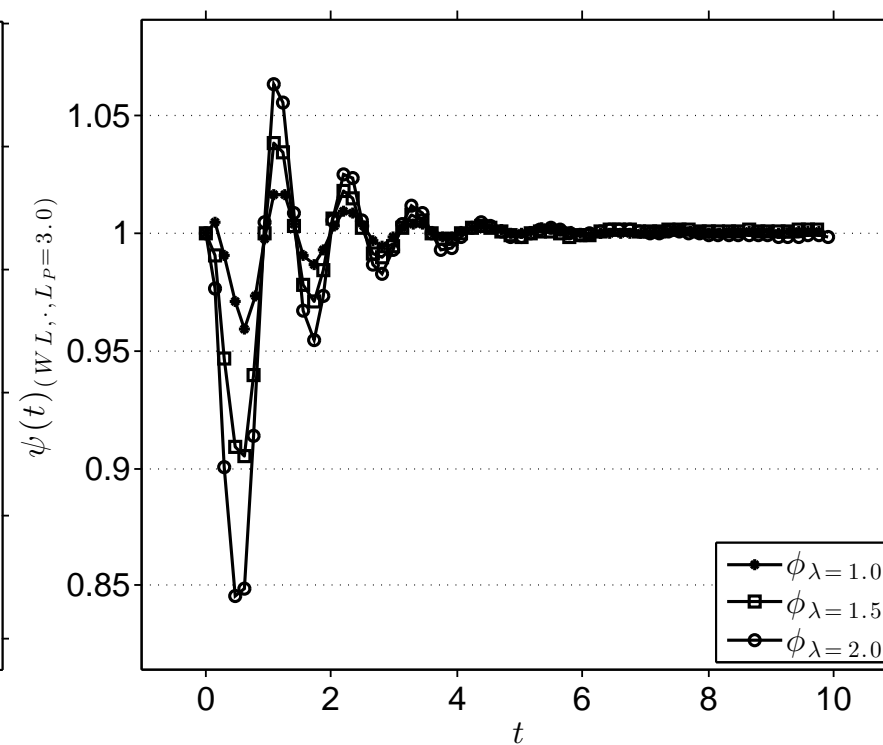
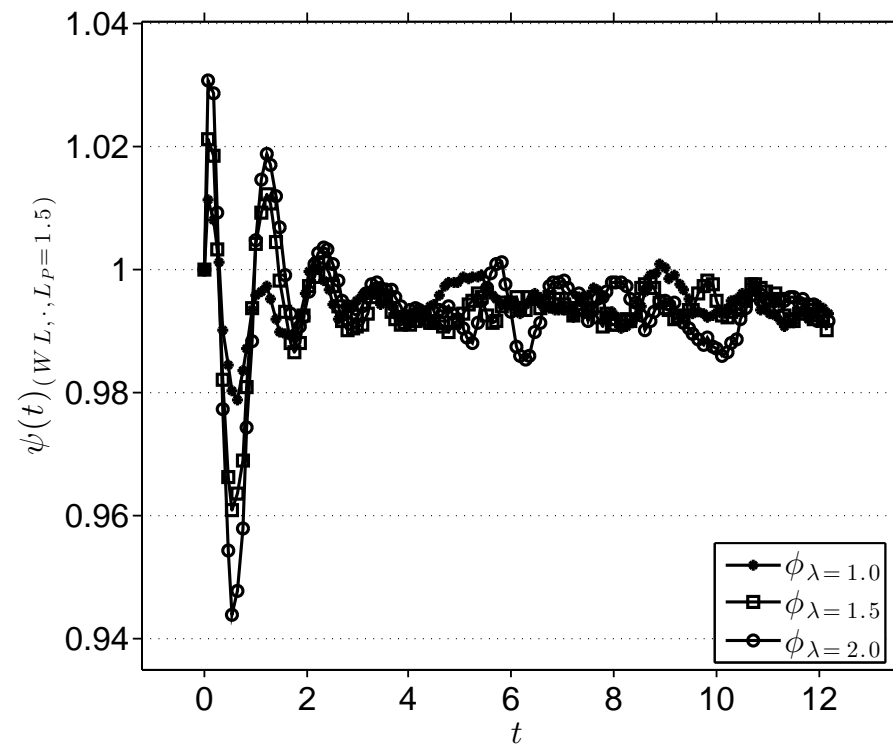
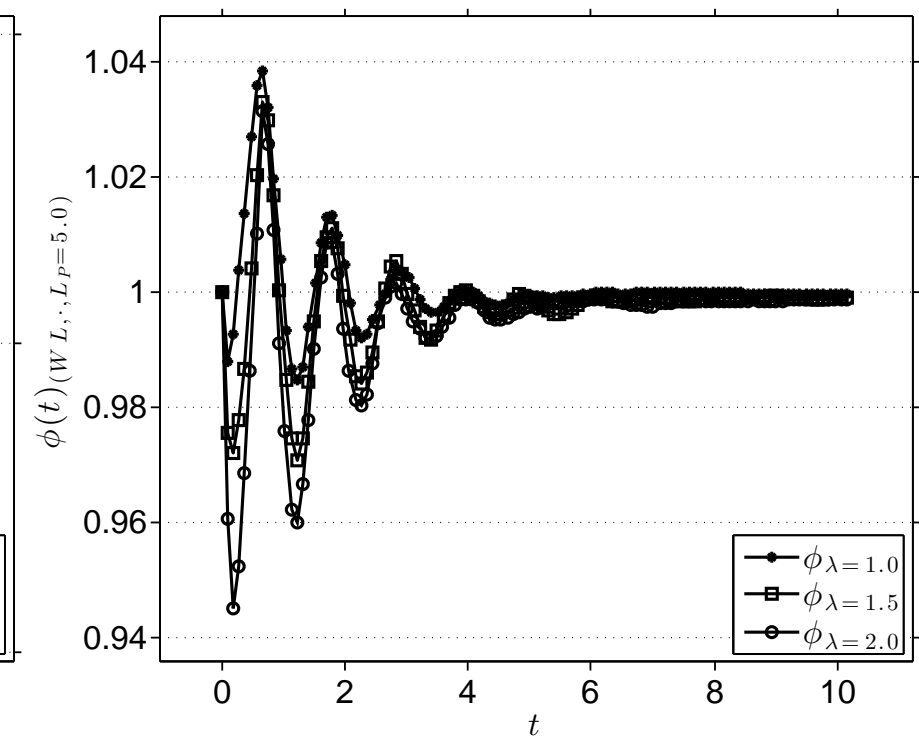
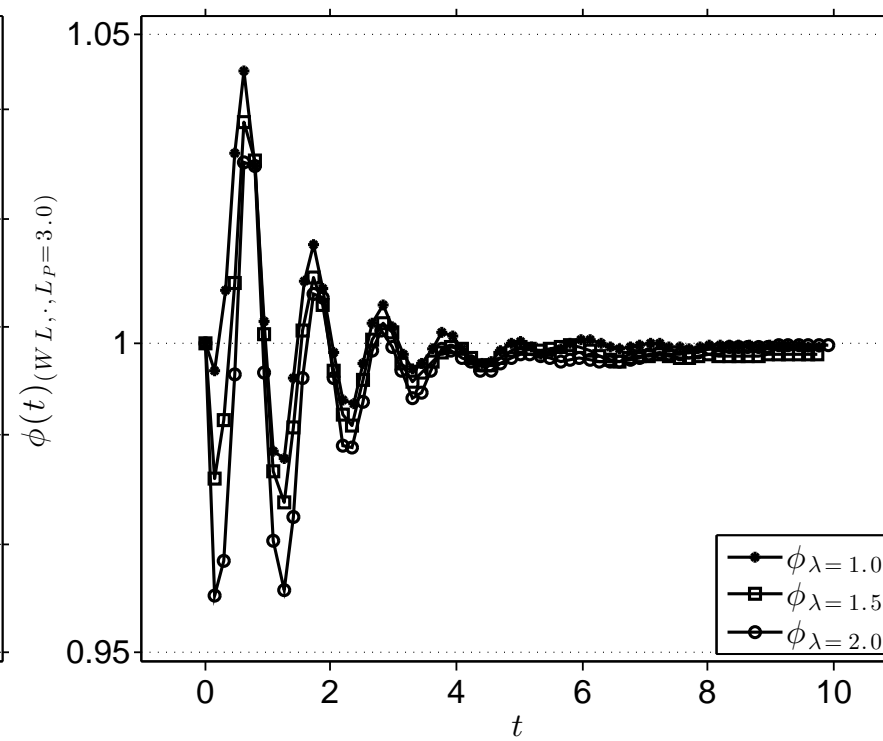
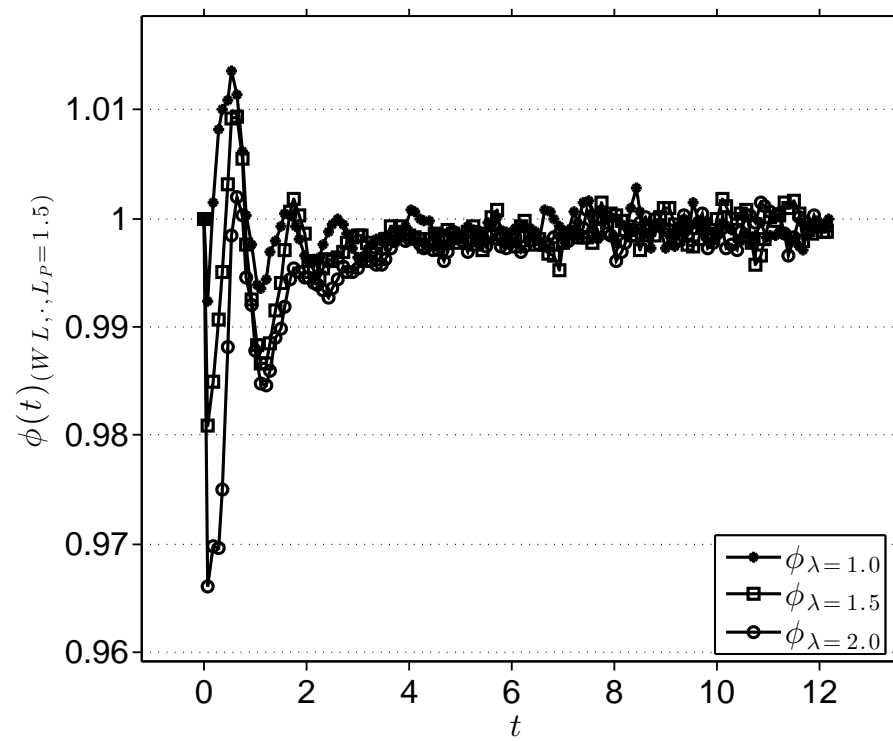


# Drop shape variation

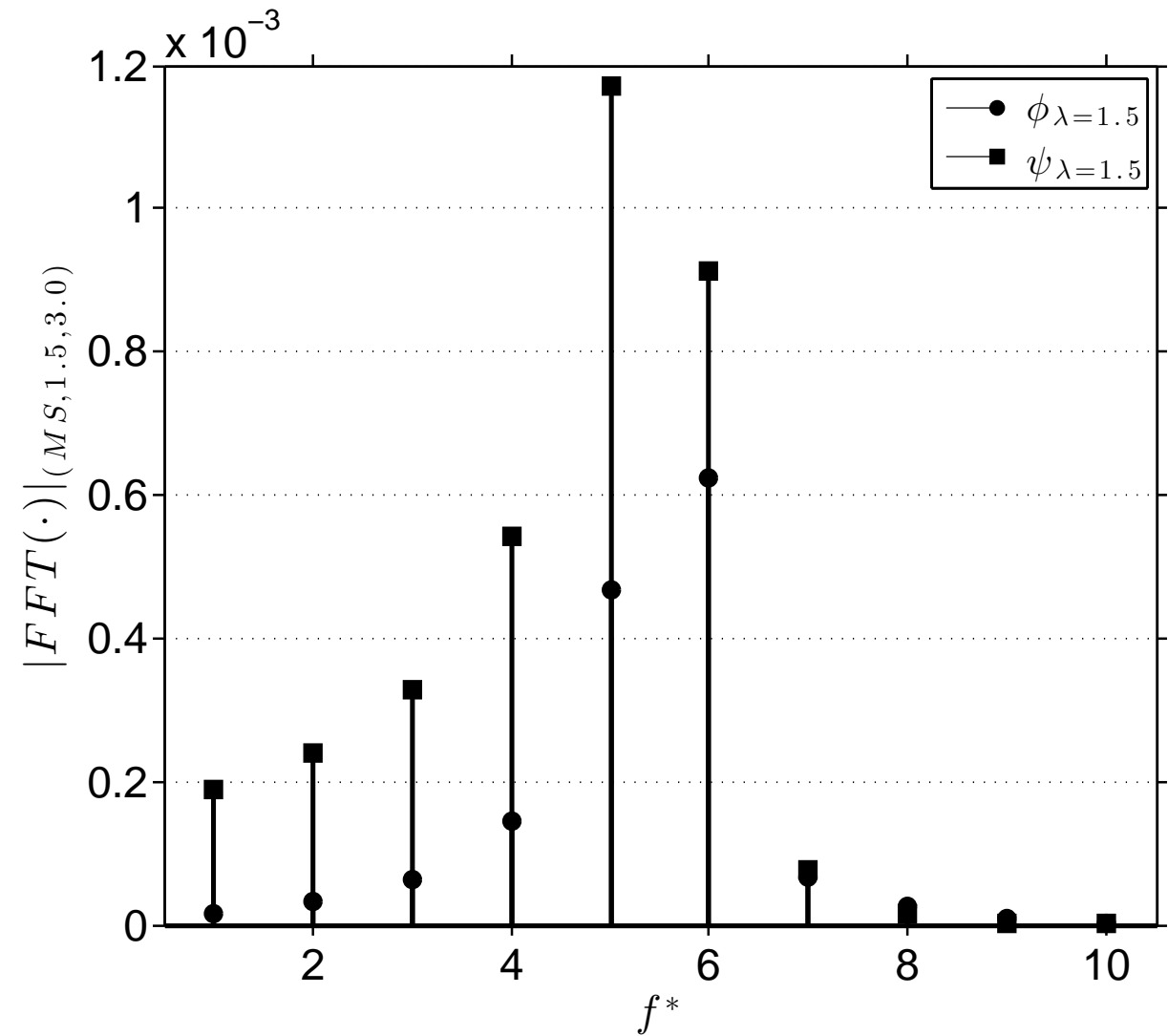
$(MS, \cdot, \cdot); \phi, \psi$



$(WL, \cdot, \cdot); \phi, \psi$



# Spectrum analysis

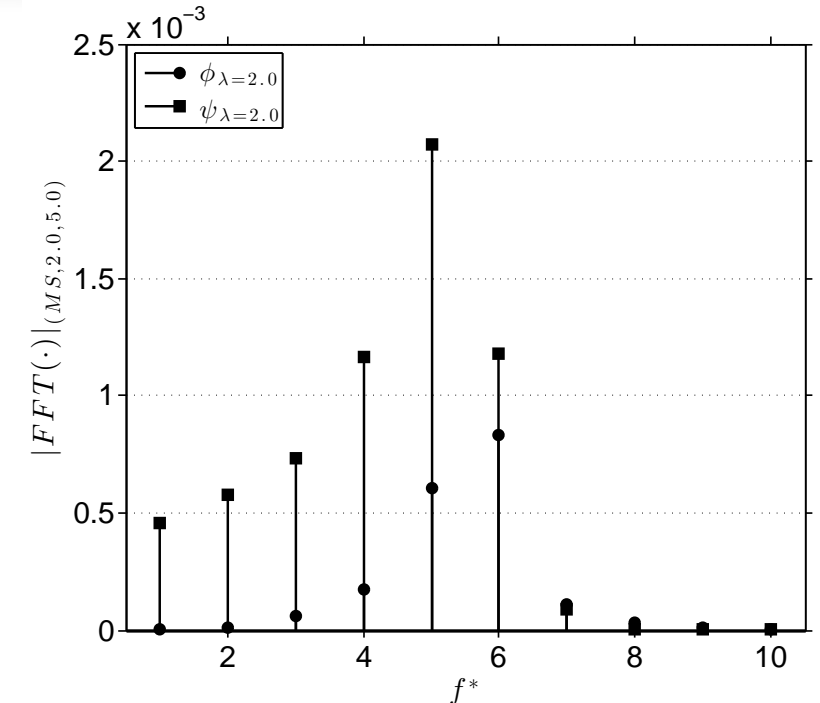
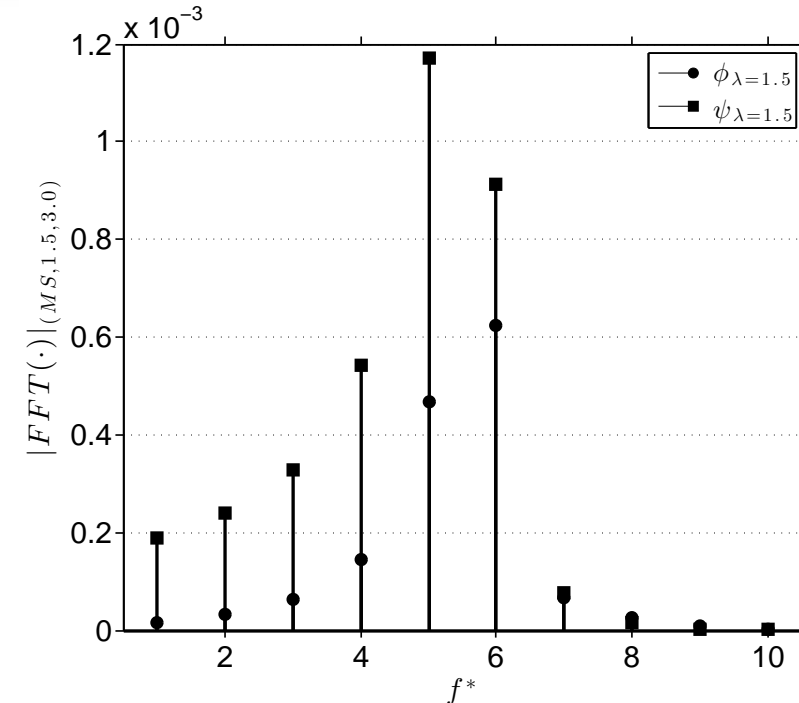
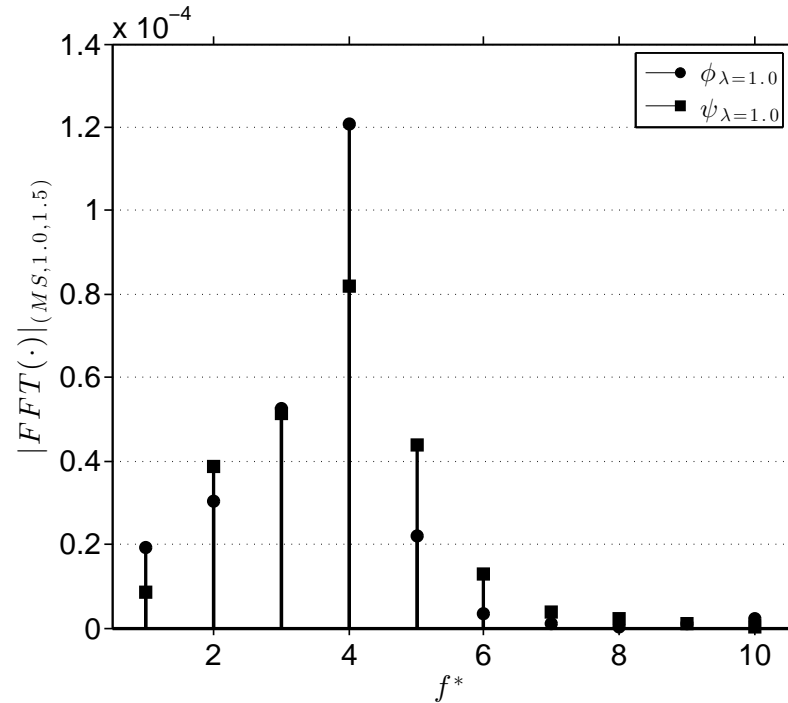


FFT-based spectrum

harmonic modes vs.  
disturbance energy

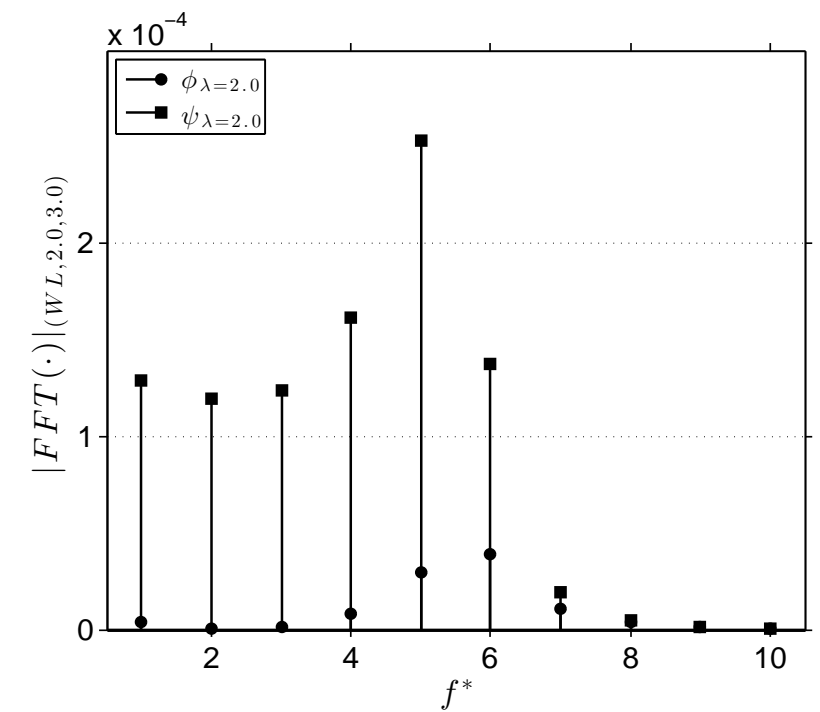
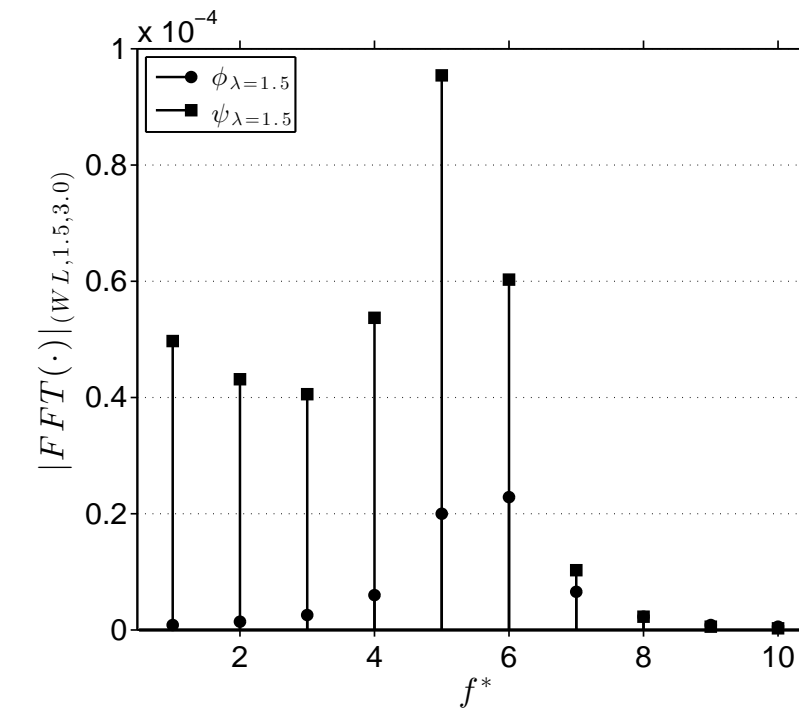
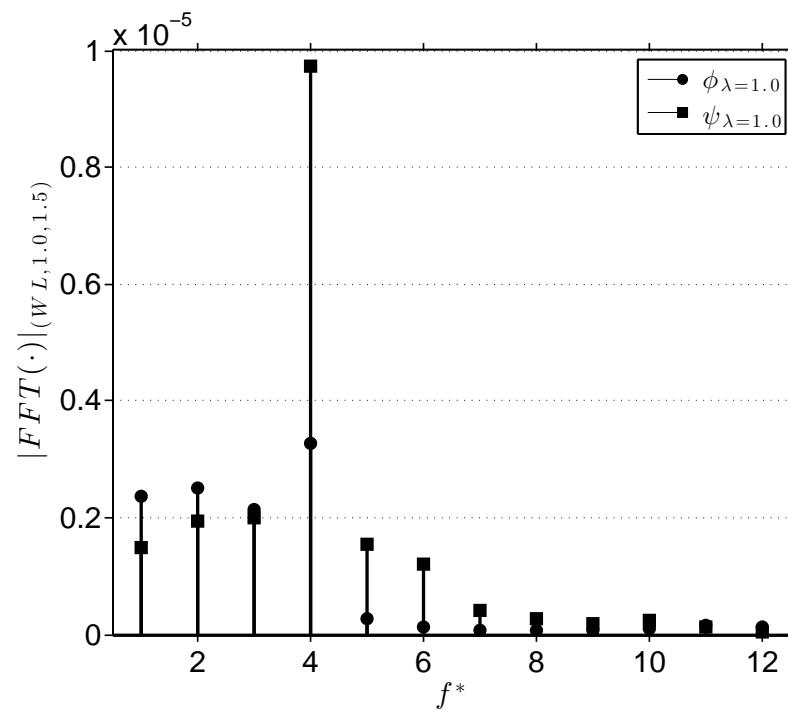
$(MS, 1.5, 3.0)$

$$|FFT[F(t)]| = FFT[F(t)] \overline{FFT[F(t)]};$$
$$F(t) = \phi_{\lambda}(t), \psi_{\lambda}(t)$$

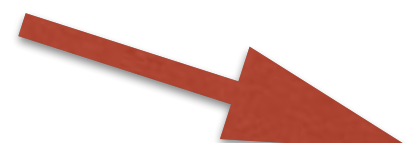


family MS - upper

family WL - lower



highest values

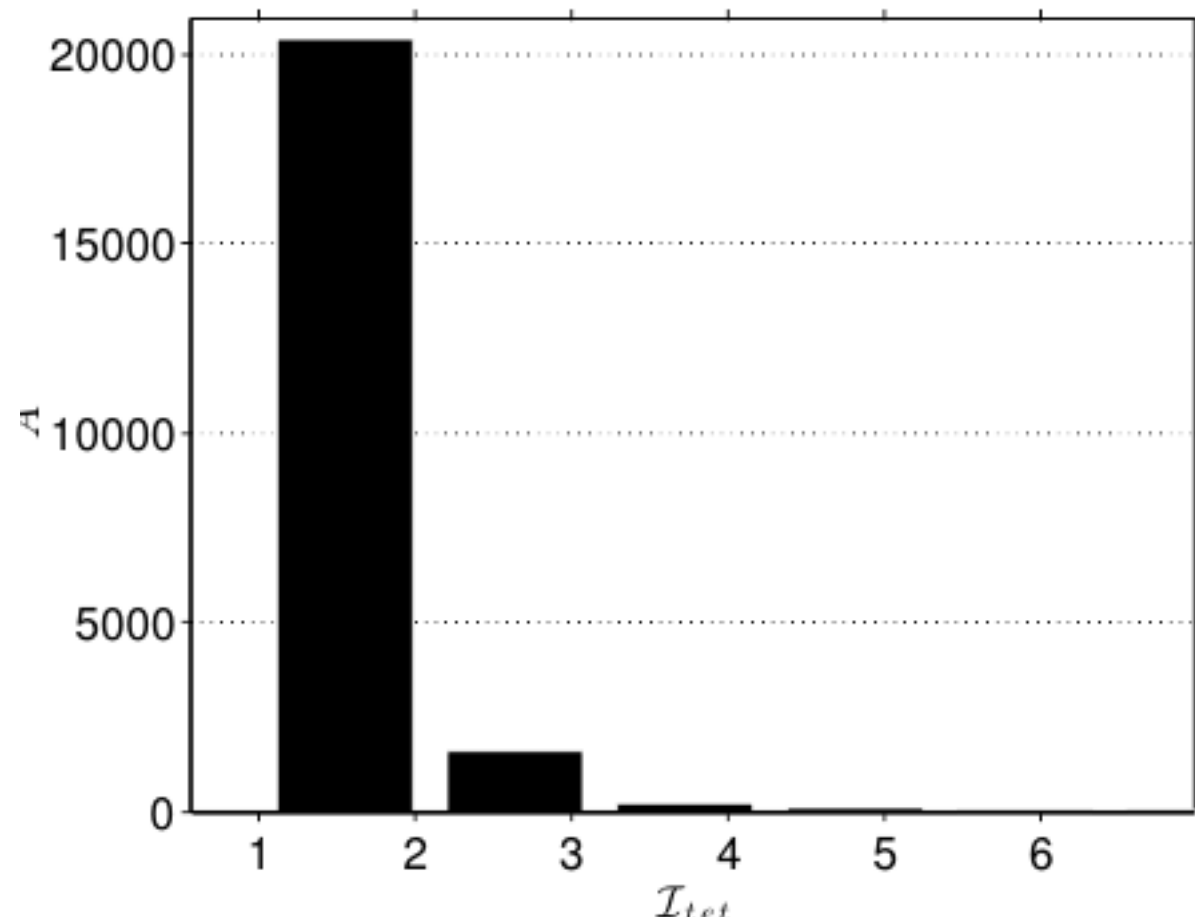


disturbance  
maximum energy  
and  
associated modes

Test Configuration (Ref, $\lambda$ , $L_P$ )	Elongation: $\phi$ $E_\phi$	Elongation: $\phi$ $f_\phi^*$	Flatness: $\psi$ $E_\psi$	Flatness: $\psi$ $f_\psi^*$
(MS, 1.0, 1.5)	0.1209e-03	4	0.8209e-04	4
(MS, 1.5, 1.5)	0.1371e-03	4	0.2307e-03	4
(MS, 2.0, 1.5)	0.2724e-03	4	0.5173e-03	4
(MS, 1.0, 3.0)	0.5823e-03	6	0.6555e-03	6
(MS, 1.5, 3.0)	0.6240e-03	6	1.2000e-03	5
(MS, 2.0, 3.0)	0.7976e-03	6	2.2000e-03	5
(MS, 1.0, 5.0)	0.5204e-03	6	0.5398e-03	5
(MS, 1.5, 5.0)	0.6744e-03	6	1.4000e-03	5
(MS, 2.0, 5.0)	0.8320e-03	6	2.1000e-03	5
(WL, 1.0, 1.5)	0.3273e-05	4	0.9720e-05	4
(WL, 1.5, 1.5)	0.6780e-05	4	2.9883e-05	4
(WL, 2.0, 1.5)	0.9122e-05	4	5.4396e-05	3
(WL, 1.0, 3.0)	1.9835e-05	5	1.5984e-05	5
(WL, 1.5, 3.0)	0.2279e-04	6	0.9535e-04	5
(WL, 2.0, 3.0)	0.3907e-04	6	2.5348e-04	5
(WL, 1.0, 5.0)	2.1435e-05	5	2.7042e-05	5
(WL, 1.5, 5.0)	0.3822e-04	5	1.1677e-04	5
(WL, 2.0, 5.0)	0.5176e-04	5	2.7757e-04	5

# Tetrahedral mesh quality

circumradius-to-inradius ratio



$$\mathcal{J}_{tet}(t) = \left[ \frac{R_{out}(t)}{3R_{in}(t)} \right]_{tet}$$

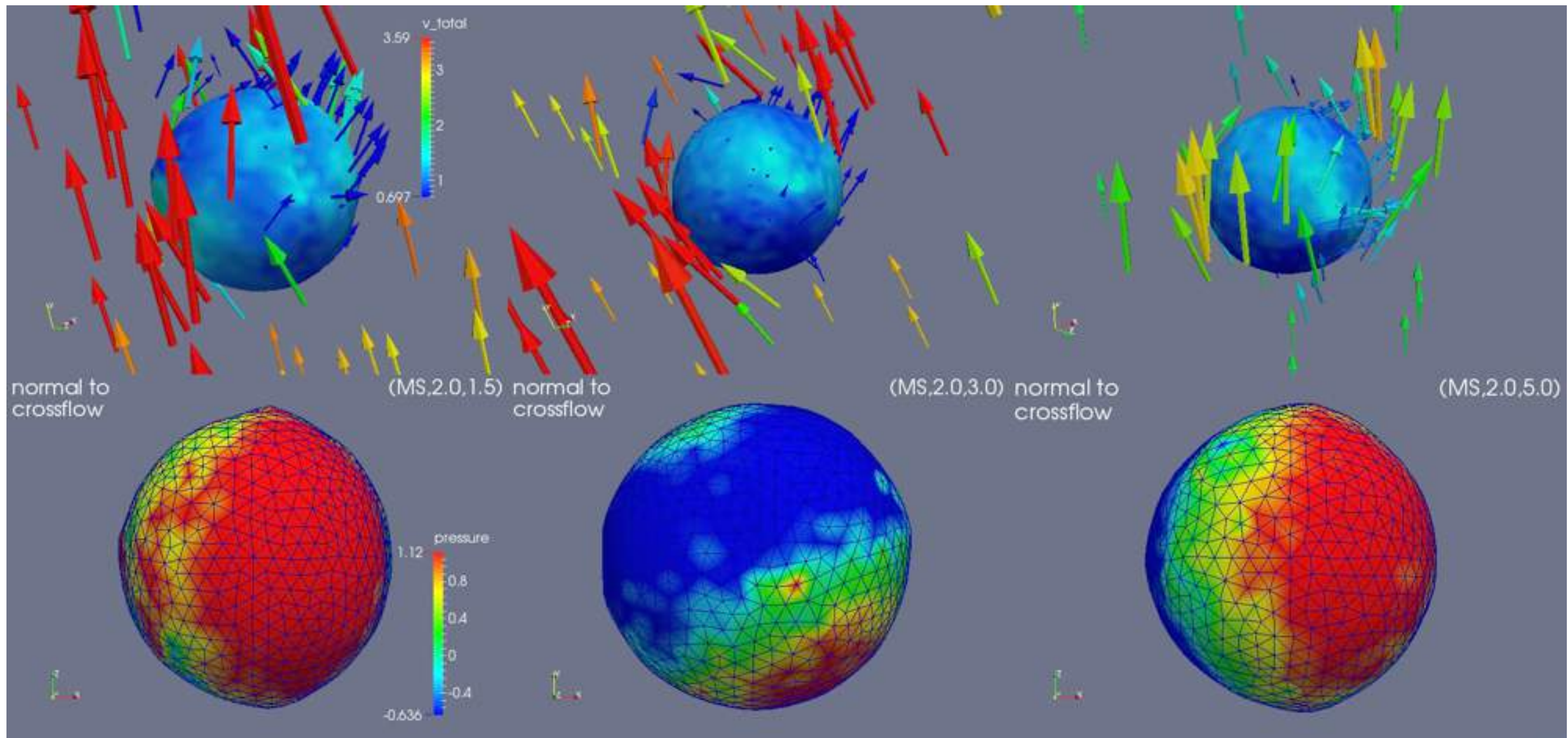
statistical histograms  
follow a similar behaviour

(MS,  $\lambda = 2.0$ ,  $L_P = 5.0$ )

# Table of quality indicators

Test Configuration $(Ref, \lambda, L_P)$	Time Instant $t_A$	Number of Elements $A_{\mathcal{J}}^{max}$	Quality Percentage $\mathcal{O}\%$
$(MS, 1.0, 1.5)$	1.03	17881	95.86
$(MS, 1.5, 3.0)$	8.50	20748	87.42
$(MS, 2.0, 5.0)$	25.47	20421	91.54
$(WL, 1.5, 1.5)$	8.17	17060	96.71
$(WL, 2.0, 3.0)$	9.68	21229	91.88
$(WL, 2.0, 5.0)$	13.22	18479	92.20

# Sample simulations



# Some conclusions

- Flow properties: > or < sensibility to shape change
- Narrowing the spacing -> influence on trajectory
- Disturbance dominant modes for elongation/ flatness -> concentrated between 3 and 6;
- Mesh statistical indicators -> very good mesh quality;

# Acknowledgments

- CAPES and CNPq, for the grants;
- UERJ staff and mates;
- LTCM/EPFL, on behalf of Prof. John R. Thome;
- The jury;
- The audience;

# The end... Thanks for listening!



**“Let’s go to Cappadocia, because at least  
one trail will lead us to the treasure!”**